UNIVERSIDADE FEDERAL DE PERNAMBUCO

CENTRO DE BIOCIÊNCIAS

PROGRAMA DE PÓS GRADUAÇÃO EM BIOLOGIA VEGETAL

THIAGO HENRIQUE DO NASCIMENTO

REVISITANDO A EVOLUÇÃO CROMOSSÔMICA DE *Phaseolus* L. (Leguminosae) POR MEIO DE OLIGO-FISH

RECIFE-PE

2022

THIAGO HENRIQUE DO NASCIMENTO

REVISITANDO A EVOLUÇÃO CROMOSSÔMICA DE *Phaseolus* L. (Leguminosae) POR MEIO DE OLIGO-FISH

Dissertação apresentada ao Programa de Pós-Graduação em Biologia Vegetal da Universidade Federal de Pernambuco, na Área de Sistemática e Evolução, na linha de pesquisa de Citogenética e Citotaxonomia, como requisito para obtenção do grau de Mestre em Biologia Vegetal.

Orientadora: Prof.ª Dr.ª Andrea Pedrosa-Harand (Dept. Botânica, UFPE)

RECIFE-PE

2022

Catalogação na Fonte
Bibliotecário: Marcos Antonio Soares da Silva
CRB4/1381

Nascimento, Thiago Henrique do.
Revisitando a evolução crosmossômica de *Phaseolus L. (Leguminosae)* por meio de oligo-fish. / Thiago Henrique do Nascimento . – 2022.

87 f. : il., fig.; tab.

Orientadora:Andrea Pedrosa-Harand.

.

Dissertação (mestrado) – Programa de Pós-Graduação em Biologia Vegetal da Universidade Federal de Pernambuco, 2022.

Inclui referências.

1. Evolução cromossômica. 2. Oligo-FISH. 3. Phaseolus. 4. Pintura cromossômica. 5. Rearranjos estruturais. I. Pedrosa-Harand, Andrea (Orient.). II. Título

580 CDD (22.ed.) UFPE/CB – 2024-047

THIAGO HENRIQUE DO NASCIMENTO

REVISITANDO A EVOLUÇÃO CROMOSSÔMICA DE *Phaseolus* L. (Leguminosae) POR MEIO DE OLIGO-FISH

Aprovado em: 25/02/2022

BANCA EXAMINADORA

Membros Titulares:

Prof.ª Dr.ª Andrea Pedrosa-Harand- UFPE

Prof.ª Dr.ª Giovana Torres- UFLA

Prof. Dr. Luiz Gustavo Rodrigues Souza- UFPE

Membros Suplentes:

Prof. Dr. Marcelo dos Santos Guerra Filho- UFPE

Prof. Dr. Reginaldo de Carvalho- UFRPE

Recife-PE

2022

Eu cheguei de muito longe

E a viagem foi tão longa

E na minha caminhada

Obstáculos da estrada, mas enfim aqui estou [...]

Erasmo Carlos

Dedico aos meus Pais, que com muito esforço me ensinaram o valor da Educação.

AGRADECIMENTOS

Gostaria de agradecer aos meus Pais, minha Mãe-Maria (Vó) e minha tia Viviane, sem o apoio deles seria impossível ter chegado até aqui. Lhes agradeço por terem me ensinado desde muito cedo o valor da educação e seu efeito transformador.

Agradeço aos colegas do Laboratório de Citogenética e Evolução Vegetal, tenho certeza que aprendi com cada pessoa com quem tive contato durante esses anos. Em especial, quero agradecer a Jéssica Nascimento, Amanda Santos, Amália Ibiapino e Yennifer Mata-Sucre (da qual sinto muita falta) por todos os momentos compartilhados, eles foram de muita importância para mim e certamente os guardarei em minhas memórias para sempre. Quero agradecer também a Andrea Pedrosa-Harand pela orientação e pelos momentos de discussão que, embora às vezes acalorados, sempre são repletos de trocas e nesse movimento vamos crescendo juntos. A Gustavo Souza, que embora não tenhamos tido muito contato durante meu mestrado pandêmico, sou grato pelos conhecimentos compartilhados durante as disciplinas. Quero agradecer também a Marcelo Guerra, que nos últimos meses tem compartilhado seus conhecimentos e vivências comigo tornando os sábados sempre muito agradáveis.

"Which is more important," asked Big Panda, "the journey or the destination?"

"The company." said Tiny Dragon.

Por último, e não menos importante, quero agradecer ao Programa de Pós-Graduação em Biologia Vegetal, à CAPES e à Universidade Federal de Pernambuco pelo apoio e infraestrutura que viabilizaram a realização dos trabalhos aqui compilados.

Meus sinceros agradecimentos.

RESUMO

O gênero *Phaseolus* L. (Leguminosae) é constituído por cerca de 90 espécies neotropicais. Estudos citogenéticos têm revelado relativa estabilidade cariotípica (2*n* = 22), exceto pelo clado Leptostachyus, composto por *P. macvaughii* Delgado, *P. micranthus* Hook. & Arn. e *P. leptostachyus* Benth. (2*n* = 20), que sofreu disploidia e outros rearranjos cromossômicos. Embora tenha sido alvo de mapeamento por BAC-FISH, o cariótipo de *P. leptostachyus* ainda não foi esclarecido, assim como não está claro o quão rearranjado é este cariótipo em comparação a outros clados. O presente estudo teve como objetivo revisitar a evolução cromossômica em espécies de *Phaseolus* por meio de mapeamento comparativo com o sistema de identificação oligo-FISH *barcode*, pintura cromossômica, DNAr e um *repeat* centromérico (CentPv1) em nove espécies do gênero, sendo analisados dois acessos de *P. vulgaris*, um de origem andina e outro mesoamericana. Para tanto, preparações citológicas foram hibridizadas *in situ* com sondas oligonucleotídicas para o mapeamento comparativo de todos os pares cromossômicos. Foi possível, em um primeiro capítulo, desenvolver e implementar o primeiro sistema de identificação oligo-FISH *barcode* para leguminosas em *V. unguiculata* e *P. vulgaris*, o qual foi eficiente e possibilitou a identificação de novos rearranjos estruturais entre as espécies. E, em um segundo capítulo, foi possível mensurar a taxa de evolução cromossômica (rearranjos/milhão de anos) em uma ampla amostragem, revelando uma alta taxa de evolução cromossômica no clado Leptostachyus, em especial em *P. leptostachyus*, o que sugere a possibilidade de que essa seja a planta com maior reestruturação genômica em um curto espaço de tempo evolutivo.

Palavras-chave: evolução cromossômica; oligo-FISH; *Phaseolus*; pintura cromossômica; rearranjos estruturais.

ABSTRACT

Phaseolus L. (Leguminosae) is constituted by ~90 Neotropical species. Cytogenetic studies have revealed relative karyotypic stability (2*n* = 22), except for the clade Leptostachyus, composed by *P. macvaughii* Delgado, *P. micranthus* Hook. & Arn. and *P. leptostachyus* Benth. (2*n* = 20), which has undergone dysploidy and other chromosome rearrangements. Although it has been the target of BAC-FISH mapping, the karyotype of *P. leptostachyus* has not yet been clarified, as well as it is not clear how rearranged this karyotype is compared to other clades. The present study aimed to revisit the chromosome evolution in *Phaseolus* by comparative mapping with a oligo-FISH barcode identification system, chromosome painting, rDNA and a centromeric repeat (CentPv1) in nine species of the genus, including two accessions of *P. vulgaris*, one Andean and one of Mesoamerican origin. For this, cytological preparations were hybridized *in situ* with oligonucleotide probes for the comparative mapping of all chromosome pairs. In the first chapter, we developed and implemented the first oligo-FISH barcode identification system for legumes in *V. unguiculata* and *P. vulgaris*, which was efficient and allowed the identification of new structural rearrangements between the species. In a second chapter, we measured the chromosome evolution rate (rearrangements/million years) in a large sample, revealing a high chromosome evolution rate in the Leptostachyus clade, especially in *P. leptostachyus*, suggesting the possibility that this is the plant with the greatest genomic restructuring in a short period of the evolutionary time.

Keywords: chromosome evolution; chromosome painting; oligo-FISH; *Phaseolus*; structural rearrangements.

LISTA DE ILUSTRAÇÕES

MANUSCRITO 1- OLIGO-FISH BARCODE IN BEANS: A NEW CHROMOSOME IDENTIFICATION SYSTEM

Figure 1. Chromosome identification of *Vigna unguiculata* (*2n* = 22) and *Phaseolus vulgaris* (*2n* = 22) based on *V. unguiculata* oligo-FISH barcode. Two oligo-FISH probe sets (red and green) hybridized on mitotic metaphase chromosomes of *V. unguiculata* (a) and *P. vulgaris* (b). Homologous chromosomes in **a** and **b** were paired in karyograms to identify the 11 chromosome pairs of *V. unguiculata* (c) and *P. vulgaris* (d). Each chromosome shows a unique pattern of oligo-FISH red and/or green signals. Chromosomes were counterstained in DAPI (pseudocoloured in grey). Idiograms of the barcode for both species using the *V. unguiculata* reference genome and considering the conserved sequences of *P. vulgaris* genome (**e**, *V. unguiculata* and **f**, *P. vulgaris*). Chromosomes were named according to the species name abbreviations (*Vu* and *Pv*), followed by their chromosome numbering. Each region was selected and named according to its position in *V. unguiculata* pseudomolecules starting at 0 Mb in alphabetical order. Bars in **a**-**b** = 5 µm and in **c**-**d** = 10 µm ……..48

Figure 2. Circular representation of pseudomolecules (internal) and chromosomes (external) of *Vigna unguiculata* (left side) and *Phaseolus vulgaris* (right side) showing the position of oligo barcode, BAC, rDNA and markers. Each chromosome and pseudomolecule start at 0 Mb, indicating its orientation in the present representation. Barcode markers are represented by continuous lines, while the BAC markers by dashed lines. The colour of each chromosome marker was defined in accordance with *V. unguiculata* chromosomes/ pseudomolecules: *Vu*1 (dark blue), *Vu*2 (light green), *Vu*3 (red), *Vu*4 (gold), *Vu*5 (brown), *Vu*6 (purple), *Vu*7 (dark green), *Vu*8 (light pink), *Vu*9 (yellow), *Vu*10 (light blue), *Vu*11 (magenta). DNAr 5S and 35S marks colours were represented by red and green, respectively. Labels of markers that colocalize are separated by "/" and of markers that are adjacent, by "-". The first label represents the marker that is closer to 0 Mb (from right to left in *Vu* and from left to right in *Pv*). The orientation of some pseudomolecules (*Pv*2, *Pv*3, *Pv*4, *Pv*7, *Pv*9, *Pv*10, and *Pv*11)

and chromosomes (*Pv*2, *Pv*3, *Pv*4, *Pv*7, *Pv*9, *Pv*11, and *Vu*5) was inverted for a better visualization of synteny and collinearity ……..49

Figure 3. Circular representation of the chromosomes 1, 5, and 8 of *Vigna unguiculata* (*Vu*) and *Phaseolus vulgaris* (*Pv*), showing the translocation complex among them (a), and the reciprocal translocation between chromosomes 2 and 3 (b) both identified using the oligo barcode and BAC probes. The measurement scale is presented in Mb. Each chromosome starts at 0 Mb, indicating its orientation in the present representation. Barcode markers are represented by continuous lines, while the BAC markers by dashed lines ……50

Figure 4. Circular representation of chromosomes 7 (a) and 9 (b) of *Vigna unguiculata* (*Vu*) and *Phaseolus vulgaris* (*Pv*), both suggesting a centromere repositioning. The measurement scale is presented in Mb. Each chromosome starts at 0 Mb, indicating its orientation in the present representation. Barcode markers are represented by continuous lines, while the BAC markers by dashed lines ……...…….51

Figure 5. Circular representation of chromosomes 4 (a) and 10 (b) of *Vigna unguiculata* (*Vu*) and *Phaseolus vulgaris* (*Pv*), evidencing a pericentric (a), and a paracentric (b) inversion, respectively. The measurement scale is presented in Mb. Each chromosome starts at 0 Mb, indicating its orientation in the present representation. Barcode markers are represented by continuous lines, while the BAC markers by dashed lines ……..…52

MANUSCRITO 2- OLIGO-FISH REVEALS THE SPEED RACE IN *PHASEOLUS* BEANS CHROMOSOME EVOLUTION

Figure 1. Chromosome identification by oligo-FISH barcode, *Pv2* and *Pv3* painting, 5S and 35S rDNA and CentPv1 centromeric repeat in *Phaseolus* species. **(a** and **a')** *P. microcarpus* (*Pmi*), insets in **a** highlight the pericentric inversion in *Pmi2,* the deletion of one red signal in *Pmi3* and small signals in *Pmi4* and *Pmi5*. **(b** and **b')** *P. filiformis*, insets in **b** and **b'** display the small green barcode signal in *Pfi3* and small signals in *Pfi5*, besides of segment of *Pfi3* translocated to *Pfi7,* respectively. **(c** and

c') *P. acutifolius* (*Pac*), insets in **c** show details of *Pac2* and *Pac3*. **(d** and **d')** *P. coccineus* (*Pco*), inserts in **d'** evidence the CentPv1 centromeric signal in *Pco6* co-localized with 5S rDNA locus. **(e** and **e')** *P. vulgaris* 'G19833' (*Pv* 'G19833'), insets in **e'** evidence a small 35S rDNA *locus* in *Pv4*. **(f** and **f')** *P. vulgaris* 'BAT93' (*Pv* 'BAT93'), insets in **f** evidence weak signals in *Pv2*, *4* and *11*, while insert in **f'** amplify the 5S rDNA locus in *Pv10*. **(g** and **g')** *P. dumosus* (*Pdu*), inserts in **g'** highlight smaller 35S rDNA loci. **(h** and **h')** *P. leptostachyus* (*Ple*) with inset in **h** evidencing small signals in *Ple2*. **(i** and **i')** *P. macvaughii* (*Pma*), inserts in **i** display signals of *Pma1*, *2* and *3*. **(j** and **j')** *P. lunatus* (*Plu*), insert in **j** evidences a small green signal in *Plu8*. Bar corresponds to 5 µm ……..78

Figure 2. Karyograms of the nine analysed *Phaseolus* species and two *P. vulgaris* accessions plotted in a phylogenetic tree. For each species, the upper lane shows the barcode signals in green and red, and the bottom lane shows the *Pv*2 (green) and *Pv*3 (red) painting probes, as well as the 5S (yellow) and 35S (purple) rDNA probes. For *P. coccineus*, *P. dumosus* and *P. vulgaris*, CentPv1 probe (blue) is present in the centromeric region of some chromosome pairs. The chromosomes are ordered according to putative orthology to *P. vulgaris*, with centromere aligned by a dotted white line. The arrowheads point to differences in the barcode or painting pattern in comparison to *P. vulgaris* ……*89*

Figure 3. Schematic representation of *Phaseolus* karyotypes based on the distribution of oligo-FISH barcode signals (green and red dots), painting (green and red segments for *Pv2* and *Pv3*, respectively), 5S (yellow dots) and 35S (purple segments) rDNA loci and CentPv1 (blue segments at centromeric regions of *P. coccineus, P. dumosus and P. vulgaris*). Vertical arrows in different directions represent inversions (except for the indication of the hybrid origin of *P. dumosus*), Tr translocations, while NCF represents Nested Chromosome Fusion; minus signs represent deletions, while plus signs represent duplications of signals. Exclusive rDNA sites are indicated with black dots. Independent and shared rearrangements are indicated in the nodes and clades of the dated phylogenetic tree. Rearrangements in rDNA loci are represented in blue and rearrangements detected by oligo-FISH probes in red. All codes are preceded by the occurrence number and followed by the respective rearranged ortholog. In the right side, numbers after G and R letters represent the total number of barcode green and red signals, respectively ……80

Figure 4. Schematic representation of the complex translocation involving chromosomes 1, 3 and 7 of *P. filiformis*. *Pfi*1 probably received a segment from *Pfi*7 containing one barcode red signal and donated a segment to *Pfi*3 containing one barcode green signal. *Pfi*3 donated a segment to *Pfi*7 detected by the red painting probe …….....81

Figure S1. *P. leptostachyus* zygotene exhibiting more than one 5S rDNA loci ……82

Figure S2. Phylogenetic tree based on the circular plastidial contigs ……...83

LISTA DE TABELAS

MANUSCRITO 1- OLIGO-FISH BARCODE IN BEANS: A NEW CHROMOSOME IDENTIFICATION SYSTEM

Table S1. Genomic positions of oligo barcode and BAC markers in the reference genome of *Vigna unguiculata* (*Vu*) showing the scores of BLAST search, as well as the positions in bp. a Total size and centromere regions by Lonardi et al. (2019). b BACs from V. unguiculata were previous used by Oliveira et al. (2020) and Martins et al. (2021) and are available at HarvEST:cowpea (harvest.ucr.edu). The colour of each chromosome marker was defined in accordance with Fig. 2 description …….....52

Table S2. Genomic positions of oligo barcode and BAC markers in the reference genome of *Phaseolus vulgaris* (*Pv*) showing the scores of BLAST search, as well as the positions in bp. Genomic positions of oligo barcode and BAC markers in the reference genome of Phaseolus vulgaris (Pv) showing the scores of BLAST search, as well as the positions in bp. a Total size and centromere regions by Schmutz et al. (2014). c Gene markers ID and accessions for BAC sequences available at NCBI GenBank and EMBL-EBI. The colour of each chromosome marker was defined in accordance with Fig. 2 description ……..……....52

Table S3. Chromosome positions of oligo barcode and BAC markers on *Vigna unguiculata* idiogram. Total chromosome size and position of centromere in bp are also

indicated. The colour of each chromosome marker was defined in accordance with Fig. 2 description …….....52

Table S4. Chromosome positions of oligo barcode and BAC markers on *Phaseolus vulgaris* idiogram. Total chromosome size and position of centromere in bp are also indicated. The colour of each chromosome marker was defined in accordance with Fig. 2 description …...……52

MANUSCRITO 2- OLIGO-FISH REVEALS THE SPEED RACE IN *PHASEOLUS* BEANS CHROMOSOME EVOLUTION

Table 1. Summary of the chromosomal rearrangement number and type, ages (in My) of each clade and their respective chromosomal evolution rates calculated separately for structural rearrangements (CE) and changes in rDNA (CErDNA)…….....75

Table S1. Accessions of sequencing data deposited in GenBank …….84

SUMÁRIO

1. APRESENTAÇÃO 14

2. FUNDAMENTAÇÃO TEÓRICA 16

2.1. O gênero *Phaseolus* L. 16

2.2. Estudos citogenéticos em *Phaseolus* L. 16

2.3. Oligo-FISH 18

REFERÊNCIAS BIBLIOGRÁFICAS 19

3. ARTIGO 1 25

4. ARTIGO 2 53

5. CONCLUSÕES 85

6. ANEXOS 86

6.1. Regras para submissão no periódico Theoretical and Appplied Genetics 86

6.2. Regras para submissão no periódico The Plant Journal 87

1. APRESENTAÇÃO

A citogenética foi fortemente impactada pelos avanços do sequenciamento de nova geração (do inglês, *Next Generation Sequencing* - NGS) e da bioinformática nos últimos anos. As plataformas NGS possibilitaram o sequenciamento de um maior número de genomas, o que, aliado ao desenvolvimento de novas ferramentas, proporcionaram uma abordagem ainda mais sofisticada à citogenética (CHÈVRE et al., 2018). O sequenciamento NGS possibilitou, por exemplo, a identificação de uma enorme quantidade de sequências de DNA cópia única, úteis para a distinção de cromossomos individuais e para comparação entre genomas de forma ainda mais detalhada. Atualmente, essas sequências podem ser usadas na técnica de Hibridização *in situ* Fluorescente (do inglês, *Fluorescent In Situ Hibridization* - FISH) por meio da síntese de sondas oligonucleotídicas (oligo-FISH) direcionadas a regiões de interesse (JIANG, 2019). O feijão comum, *Phaseolus vulgaris*, foi uma das muitas espécies de plantas que teve seu genoma completo sequenciado a partir de técnicas NGS (SCHMUTZ et al., 2014), permitindo não apenas a sua melhor caracterização, mas também de seu gênero.

O gênero *Phaseolus* L. compreende cerca de 90 espécies (POWO, 2021) com idade estimada entre 6 e 8 milhões de anos (Ma), separadas em dois clados principais (clado A e B), os quais são subdivididos em oito grupos. Algumas de suas espécies possuem elevado potencial econômico e valor nutricional, a exemplo de *P. vulgaris* L. (feijão comum) e *P. lunatus* L. (fava), ambas pertencentes ao clado B e aos grupos Vulgaris e Lunatus, respectivamente. (DELGADO-SALINAS; BIBLER; LAVIN, 2006).

Caracterizações citogenéticas de espécies do gênero vêm sendo realizadas e têm revelado informações relevantes para a compreensão de sua evolução. As espécies se caracterizam como exclusivamente diploides ($2n = 22$) e relativamente estáveis, com exceção das espécies que compõem o grupo Leptostachyus (FONSÊCA; PEDROSA-HARAND, 2017). Estas apresentam um número reduzido de cromossomos ($2n = 20$) proveniente de disploidia, associada a uma variedade de eventos de rearranjos cromossômicos, como inserção cêntrica, translocações e inversões (FONSÊCA; FERRAZ; PEDROSA-HARAND, 2016).

Estudos de BAC-FISH permitiram a construção de mapas citogenéticos para *P. vulgaris* (FONSÊCA et al., 2010), *P. lunatus* (BONIFÁCIO et al., 2012), *P. macvaughii* (FERRAZ; FONSÊCA; PEDROSA-HARAND, 2020) e *P. microcarpus* Mart. (FONSÊCA; PEDROSA-HARAND, 2013), bem como o reconhecimento de múltiplos rearranjos em *P. leptostachyus* (FONSÊCA; FERRAZ; PEDROSA-HARAND, 2016). No entanto, ainda há dúvidas sobre a origem e dinâmica desses rearranjos e se esses eventos são restritos a esse grupo. Isso porque a

técnica de BAC-FISH permite o mapeamento de uma ou duas sequências únicas por vez, dificultando o reconhecimento simultâneo de todos os pares cromossômicos. Por isso, o mapeamento do conjunto cromossômico de uma espécie é bastante laborioso, levando a um número reduzido de espécies mapeadas até então. Uma vez que o cariótipo de *P. leptostachyus* apresentou várias translocações e inversões, além da inserção cêntrica, não foi possível estabelecer um mapa citogenético para essa espécie usando BAC-FISH apenas, o que impossibilita uma avaliação mais precisa sobre o número de rearranjos e sua taxa de evolução em comparação aos outros clados.

O sequenciamento do genoma de *P. vulgaris* (SCHMUTZ et al., 2014; VLASOVA et al., 2016) e de espécies próximas como *Vigna unguiculata* [L.] Walp. (LONARDI et al., 2019), no entanto, tem possibilitado o desenvolvimento de novas ferramentas para investigar a evolução de *Phaseolus* e gêneros próximos, como sondas oligonucleotídicas que permitem o reconhecimento dos cromossomos de forma mais eficiente (DO VALE MARTINS *et al.*, 2021). Sendo assim, dispomos agora de ferramentas que nos possibilitam responder a diversas perguntas, como: 1) Quantos e quais rearranjos moldaram o cariótipo de *P. leptostachyus*? 2) Os rearranjos presentes em *P. leptostachyus* são compartilhados com outras espécies do gênero? 3) Quão acelerada é a taxa de evolução de *P. leptostachyus* em comparação às outras linhagens?

O presente trabalho teve como objetivo analisar a evolução cromossômica de uma amostragem ampliada do gênero *Phaseolus* por meio do mapeamento comparativo com o sistema de identificação oligo-FISH *barcode* e pintura cromossômica. Para isso, um sistema de oligo-FISH *barcode* foi desenvolvido para o feijão comum no Capítulo 1 e utilizado em conjunto com outras sondas em dez acessos de *Phaseolus* no Capítulo 2. Além disso, o presente trabalho forneceu o arcabouço citogenético para futuros estudos genômicos que pretendem investigar a origem da reorganização genômica do grupo Leptostachyus.

2. FUNDAMENTAÇÃO TEÓRICA

2.1. O gênero *Phaseolus* L.

O gênero *Phaseolus* L. pertence à família Leguminosae L. (Fabaceae), a qual se caracteriza como a terceira maior família dentro das angiospermas, sendo superada apenas pelas famílias Orchidaceae Juss. e Asteraceae L. Possui cerca de 90 espécies, com ampla distribuição entre o sudoeste canadense e o norte argentino, com a maior parte de sua diversidade concentrada no México (BROUGHTON et al., 2003; LEWIS et al., 2005; MERCADO-RUARO; DELGADO-SALINAS; CHIANG, 2009; POWO, 2021).

Utilizando as regiões ITS com o DNA ribossomal nuclear 5,8S e o loco *trn*K como marcadores filogenéticos, o gênero foi dividido em dois clados monofiléticos principais (A e B) subdivididos em oito agrupamentos designados como grupos, além de algumas espécies de posicionamento incerto: *Phaseolus glabellus* Piper., *P. macrolepis* Piper., *P. microcarpus* Mart. e *P. oaxacanus* Rose. O gênero foi datado em cerca de 6 a 8 milhões de anos (Ma), de acordo com a taxa de substituição presente nas sequências dos dois marcadores, sendo o grupo Vulgaris o mais antigo (1,8-3,9 Ma) e os grupos Filiformis, Pedicellatus e Polystachius os mais recentes, com cerca de 1 Ma. O grupo Leptostachyus composto por três espécies (*P. macvaughii*, *P. micranthus* e *P. leptostachyus*) tem idade estimada entre 1,7-3,4 Ma (DELGADO-SALINAS et al., 2006).

O gênero apresenta espécies com significativo potencial alimentício e econômico. Há milênios tem sido parte essencial da alimentação humana, com eficácia na complementação proteica e vitamínica. Também se mostra adaptável a diferentes nichos e com alto grau de diversificação (BROUGHTON et al., 2003). De acordo com dados da FAO (*Food and Agricultural Organization*), somente no Brasil, a produção de grãos de *Phaseolus* em 2018 chegou a cerca de 2,9 milhões de toneladas. Por esses motivos, vem sendo alvo de vários estudos de importância agronômica e biológica.

2.2. Estudos citogenéticos em *Phaseolus* L.

Um dos primeiros estudos sobre a organização dos cromossomos em espécies do gênero foi o desenvolvido por Karpechenko (1925), tendo como principal resultado a identificação do número cromossômico $2n = 22$ para algumas espécies do clado B, como: *P. coccineus* L., *P.vulgaris* L., *P. acutifolius* A. Gray. e *P. lunatus* L. Posteriormente, estudos mostraram que

outras espécies, em especial aquelas pertencentes ao grupo Leptostachyus, possuíam o conjunto haploide reduzido, com *n* = 10, passando assim a serem consideradas disploides e parte de um mesmo clado (MERCADO-RUARO; DELGADO-SALINAS, 1996, 1998).

Por meio do uso de corantes fluorescentes como a cromomicina A3 (CMA) e o 4',6'-diamino-2-fenil-indol (DAPI) aliados à FISH com sondas de DNAr 5S e 35S (18S-5.8S-25S), tornou-se possível a observação de padrões de bandas que diferiam em distribuição e quantidade entre cultivares de *P. vulgaris*, além de revelar provável ortologia entre cromossomos de *P. vulgaris* e *P. coccineus*, bem como entre os de *P acutifolius* e *P. lunatus* (MOSCONE et al., 1999). Também foi observada a prevalência de pelo menos um par de cromossomos com a região terminal marcada por uma banda CMA+ em espécies como *P. vulgaris* (FONSÊCA et al., 2010), *P. lunatus* (BONIFÁCIO et al., 2012) e *P. leptostachyus* (FONSÊCA; FERRAZ; PEDROSA-HARAND, 2016). O bandeamento CMA/DAPI corroborou o posicionamento de *P. microcarpus* no clado A, pois a espécie apresentou fraca marcação CMA+ na região pericentromérica de apenas seis pares cromossômicos, padrão este diferente das espécies analisadas do clado B (FONSÊCA; PEDROSA-HARAND, 2013).

Adicionalmente, marcadores moleculares de mapas de ligação do feijão comum (FREYRE et al., 1998; HOUGAARD et al., 2008; VALLEJOS; SAKIYAMA; CHASE, 1992) foram utilizados para selecionar Cromossomos Artificiais de Bactérias (do inglês, *Bacterial Artificial Chromosomes* - BACs), passando a ser largamente usados como sondas cromossomo-específicas na identificação cromossômica e no mapeamento comparativo entre as espécies, a exemplo de *P. lunatus* (BONIFÁCIO et al., 2012) e *P. microcarpus* (FONSÊCA; PEDROSA-HARAND, 2013), além de serem transferíveis para espécies do gênero irmão *Vigna* Savi, como *Vigna unguiculata* (L.) Walp. (VASCONCELOS et al., 2015) e *V. aconitifolia* (Jacq.) Marechal (OLIVEIRA et al., 2020). O uso de BAC-FISH nessas espécies permitiu identificar inversões e translocações entre alguns cromossomos, como entre os cromossomos 2 e 3 de *Phaseolus* e *Vigna*, que além de translocação entre os dois gêneros, apresentou diferentes inversões em várias espécies. No entanto, não foi possível mapear todos os cromossomos dos complementos, como o cromossomo 5, cuja marca de *P. vulgaris* não apresentou sinal em nenhuma outra espécie. Desse modo, a identificação de todos os cromossomos em um número maior de espécies seria útil para identificar possíveis rearranjos adicionais.

Espécies pertencentes ao grupo Leptostachyus, quando submetidas a BAC-FISH, apresentaram uma grande quantidade de rearranjos cromossômicos observados em quase todos os pares, como uma inserção cêntrica e translocações, detectadas pela primeira vez no gênero, além de inversões paracêntricas e pericêntricas. Das três espécies pertencentes ao grupo, duas

espécies foram analisadas, *P. leptostachyus* , com maior número de rearranjos, porém não elucidados devido às limitações da técnica de BAC-FISH (FONSÊCA; FERRAZ; PEDROSA-HARAND, 2016) e *P. macvaughii* , com bem menos rearranjos em comparação com *P. leptostachyus* (FERRAZ; FONSÊCA; PEDROSA-HARAND, 2020). Esses estudos apontam para a hipótese de que houve uma alta taxa de evolução cariotípica em *P. leptostachyus*, com grande acúmulo de rearranjos, porém quantos e quais foram esses rearranjos não está claro, pois os cromossomos envolvidos não puderam ser identificados.

Sequências repetitivas como DNAs satélites já foram mapeadas em espécies do gênero, a exemplo de CentPv1 (também conhecido como Nazca) e do CentPv2, ambos localizados na região centromérica dos cromossomos de *P. vulgaris* e distribuídos em dois conjuntos cromossômicos distintos, o que sugere uma evolução independente para ambas as sequências (IWATA et al., 2013). Outros satélites localizados nas regiões pericentroméricas e subteloméricas também foram estudados no gênero: como o satélite CC4, similar a regiões intergênicas do DNAr 35S, que se tornou um DNA satélite independente no grupo Vulgaris (ALMEIDA et al., 2012) e *khipu*, um satélite associado a genes de resistência que constitui parte da heterocromatina subtelomérica de *Phaseolus vulgaris* (RIBEIRO et al., 2017). Em estudo posterior, Ribeiro et al., (2020) identificaram e analisaram retroelementos do tipo LTR (do inglês, *Long Terminal Repeats*) e um conjunto de DNAs satélites (*Pac*SAT363, *Pco*SAT339 e *Pco*SAT36) em *P. vulgaris*, *P. acutifolius e P. coccineus,* localizados principalmente nas regiões centroméricas/pericentroméricas e subterminais, mostrando assim a heterogeneidade e rápida evolução desses sítios nessas espécies. Alguns dos satélites descritos acima como *khipu* e CentPv puderam ser detectados na técnica de hibridização *in situ* por meio de sondas oligonucleotídicas, o que permitiu detectar variantes dessas sequencias em alguns cromossomos, sendo uteis em sua caracterização.

2.3. Oligo-FISH

Os primeiros experimentos de FISH utilizando oligonucleotídeos se baseavam no uso de repetições de sequências simples (do inglês, *Simple Sequence Repeats* - SSRs) empregadas como sondas para identificação cromossômica em várias espécies de plantas. Em seguida, oligonucleotídeos específicos para sequências de DNA satélite e outras repetições em tandem maiores passaram a ser utilizados como sondas, trazendo uma maior praticidade na obtenção das sondas para FISH, que antes dependiam de clonagem ou PCR. Atualmente, regiões cromossômicas específicas ou cromossomos inteiros podem ser selecionados e sintetizados em

conjuntos de oligos, marcados e utilizados como sondas para discriminar essas regiões por oligo-FISH (JIANG, 2019). Como a maioria dos grupos vegetais contam, quando muito, com apenas um genoma de referência, e *Phaseolus* possui apenas 4 espécies com genoma montados, a oligo-FISH permite a comparação entre espécies a partir do desenvolvimento de sonda do genoma montado e utilização das mesmas nas espécies relacionadas não sequenciadas.

O primeiro trabalho com o uso de oligo-FISH para a pintura de cromossomos em plantas foi realizado por HAN et al. (2015). Nesse estudo, foram desenvolvidas sondas (com cerca de 25.000 oligos cada) para a pintura dos cromossomos 3 e 7 de *Cucumis sativus* L., o pepino. Além de identificá-los, a análise foi estendida para outras espécies do gênero, incluindo poliploides e híbridos interespecíficos. Em seguida, estudos com alterações da técnica foram replicados para outras espécies como o morango (*Fragaria vesca* Benth.; QU et al., 2017), espécies do gênero *Populus* L. (XIN et al., 2019), banana (*Musa* spp.; ŠIMONÍKOVÁ et al., 2019) , trigo (*Triticum aestivum* L.; SONG et al., 2020) e no feijão comum (*Phaseolus vulgaris* L.; DO VALE MARTINS et al., 2021).

Em 2018, BRAZ et al. estabeleceram a oligo-FISH *barcode*, um novo sistema de identificação cromossômica. Dois conjuntos de cerca de 27.000 oligonucleotídeos cada foram distribuídos em 13 sinais visualizados em verde e 13 em vermelho, permitindo, em conjunto, identificar de forma única cada par cromossômico de espécies do gênero *Solanum* L., como a batata cultivada (*Solanum tuberosum* L.), além de permitir a identificação de cromossomos ortólogos em espécies relativamente distantes como a batata (*Solanum etuberosum* L.) e a beringela (*Solanum melongena* L.), desde que esses genomas apresentem poucos rearranjos entre si. Desde então, outros estudos com o uso da oligo-FISH *barcode* em plantas têm sido reportados, como em espécies de milho (*Zea* spp.; BRAZ et al., 2020), arroz (*Oryza* spp.; LIU et al., 2020), cana de açúcar (PIPERIDIS; D'HONT, 2020) e, mais recentemente, como parte desse trabalho, foi desenvolvido o primeiro sistema oligo-FISH *barcode* para leguminosas com base no genoma de *Vigna unguiculata* e *Phaseolus vulgaris*, todos com resultados promissores para o entendimento da evolução cromossômica.

REFERÊNCIAS BIBLIOGRÁFICAS

ALMEIDA, Cícero; FONSÊCA, Artur; DOS SANTOS, Karla Galvão Bezerra; MOSIOLEK, Magdalena; PEDROSA-HARAND, Andrea. Contrasting evolution of a satellite DNA and its ancestral IGS rDNA in *Phaseolus* (Fabaceae). **Genome / National Research Council**

Canada = Génome / Conseil national de recherches Canada, *[S. l.]*, v. 55, n. 9, p. 683–689, 2012. DOI: 10.1139/g2012-059. Acesso em 10 jun.

BONIFÁCIO, Eliene Mariano; FONSÊCA, Artur; ALMEIDA, Cícero; DOS SANTOS, Karla G. B.; PEDROSA-HARAND, Andrea. Comparative cytogenetic mapping between the lima 14 bean (*Phaseolus lunatus* L.) and the common bean (*P. vulgaris* L.). **Theoretical and Applied Genetics**, *[S. l.]*, v. 124, n. 8, p. 1513–1520, 2012. DOI: 10.1007/s00122-012-1806-x. Acesso em: 10 jun. 2021.

BRAZ, Guilherme T.; DO VALE MARTINS, Lívia; ZHANG, Tao; ALBERT, Patrice S.; BIRCHLER, James A.; JIANG, Jiming. A universal chromosome identification system for maize and wild *Zea* species. **Chromosome Research**, *[S. l.]*, v. 28, n. 2, p. 183–194, 2020. DOI: 10.1007/s10577-020-09630-5. Acesso em: 10 jun. 2021.

BRAZ, Guilherme T.; HE, Li; ZHAO, Hainan; ZHANG, Tao; SEMRAU, Kassandra; ROUILLARD, Jean-Marie; TORRES, Giovana A.; JIANG, Jiming. Comparative Oligo-FISH Mapping: An Efficient and Powerful Methodology To Reveal Karyotypic and Chromosomal Evolution. **Genetics**, *[S. l.]*, v. 208, n. 2, p. 513–523, 2018. DOI: 10.1534/genetics.117.300344. Acesso em: 11 jun. 2021.

BROUGHTON, W. J.; HERN; AACUTE; NDEZ, G.; BLAIR, M.; BEEBE, S.; GEPTS, P.; VANDERLEYDEN, J. Beans (*Phaseolus* spp.) - model food legumes. **Plant and Soil**, *[S. l.]*, v. 252, n. 1, p. 55–128, 2003. Acesso em: 12 jun. 2021.

CHÈVRE, Anne-Marie; MASON, Annaliese S.; CORITON, Olivier; GRANDONT, Laurie; JENCZEWSKI, Eric; LYSAK, Martin A. Cytogenetics, a Science Linking Genomics and Breeding: The *Brassica* Model. *In*: LIU, Shengyi; SNOWDON, Rod; CHALHOUB, Boulos (org.). **The *Brassica napus* Genome**. Compendium of Plant GenomesCham: Springer International Publishing, 2018. p. 21–39. DOI: 10.1007/978-3-319-43694-4_2. Acesso em: 13 jun. 2021.

DELGADO-SALINAS, Alfonso; BIBLER, Ryan; LAVIN, Matt. Phylogeny of the Genus *Phaseolus* (Leguminosae): A Recent Diversification in an Ancient Landscape. **Systematic Botany**, *[S. l.]*, v. 31, n. 4, p. 779–791, 2006. DOI: 10.1600/036364406779695960. Acesso em 15 jun. 2021.

DO VALE MARTINS, L. et al. BAC- and oligo-FISH mapping reveals chromosome evolution among *Vigna angularis*, *V. unguiculata*, and *Phaseolus vulgaris*. **Chromosoma**, 28 set.

2021. v. 130, n. 2–3, p. 133–147. DOI: 10.1007/s00412-021-00758-9. Acesso em 28 set. 2021.

FERRAZ, M. E.; FONSÊCA, A.; PEDROSA-HARAND, A. Multiple and independent rearrangements revealed by comparative cytogenetic mapping in the dysploid Leptostachyus group (*Phaseolus* L., Leguminosae). **Chromosome Research**, 2020. v. 28, n. 3–4, p. 395–405. DOI: 10.1007/s10577-020-09644-z. Acesso em 20 dez. 2020.

FONSÊCA, Artur et al. Cytogenetic map of common bean (*Phaseolus vulgaris* L.). **Chromosome Research**, *[S. l.]*, v. 18, n. 4, p. 487–502, 2010. DOI: 10.1007/s10577-010-9129-8. Acesso em 25 jun. 2020.

FONSÊCA, Artur; FERRAZ, Maria Eduarda; PEDROSA-HARAND, Andrea. Speeding up chromosome evolution in *Phaseolus*: multiple rearrangements associated with a one-step descending dysploidy. **Chromosoma**, *[S. l.]*, v. 125, n. 3, p. 413–421, 2016. DOI: 10.1007/s00412-015-0548-3 Acesso em: 16 jun. 2020.

FONSÊCA, Artur; PEDROSA-HARAND, Andrea. Karyotype stability in the genus *Phaseolus* evidenced by the comparative mapping of the wild species *Phaseolus microcarpus*. **Genome**, *[S. l.]*, v. 56, n. 6, p. 335–343, 2013. DOI: 10.1139/gen-2013-0025. Acesso em: 16 jun. 2020.

FONSÊCA, Artur; PEDROSA-HARAND, Andrea. Cytogenetics and Comparative Analysis of *Phaseolus* Species. *In*: PÉREZ DE LA VEGA, Marcelino; SANTALLA, Marta; MARSOLAIS, Frédéric (org.). **The common bean genome**. Compendium of Plant Genomes: Springer International Publishing, 2017. p. 57–68. DOI: 10.1007/978-3-319-63526-2_3. Acesso em: 17 jun. 2020.

FREYRE, R. et al. Towards an integrated linkage map of common bean. Development of a core linkage map and alignment of RFLP maps. **Theoretical and Applied Genetics**, *[S. l.]*, v. 97, n. 5–6, p. 847–856, 1998. DOI: 10.1007/s001220050964. Acesso em: 17 jun. 2020.

HAN, Yonghua; ZHANG, Tao; THAMMAPICHAI, Paradee; WENG, Yiqun; JIANG, Jiming. Chromosome-Specific Painting in *Cucumis* Species Using Bulked Oligonucleotides. **Genetics**, *[S. l.]*, v. 200, n. 3, p. 771–779, 2015. DOI: 10.1534/genetics.115.177642. Acesso em: 18 jun. 2020.

HOUGAARD, Birgit Kristine et al. Legume anchor markers link syntenic regions between *Phaseolus vulgaris, Lotus japonicus, Medicago truncatula* and *Arachis*. **Genetics**, *[S. l.]*,

v. 179, n. 4, p. 2299–2312, 2008. DOI: 10.1534/genetics.108.090084. Acesso em 30 mar. 2020

IWATA, Aiko et al. Identification and characterization of functional centromeres of the common bean. **Plant Journal**, *[S. l.]*, v. 76, n. 1, p. 47–60, 2013. DOI: 10.1111/tpj.12269. Acesso em 15 mar. 2020.

JIANG, Jiming. Fluorescence *in situ* hybridization in plants: recent developments and future applications. **Chromosome Research**, *[S. l.]*, v. 27, n. 3, p. 153–165, 2019. DOI: 10.1007/s10577-019-09607-z. Acesso em 25 abr. 2021.

KARPECHENKO, G. D. On the chromosomes of the Phaseolineae. **Bull. Appl. Bot and Plant Breeding**, *[S. l.]*, v. 14, p. 143–148, 1925.

LEWIS, Gwilym; SCHRIRE, Brian; MACKINDER, Barbara; LOCK, Mike. **Legumes of the world**. 1 ed. London, UK: Royal Botanic Garden, Kew, 2005.

LIU, Xiaoyu et al. Dual-color oligo-FISH can reveal chromosomal variations and evolution in *Oryza* species. **Plant Journal**, *[S. l.]*, v. 101, n. 1, p. 112–121, 2020. DOI: 10.1111/tpj.14522. Acesso em 17 de mai. 2021.

LONARDI, Stefano et al. The genome of cowpea (*Vigna unguiculata* [L.] Walp.). **Plant Journal**, *[S. l.]*, v. 98, n. 5, p. 767–782, 2019. DOI: 10.1111/tpj.14349. Acesso em 23 jun. 2020.

MERCADO-RUARO, Pedro; DELGADO-SALINAS, Alfonso. Karyological studies in several Mexican species of *Phaseolus* L. and *Vigna* Savi (Phaseolinae, Fabaceae). *In*: **Advances in legume systematics 8, Legumes of economic importance**. [s.l.] : Royal Botanic Gardens, Kew., 1996. p. 83–87.

MERCADO-RUARO, Pedro; DELGADO-SALINAS, Alfonso. Karyotypic studies on species of *Phaseolus* (Fabaceae: Phaseolinae). **American Journal of Botany**, *[S. l.]*, v. 85, n. 1, p. 1–9, 1998. DOI: 10.2307/2446547. Acesso em: 21 jun. 2020.

MERCADO-RUARO, Pedro; DELGADO-SALINAS, Alfonso; CHIANG, Fernando. Taxonomic re-assessment of *Phaseolus* dasycarpus (Leguminosae): Systematic position, chromosome studies and re-description. **Brittonia**, *[S. l.]*, v. 61, n. 1, p. 8–13, 2009. DOI: 10.1007/s12228-008-9048-6. Acesso em: 21 jun. 2020.

MOSCONE, Eduardo A.; KLEIN, Franz; LAMBROU, Maria; FUCHS, Jörg; SCHWEIZER, Dieter. Quantitative karyotyping and dual-color FISH mapping of 5S and 18S-25S rDNA probes in the cultivated *Phaseolus* species (Leguminosae). **Genome**, *[S. l.]*, v. 42, n. 6, p. 1224–1233, 1999. DOI: 10.1139/g99-070. Acesso em 30 mar. 2020.

OLIVEIRA, Ana Rafaela da S.; MARTINS, Lívia do Vale; BUSTAMANTE, Fernanda De O.; MUÑOZ-AMATRIAÍN, María; CLOSE, Timothy; DA COSTA, Antônio F.; BENKO-ISEPPON, Ana Maria; PEDROSA-HARAND, Andrea; BRASILEIRO-VIDAL, Ana Christina. Breaks of macrosynteny and collinearity among moth bean (*Vigna aconitifolia*), cowpea (*V. unguiculata*), and common bean (*Phaseolus vulgaris*). **Chromosome Research**, [S. l.], 2020. DOI: 10.1007/s10577-020-09635-0. Acesso em: 25 jul. 2020.

PIPERIDIS, N.; D'HONT, A. Sugarcane genome architecture decrypted with chromosome-specific oligo probes. **The Plant Journal**, 12 set. 2020. v. 103, n. 6, p. 2039–2051. DOI: 10.1111/tpj.14881. Acesso em: 24 nov. 2021

POWO.Plants of the World Online. Jardim Botânico Real, Kew, 2021. Disponivel em: http://www.plantsoftheworldonline.org/. Acesso em: 14 dez. 2021

QU, Manman; LI, Kunpeng; HAN, Yanli; CHEN, Lei; LI, Zongyun; HAN, Yonghua. Integrated Karyotyping of Woodland Strawberry (*Fragaria vesca*) with Oligopaint FISH Probes. **Cytogenetic and Genome Research**, *[S. l.]*, v. 153, n. 3, p. 158–164, 2017. DOI: 10.1159/000485283. Acesso em: 22 jun. 2020.

RIBEIRO, Tiago; DOS SANTOS, Karla G. B.; RICHARD, Manon M. S.; SÉVIGNAC, Mireille; THAREAU, Vincent; GEFFROY, Valérie; PEDROSA-HARAND, Andrea. Evolutionary dynamics of satellite DNA repeats from *Phaseolus* beans. **Protoplasma**, *[S. l.]*, v. 254, n. 2, p. 791–801, 2017. DOI: 10.1007/s00709-016-0993-8. Acesso em: 22 jun. 2020.

RIBEIRO, Tiago; VASCONCELOS, Emanuelle; DOS SANTOS, Karla G. B.; VAIO, Magdalena; BRASILEIRO-VIDAL, Ana Christina; PEDROSA-HARAND, Andrea. Diversity of repetitive sequences within compact genomes of *Phaseolus* L. beans and allied genera *Cajanus* L. and *Vigna* Savi. **Chromosome Research**, *[S. l.]*, v. 28, n. 2, p. 139–153, 2020. DOI: 10.1007/s10577-019-09618-w.Acesso: 25 jul.2020

SCHMUTZ, Jeremy et al. A reference genome for common bean and genome-wide analysis of dual domestications. **Nature Genetics**, *[S. l.]*, v. 46, n. 7, p. 707–713, 2014. DOI: 10.1038/ng.3008. Acesso em: 22 jun. 2020.

ŠIMONÍKOVÁ, Denisa; NĚMEČKOVÁ, Alžbeěta; KARAFIÁTOVÁ, Miroslava; UWIMANA, Brigitte; SWENNEN, Rony; DOLEŽEL, Jaroslav; HŘIBOVÁ, Eva. Chromosome Painting Facilitates Anchoring Reference Genome Sequence to Chromosomes *In Situ* and Integrated Karyotyping in Banana (*Musa* Spp.). **Frontiers in Plant Science**, *[S. l.]*, v. 10, n. November, p. 1–12, 2019. DOI: 10.3389/fpls.2019.01503.

SONG, Xinying et al. Development and application of oligonucleotide-based chromosome painting for chromosome 4D of *Triticum aestivum* L. **Chromosome Research**, *[S. l.]*, v. 28, n. 2, p. 171–182, 2020. DOI: 10.1007/s10577-020-09627-0. Acesso em: 24 jun. 2020.

VALLEJOS, C. E.; SAKIYAMA, N. S.; CHASE, C. D. A molecular marker-based linkage map of *Phaseolus vulgaris* L. **Genetics**, *[S. l.]*, v. 131, n. 3, p. 733–740, 1992.

VASCONCELOS, Emanuelle Varão; DE ANDRADE FONSÊCA, Artur Fellipe; PEDROSA-HARAND, Andrea; DE ANDRADE BORTOLETI, Kyria Cilene; BENKO-ISEPPON, Ana Maria; DA COSTA, Antônio Félix; BRASILEIRO-VIDAL, Ana Christina. Intra- and interchromosomal rearrangements between cowpea [*Vigna unguiculata* (L.) Walp.] and common bean (*Phaseolus vulgaris* L.) revealed by BAC-FISH. **Chromosome Research**, *[S. l.]*, v. 23, n. 2, p. 253–266, 2015. DOI: 10.1007/s10577-014-9464-2. Acesso em 02 mar. 2020.

VLASOVA, Anna et al. Genome and transcriptome analysis of the Mesoamerican common bean and the role of gene duplications in establishing tissue and temporal specialization of genes. **Genome Biology**, *[S. l.]*, v. 17, n. 1, p. 1–18, 2016. DOI: 10.1186/s13059-016-0883-6. Acesso em: 25 jun. 2020.

XIN, Haoyang; ZHANG, Tao; WU, Yufeng; ZHANG, Wenli; ZHANG, Pingdong; XI, Mengli; JIANG, Jiming. An extraordinarily stable karyotype of the woody *Populus* species revealed by chromosome painting. **The Plant Journal**, *[S. l.]*, v. 101, n. 2, p. 253–264, 2019. DOI: 10.1111/tpj.14536. Acesso em: 29 jun. 2020.

3. ARTIGO 1

Artigo publicado no periódico *Theoretical and Applied Genetics*

doi:10.1007/s00122-021-03921-z

Primeira autoria compartilhada

Oligo-FISH barcode in beans: a new chromosome identification system

Fernanda de Oliveira Bustamante[1, 2§], Thiago Henrique do Nascimento[3§], Claudio Montenegro[3], Sibelle Dias[1], Lívia do Vale Martins[1,4], Guilherme Tomaz Braz[5], Ana Maria Benko-Iseppon[1], Jiming Jiang[5, 6], Andrea Pedrosa-Harand[3✉], Ana Christina Brasileiro-Vidal[1✉]

[1]Departamento de Genética, Universidade Federal de Pernambuco, Recife, PE, Brazil
[2]Universidade do Estado de Minas Gerais, Unidade Divinópolis, MG, Brazil (Present address)
[3]Departamento de Botânica, Universidade Federal de Pernambuco, Recife, PE, Brazil
[4]Departamento de Biologia, Universidade Federal do Piauí, Teresina, PI, Brazil (Present address)
[5]Department of Plant Biology, Michigan State University, East Lansing, MI, USA
[6]Department of Horticulture, Michigan State University, East Lansing, MI 48824, USA

✉ For correspondence (e-mail: ana.vidal@ufpe.br; andrea.harand@ufpe.br).
§These authors contributed equally to this work.

Fernanda de Oliveira Bustamante - ORCID: 0000-0002-2826-5217
Thiago Henrique do Nascimento - ORCID: 0000-0002-7742-0260
Claudio César Montenegro Júnior - ORCID: 0000-0003-2089-1608
Sibelle Dias - ORCID: 0000-0002-1677-6677
Lívia do Vale Martins - ORCID: 0000-0003-4645-9055
Guilherme Tomaz Braz - ORCID: 0000-0002-0803-7778
Ana Maria Benko-Iseppon - ORCID: 0000-0002-0575-3197
Jiming Jiang – ORCID: 0000-0002-6435-6140
Andrea Pedrosa-Harand - ORCID: 0000-0001-5213-4770

Ana Christina Brasileiro-Vidal - ORCID: 0000-0002-9704-5509

Running head: Oligo-FISH barcode in beans

ABSTRACT

Current status on plant cytogenetic and cytogenomic research has allowed the selection and design of oligo-specific probes to individually identify each chromosome of the karyotype in a target species. Here, we developed the first chromosome identification system for legumes based on oligo-FISH barcode probes. We selected conserved genomic regions between *Vigna unguiculata* (*Vu*, cowpea) and *Phaseolus vulgaris* (*Pv*, common bean) (diverged ~9.7-15 Mya), using cowpea as a reference, to produce a unique barcode pattern for each species. We combined our oligo-FISH barcode pattern with a set of previously developed FISH probes based on BACs and ribosomal DNA sequences. In addition, we integrated our FISH maps with genome sequence data. Based on this integrated analysis, we confirmed two translocation events (involving chromosomes 1, 5, and 8; and chromosomes 2 and 3) between both species. The application of the oligo-based probes allowed us to demonstrate the participation of chromosome 5 in the translocation complex for the first time. Additionally, we detailed a pericentric inversion on chromosome 4, and identified a new paracentric inversion on chromosome 10. We also detected centromere repositioning associated with chromosomes 2, 3, 5, 7, and 9, confirming previous results for chromosomes 2 and 3. This first barcode system for legumes can be applied for karyotyping other Phaseolinae species, especially non-model, orphan crop species lacking genomic assemblies and cytogenetic maps, expanding our understanding of the chromosome evolution and genome organization of this economically important legume group.

Keywords: centromeric repositioning, chromosome evolution, inversion, oligo probes, *Phaseolus vulgaris*, translocation, *Vigna unguiculata*

DECLARATIONS

Funding

This work was supported by CNPq (Conselho Nacional de Desenvolvimento Científico e Tecnológico) Grant no. 421968/2018-4, 313527/2017-2, 310804/2017-5, 433931/2018-3, and 442019/2019-0, and FACEPE (Fundação de Amparo à Ciência e Tecnologia do Estado de Pernambuco) Grant no. APQ-0390-2.02/19.

Conflicts of interest/Competing interest

The authors declare no conflicts of interest.

Availability of data and material

All data generated or analyzed during this study are included as supplementary materials.

Code Availability:

Not applicable

Authors contributions

FOB: designed oligo system, provided resources for the oligo-FISH experiments and wrote the paper. THN: conducted oligo-FISH experiments, analyzed the sequence synteny data, constructed Circos images and wrote the paper. CCMJ: analyzed the sequence synteny data, constructed the Circos images and helped writing the paper. SD: conducted the oligo-FISH experiments and analyzed the sequence synteny data. LVM: analyzed and processed the oligo-FISH images and helped writing the paper. GTB: labeled the oligo-FISH probes. AMBI: discussed the results. JJ: discussed the results and provided resources for the oligo probe labeling. APH: designed this research and writing the manuscript, discussed the results and provided resources for the oligo-FISH experiments. ACBV: designed this research, the images and writing the manuscript and discussed the results. All authors read and approved the final version of the paper.

Ethical approval

Not applicable

Concent to participate

Not applicable

Consented for publication

Not applicable

Key message

An Oligo-FISH barcode system was developed for two model legumes, allowing the identification of all cowpea andcommon bean chromosomes in a single FISH experiment, and revealing new chromosome rearrangements. The FISH barcode system emerges as an effective tool to understand the chromosome evolution of economically important legumes and their related species.

Acknowledgments

We thank Embrapa Meio-Norte (Teresina, Piauí, Brazil) and Embrapa Cenargen (Brasília, Distrito Federal, Brazil) for providing the *V. unguiculata* and *P. vulgaris* seeds, respectively. We thank CNPq (Conselho Nacional de Desenvolvimento Científico e Tecnológico) Grant no. 421968/2018-4, 313527/2017-2, 310804/2017-5, 433931/2018-3, and 442019/2019-0, and FACEPE (Fundação de Amparo à Ciência e Tecnologia do Estado de Pernambuco) Grant no. APQ-0390-2.02/19 for the financial support. We also thank CAPES (Coordenação de Aperfeiçoamento de Pessoal de Nível Superior), and FACEPE for the scholarships.

INTRODUCTION

The development of a karyotype is essential to gain insights into the chromosome organization and evolution of related species. The early 1980s represented the beginning of the molecular cytogenetic era with the advent of FISH (Fluorescent *In Situ* Hybridization) technique (Langer-Safer et al. 1982). FISH provides a powerful tool for individual chromosome identification by using a wide range of DNA probes, including large-insert genomic DNA clones, such as BACs (Bacterial Artificial Chromosomes) (Jiang and Gill 1994, 2006; reviewed by Jiang 2019). Advances in sequencing technologies, with availability of genome sequences from an increasing number of species, and massive synthesis of oligonucleotides (oligos), have allowed the design of new probes for FISH, such as oligopainting (Beliveau et al. 2012). These probes can be developed from any species with a sequenced and assembled genome and can be used in karyotype analyses of related species (Jiang 2019).

In plants, chromosome painting with oligo-based probes have been used to determine karyotypes and investigate chromosome rearrangements, meiotic pairing and recombination in a wide range of species (Han et al. 2015; Qu et al. 2017; Braz et al. 2018; He et al. 2018; Hou et al. 2018; Meng et al. 2018; Xin et al. 2018; Albert et al. 2019; Martins et al. 2019; Šimoníková et al. 2019; Zhao et al. 2019; Bi et al. 2020; Bielski et al. 2020; Braz et al. 2021; He et al. 2020;

Li et al. 2020; Liu et al. 2020; Piperidis and D'Hont 2020; Song et al. 2020). Oligos selected from multiple regions from multiple chromosomes can be used to produce a barcode signal pattern for an individual chromosome pair, allowing the identification of a complete set of individual chromosomes in a single FISH experiment (Braz et al. 2018). So far, the oligo-FISH barcode system has been established in a few species, including potato (Braz et al. 2018), maize (Braz et al. 2020a; 2021), rice (Liu et al. 2020), sugarcane (Meng et al. 2020; Piperidis and D'Hont 2020), *Ipomoea* taxa (Chen et al. 2020) and Triticeae tribe (Li et al. 2020).

Vigna Savi and *Phaseolus* L. (Leguminosae family, Phaseoloid clade, Phaseolinae subtribe) are phylogenetically related genera, which diverged about 9.7-15 million years ago (Mya) (Li et al. 2013; Garcia et al. 2020). The group includes socioeconomically important species, such as *Vigna unguiculata* (L.) Walp. (cowpea) and *Phaseolus vulgaris* L. (common bean), essential crops for global food security and human population nutrition, especially in developing countries (Broughton et al. 2003; Gepts et al. 2008; Freire-Filho et al. 2011; Boukar et al. 2016). Most *Phaseolus* and *Vigna* species have $2n = 2x = 22$ chromosomes, which are in small size (1-4 μm) and morphological similarity varying from meta- to submetacentric chromosomes (Darlington and Wylie 1955; Forni-Martins 1986; Mercado-Ruaro and Delgado-Salinas 1996, 1998; Venora et al. 1999; Mercado-Ruaro and Delgado-Salinas 2000).

A BAC-FISH based cytogenetic map was first established for *P. vulgaris* (Fonsêca et al. 2010). The established BAC markers were used for comparative mapping in *P. lunatus* (Bonifácio et al. 2012; Almeida and Pedrosa-Harand 2013) and *P. microcarpus* (Fonsêca and Pedrosa-Harand 2013) and revealed a generally high degree of macrosynteny among these species and collinearity breaks due to a few inversions. In turn, in the Leptostachyus group of species ($2n = 20$), the BAC markers revealed several translocations and a nested chromosome fusion that resulted in descending dysploidy (Fonsêca et al. 2016; Ferraz et al. 2020). BACs from *P. vulgaris* were also hybridized to *V. unguiculata* chromosomes and allowed identification of macrosynteny breaks involving a duplication, translocations, and inversions between species (Vasconcelos et al. 2015). Other studies included application of *V. unguiculata* BACs in genetic and physical map integration (Iwata-Otsubo et al. 2016), besides *V. unguiculata* and *P. vulgaris* BACs for BAC-FISH maps for *V. angularis* (Martins et al. 2021) and *V. aconitifolia* (Oliveira et al. 2020). These studies enabled the expansion of the comparative cytogenetic analyses between *Vigna* and *Phaseolus* species. Although BAC-FISH is highly informative, it is a laborious process and technically challenging to identify all chromosomes in the same metaphase cells, limiting its application to a small number of species.

The availability of sequenced and assembled genomes for *V. unguiculata* (1C = 640 Mb; Lonardi et al. 2019) and *P. vulgaris* (1C = 587 Mb; Schmutz et al. 2014) allows designing oligo-FISH probes for both genomes, as previously demonstrated by oligo-painting on *Vigna* and *Phaseolus* species using probes from chromosomes 2 and 3 of *P. vulgaris* (Martins et al. 2021). Here, we present a new barcode system for the chromosome identification of both species. We compared the *V. unguiculata* and *P. vulgaris* genome sequences and selected *V. unguiculata* oligo pools from conserved regions in both species so that each chromosome is associated with a unique barcode pattern. This approach will enable comparative FISH mapping and individual chromosome identification of different *Vigna* and *Phaseolus* species and potentially other related Phaseolinae members. The accurate chromosome identification will be crucial for future investigation of chromosome evolution and diversification within the subtribe, especially for the non-model species with neither assembled genome nor available cytogenetic map.

MATERIALS AND METHODS

Plant material and chromosome preparation

The root tips of germinated seeds of *V. unguiculata* 'BR14 Mulato' and *P. vulgaris* 'BAT93' from Embrapa Meio-Norte (Empresa Brasileira de Pesquisa Agropecuária, Teresina, Piauí, Brazil) and Embrapa Cenargen (Embrapa Recursos Genéticos e Biotecnologia, Brasília, Distrito Federal, Brazil), respectively, were collected and pre-treated with 2 mM 8-hydroxyquinoline for 5 h at 18 ºC, fixed in methanol: acetic acid (3:1 v/v) for 2-24 h at room temperature and stored at -20 ºC until use. For chromosome preparation, the tips were washed twice in distilled water, then submitted to enzymatic treatment of 2% pectolyase (Sigma-Aldrich), 4% cellulase (Onozuka or Sigma-Aldrich) and 20% pectinase (Sigma-Aldrich) at 37 ºC for 2 h in a humid chamber. The slides were prepared using the air dry technique (De Carvalho and Saraiva 1993) with minor modifications. Meristems were washed in distilled water, placed individually in an approximately 30◦ vertically inclined slide. Using a Pasteur pipette, cold fixative solution (methanol:acetic acid, 3:1, v:v) were dropped over the meristem, which were macerated until its total fragmentation. Afterwards, the slides were air dried by fanning, immersed in 45% acetic acid for 10 s and placed on a hot plate surface (at 42 ◦C) for 5 to 10 min.

Selection and synthesis of Oligo-FISH probes

The Oligo-FISH barcode probes were designed using the reference genome of *V. unguiculata* 'IT97K-499-35' v. 1.1 available at Phytozome (phytozome.jgi.doe.gov) and NCBI SRA BioSample accession SAMN06674009 (also ASM 411807v1) (Lonardi et al. 2019). Unique sequences of each pseudochromosome of *V. unguiculata* were selected after filtering for excluding repetitive sequences by Arbor Biosciences (Ann Arbor, MI, USA). Probes able to generate a signal on both *V. unguiculata* and *P. vulgaris* were selected by mapping the oligo probe derived from *V. unguiculata* to the *P. vulgaris* genome (v. 2.1, http:// www.phytozome.net/commonbean.php; GenBank accession ANNZ01000000; Schmutz et al. 2014) using Blastn. Only probes having a single hit in the entire *P. vulgaris* genome (Blast e-value lower than 10E-05) with this hit located on the syntenic *P. vulgaris* chromosome (Lonardi et al. 2019) were retained. Two libraries were generated, which were composed of ~27.000 oligos each of about 45 nucleotides long. Library 1 contained the oligo pool that generated the 16 signals detected in red after FISH, while library 2 contained the second oligo pool corresponding to the 14 green signals. These libraries covered together the thirty genomic regions selected for barcoding, which corresponded to ~41 megabases (Mb) of DNA sequences of *V. unguiculata* genome (Data S1 and S2) and were designed and synthesized by Arbor Biosciences (Ann Arbor, MI, USA). Each library was indirectly labeled with digoxigenin (library 1) or biotin (library 2) (Han et al. 2015). The complete sequence sets of both libraries are available at Supplementary data (Data S1 and S2).

Oligo-FISH and image processing

The oligo-FISH was conducted according to the protocol proposed by Braz et al. (2020b) with some modifications. The hybridization mix consisted of 50% formamide, 2× SSC (Saline Sodium Citrate) solution (pH 7.0), 10% dextran sulfate, 350 ng of the probe labeled with biotin-green and 200 ng of the probe labeled in digoxigenin-red, in a total volume of 10 µL per slide. The chromosomes were denatured for 5-7 min at 75 ºC and incubated for 18-72 h at 37 ºC in a humid chamber. After that, the coverslips were gently removed, stringency washes in 2× and 0.1× SSC at 42 ºC (~ 76% final stringency) were conducted, followed by a wash in 1× TNB (Tris-NaCl-Blocking) buffer. A total of 20 µL solution comprising 0.2 µL of rhodamine sheep anti-DIG (Roche) and 0.2 µL of Alexa Fluor 488 Streptavidin (Invitrogen) was applied with posterior incubation at 37 ºC for 1 h. Chromosomes were counterstained with 2 µg/mL DAPI in Vectashield antifade solution (Vector Laboratories). Chromosome images were captured with Leica DM5500B fluorescence microscope and the adjustments for brightness and contrast of images were processed using Adobe Photoshop CC (2019). The positions of each barcode

marker was measured in 20 chromatids from five metaphases per species, following Fonsêca et al. (2010), except for using the DRAWID 0.26 software (Kirov et al. 2017). The new markers were integrated into the already established maps of *V. unguiculata* (Vasconcelos et al. 2015; Oliveira et al. 2020) and *P. vulgaris* (Fonsêca et al. 2010).

In silico and integrative map analysis

The sequence set for all oligos of each barcode signal was contrasted against *V. unguiculata* 'IT97K-499-35' (ASM411807v1, GenBank ID: 8372728) and *P. vulgaris* 'G19833' (SAMN02981484, GenBank ID: 864298) genomes by BLASTn tool (NCBI platform), optimized for highly similar sequences (megaBLAST), for localizing them at the pseudomolecules considering e-value, score and identity percentage variables (Table S1). Additionally, the sequences available for BAC markers used in previous studies for both species were included. BACs from *V. unguiculata* were previously used by Oliveira et al. (2020) and Martins et al. (2021) and are available at HarvEST:cowpea (harvest.ucr.edu). The *P. vulgaris* BAC sequence accessions used for the integrated map are provided in Table S2 and were obtained by BLAST using the sequences of corresponding genetic markers used to select each BAC and provided by the studies of Vallejos et al. (1992), Murray et al. (2002), Hougaard et al. (2008) and Geffroy et al. (2009). The integrated approach was represented by circular idiograms, created using Circos software v. 0.69-9 using default parameters (Krzywinski et al. 2009), enabling an in-depth comparative analysis of the cytogenetic (outer circle) and genome (inner circle) data between *V. unguiculata* (left side) and *P. vulgaris* (right side). In order to optimize collinearity, pseudomolecules or chromosomes were eventually inverted in orientation, being the 0 Mb their initial position, as indicated in Fig. 2. The barcode signals are represented by continuous lines and BAC signals are represented by dashed lines, each with 1 Mb of length. For both chromosomes and pseudomolecules, we used the species name abbreviations (*Vu* and *Pv*) followed by their chromosome numbering. Each *V. unguiculata* chromosome is represented by a different colour (see Fig. 2 legend), evidencing *P. vulgaris* orthologous segments with the same colours. Output images (SVG format) were optimized using the CorelDraw X7 software.

RESULTS

Oligo-FISH barcode development for *V. unguiculata* and *P. vulgaris* chromosome identification

FISH using two oligo probe sets, each containing 27,000 oligos, generated 16 red and 14 green signals on *V. unguiculata* metaphase chromosomes (Fig. 1a, c). Each chromosome was numbered according to the corresponding *V. unguiculata* pseudomolecules (Fig. 2). Thus, the barcode-FISH based on the cytogenetic map was fully integrated with the current genome sequence map. In *P. vulgaris* chromosomes, the two oligo-FISH probes generated 16 red signals and 13 green signals (Fig. 1b, d). The missing green signal on *P. vulgaris* is explained by the colocalization of the barcode signals 10A and 10B on *Pv*10 (Fig. 1d, f), which are separated by 3.32 Mb. *Vigna unguiculata* and *P. vulgaris* chromosomes contained one to five or four signals, respectively, which were separated by at least ~ 6.5 Mb (6.59 Mb between 4B and 4D for *Pv*4 and 7.65 Mb between 11B and 11C for *Vu*11). Except for *Vu*7, chromosomal arms without barcode signals had the presence of rDNA loci, as observed for *Vu*6, *Vu*10, *Pv*6, *Pv*9, and *Pv*10 (Fig. 2). Barcode signals covered a region from 0.19 Mb to 1.41 Mb in length in *V. unguiculata*, and from 0.03 Mb to 4.07 Mb in *P. vulgaris* (Tables S1 and S2). Thus, it was possible to distinguish the 11 individual chromosome pairs of the two species, with each chromosome of *V. unguiculata* and *P. vulgaris* presenting a unique signal barcode pattern, which was different between species (Fig. 1).

Cytogenetic and *in silico* analysis: an integrated approach

In order to verify the differences in the barcode pattern between orthologous chromosomes and perform a more detailed comparison between species, the sequence set of each oligo barcode was mapped in its respective pseudomolecule. We integrated *in silico* and cytogenetic analyses, including the oligo-FISH barcode markers generated in this work and a set of previously developed *V. unguiculata* and *P. vulgaris* BAC-FISH markers, producing a total of 95 markers (Tables S3 and S4). Additionally, 5S and 35S rDNA sites were located in the cytogenetic maps.

We observed the same order for most markers, comparing both maps of the same species. However, we detected several discrepancies between cytogenetic and sequencing maps, including differences in chromosome sizes and morphologies, as well as distances between some markers. These discrepancies may be attributed to chromosome condensation differences between eu- and heterochromatic regions, low resolution of FISH in metaphase chromosomes, and to sequence gaps. Distortions in chromosome size were mainly observed for terminal 35S rDNA carrier chromosomes (*Vu*1, 2, 6 and 10, and *Pv*6, 9, and 10), because rDNA

sites were not present at sequencing maps (Fig. 2). The lack of rDNA sites in pseudomolecules also altered the position of markers in short versus long chromosome arms in *Vu*6 and 10. To facilitate the integration of FISH and sequencing maps, chromosomes *Vu*4, 5, 6, and 10, as well as chromosome *Pv*10, were drawn in opposite orientations in relation to their respective pseudomolecules (Fig. 2).

Barcode: improvement of *V. unguiculata* and *P. vulgaris* synteny and collinearity comparisons

Based on the position of the oligo-FISH barcode markers along the chromosomes, none of the orthologous showed a conservation of the barcode pattern across the analyzed genomes (Figs. 1, 2). Chromosomes 6, 7, 9, and 11 are largely collinear, but differences in rDNA distribution between species were observed for chromosomes 6, 9, and 11.

Translocation complexes

We confirmed two translocation complexes between *V. unguiculata* and *P. vulgaris* genomes (Figs. 1, 2). Chromosomes 1, 5 and 8 were involved in a translocation complex differentiating *Vigna* and *Phaseolus* chromosomes, as previously identified by BAC-FISH, except for the participation of *Pv*5 (Vasconcelos et al., 2015; Oliveira et al., 2020; Martins et al., submitted), which was identified for the first time here by the presence of 1A in *Pv*5 and the 5A in *Pv8*. *In silico* analysis confirmed the rearrangements by the following oligo barcode markers: *Vu*1 short arm (*Vu*1S) (1A), *Vu*1 long arm (*Vu*1L) (1B, 1C); *Vu*5S (5B, 5C), *Vu*5L (5A); *Vu*8S (8A) and *Vu*8L (8B), which were located at *Pv*1S (8A) - *Pv*1L (1B, 1C); *Pv*5S (1A, 5B) - *Pv*5L (5C); *Pv*8S (5A) - *Pv*8L (8B) (Figs. 1, 2).

A reciprocal translocation involving chromosomes 2 and 3, previously identified by BAC-FISH analysis (Vasconcelos et al. 2015; Oliveira et al. 2020; Martins et al. 2021) and chromosome painting (Martins et al. 2021), was also detected using our barcode system. In the present analysis, *Vu*2S (2A), *Vu*2L (2B, 2C); *Vu*3S (3A, 3B) and *Vu*3L (3C, 3D, 3E) markers were located at *Pv2*S (2C) - *Pv2*L (2B, 3B, 3A); *Pv*3S (2A) - *Pv*3L (3E, 3D, 3C) (Fig. 1). Additional small rearrangements, mainly involving pericentromeric regions of these two chromosomes, could be evidenced in the integrated analysis, reinforcing the centromere repositioning for chromosomes 2 and 3 described by Martins et al. (2021) (Fig. 2).

Centromere repositioning of chromosomes 5, 7 and 9

In addition to the centromere repositioning for chromosomes 2 and 3 previously described (Martins et al. 2021), changes in centromere position were also detected by oligo-FISH barcode for chromosomes 5, 7, and 9 (Figs. 1-4). While in *Vu*5 the centromere was positioned between 5A and 5B, in *Pv*5 it was located between 5B and 5C (Fig. 3a). For chromosome 7, the centromere was above 7A in *V. unguiculata*, while in *P. vulgaris* it was between 7A and 7B (Fig. 4a). For chromosome 9, the centromere was between 9A and 9B in *V. unguiculata*, and between 9B and the distal BAC H10M18 in *P. vulgaris* (Fig. 4b).

Inversions for chromosomes 4 and 10

Apart from changes in centromere position in chromosomes 2, 3, 5, 7, and 9, the barcode markers confirmed a pericentric inversion in chromosome 4 identified by Vasconcelos et al. (2015), resulting in a barcode pattern of green-red-green-red in *Pv*4 instead of green-green-red-red in *Vu*4, and detailed the regions involved in the breakpoints (Fig. 1e-f, Fig. 5a). This was confirmed by the sequence analysis, which revealed breakpoints between 4A and BAC 190C15 in *Pv*4S, and between 4B and 4D in *Pv*4L, or the corresponding regions in *Vu*4, inverting, thus, most of the chromosome (Figs. 2, 5a). We also observed a new paracentric inversion in chromosome 10, involving the segment between H025N06 and 10B in *Pv*10L (Figs. 2, 5b). This inversion resulted in the proximity of markers 10A and 10B in *P. vulgaris*, visible as a single signal in metaphase chromosomes (Figs. 1d, 1f, 5b).

DISCUSSION

A new chromosome identification system for both *V. unguiculata* and *P. vulgaris* was established in the present work. For the first time, the oligo-FISH barcode technique was used to identify legume chromosomes, by comparing sequence similarity of assembled genomes available for two species of related genera. This allowed us to design informative signal patterns for species belonging to different genera that diverged 9.7-15 Mya (Li et al. 2013; Garcia et al. 2020). We expanded the time of divergence achieved for sorghum and sugarcane (Meng et al. 2020), which diverged from a common ancestor for 8-9 Mya (Wang et al. 2010), and similar to the time of divergence of the six Solanaceae species evaluated by (Braz et al. 2018), that diverged about 15 Mya (Wu and Tanksley 2010). Our system for beans revealed new translocation complexes, inversions and changes in centromere position involving both crop species. Oligo-FISH barcode was also used to study chromosome evolution in crops such as

potato (Braz et al. 2018), rice (Liu et al. 2020), maize (Braz et al. 2020a), and sugarcane (Meng et al. 2020), identifying rearrangements as inversions, duplications and translocations.

The bean oligo-FISH barcode allowed us to identify and compare chromosomes that could not be previously analyzed cytologically, such as *Pv*5, which was identified for the first time in a translocation complex that involves chromosomes 1, 5, and 8. Furthermore, a new paracentric inversion was observed for chromosome 10, in addition to the in-depth analysis of a pericentric inversion in chromosome 4, detected cytogenetically by Vasconcelos et al. (2015). Although comparative BAC-FISH studies revealed numerous rearrangements between *V. unguiculata* and *P. vulgaris* (Vasconcelos et al. 2015; Oliveira et al. 2020), there was a lack of comparative probes for chromosome 5 and some other chromosome segments, especially in the pericentromeric region (Iwata-Otsubo et al. 2016), as observed for instance for chromosomes 4 and 10. With the establishment of the oligo-based probes, it was possible to design signals for those chromosomes and segments, including signals in more proximal positions than BACs. BAC clones may contain repetitive sequences that hinder their mapping in pericentromeric, repeat-rich chromosome regions, besides being a laborious methodology. Thus, with more genome assemblies available in the last years, it is now possible to develop more efficient and versatile chromosome identification systems, expanding and accelerating cytogenetic analyses (Jiang 2019; Braz et al. 2020b). Vasconcelos et al. (2015) have described, for instance, a pericentric inversion for chromosome 4, using subterminal BACs from *Pv*4, while we confirmed this pericentric inversion using interstitial signals for a better characterization of the pericentromeric region of chromosome 4 of both species, narrowing down the putative breakpoint regions. Martins et al. (2021) also reported a pericentric inversion for chromosome 4 comparing *V. unguiculata* and *V. angularis*, which belong to the subgenera *Vigna* and *Ceratotropis*, respectively, indicating that this inversion have occurred after subgenera separation (~3.6 Mya).

Although whole-genome comparison might be considered as the most complete way to shed light on chromosome evolution, most groups of plants still have only one reference genome, hampering comparative genomic analyses among closely related species (Varshney et al. 2012; Pecrix et al. 2018; Qin et al. 2019; Hasing et al. 2020). Additionally, rDNA loci and centromeres may be lacking in genome assemblies (Qin et al. 2019; Hasing et al. 2020). Our integrated cytogenetic and genomic approach highlighted the high level of macrosynteny and collinearity between both bean species (Lonardi et al. 2019). They revealed that some of the divergences in the barcode pattern between species were also related to changes in centromere position for chromosomes 2, 3, 5, 7, and 9. Centromere repositioning has been well documented

in plants, such as cucumber and melon (Yang et al. 2014), maize (Schneider et al. 2016), and species of the tribe Arabideae (Brassicaceae) (Mandáková et al. 2020). Repositioning events can occur by successive peri- and paracentric inversion; intrachromosomal translocation; and/or acquisition of a new centromere (Schubert and Lysak 2011; Schubert 2018). For bean chromosomes 2 and 3, a complex rearrangement was confirmed. Besides a major translocation event, minor rearrangements were observed, such as inversions, intrachromosomal translocations, and centromere repositioning by new centromere, since collinearity was not altered between *Pv*2 and *Pv*3 pericentromeric region, as discussed by Martins et al. (2021).

For chromosomes 5, 7, and 9, centromere repositioning can be due to inversions, intrachromosomal translocation and/or new centromere, although an association of the translocation complex involving chromosome 5 cannot be excluded. More markers are necessary to understand the involved mechanism for each of these centromeric changes. A recent study comparing *Phaseolus lunatus* (lima bean) and *P. vulgaris* genomes identified a complex intrachromosomal translocation within chromosome 9 (Garcia et al. 2020), which may be associated with the centromere repositioning observed between both species for this chromosome (Bonifácio et al. 2012). Further genome comparisons are necessary to confirm if this event also explains the difference observed between *P. vulgaris* and *V. unguiculata* chromosome 9, what, in this case, would suggest that *V. unguiculata* and *P. lunatus* chromosomes might represent the ancestral state. New centromere formation is common in domesticated plants, such as maize and potato (Talbert and Henikoff 2020), and is closely related to its domestication time (Schneider et al. 2016). This phenomenon may be associated with the selection of genes linked to the centromere. Thus, *Vigna* and *Phaseolus* beans, with multiple domestication events each, might be great targets to understand if domestication favors centromere repositioning.

Thus, the oligo-FISH barcode presented in this study provided the first legume chromosome identification enabling to distinguish individual chromosome pairs, besides identifying chromosome rearrangements and centromere repositioning not described previously. This technique can be applied to other crops of both genera that lack genomic information, such as moth bean [*V. aconitifolia* (Jacq.) Marechal], hairy cowpea [*Vigna luteola* (Jacq.) Benth.], wild cowpea (*Vigna vexillata* L.) yearlong (*Phaseolus dumosus* Macfad.), scarlet runner (*P. coccineus* L.), and tepary bean (*P. acutifolius* A. Gray). It will probably also be useful for infrageneric comparisons of related genera, thus helping to understand the chromosome evolution of this important group of legumes.

REFERENCES

Albert PS, Zhang T, Semrau K, et al (2019) Whole-chromosome paints in maize reveal rearrangements, nuclear domains, and chromosomal relationships. Proc Natl Acad Sci 116:1679–1685. https://doi.org/10.1073/pnas.1813957116

Almeida C, Pedrosa-Harand A (2013) High macro-collinearity between lima bean (*Phaseolus lunatus* L.) and the common bean (*P. vulgaris* L.) as revealed by comparative cytogenetic mapping. Theor Appl Genet 126:1909–1916. https://doi.org/10.1007/s00122-013-2106-9

Beliveau BJ, Joyce EF, Apostolopoulos N, et al (2012) Versatile design and synthesis platform for visualizing genomes with Oligopaint FISH probes. Proc Natl Acad Sci 109:21301–21306. https://doi.org/10.1073/pnas.1213818110

Bi Y, Zhao Q, Yan W, et al (2020) Flexible chromosome painting based on multiplex PCR of oligonucleotides and its application for comparative chromosome analyses in *Cucumis*. Plant J 102:178–186. https://doi.org/10.1111/tpj.14600

Bielski W, Książkiewicz M, Šimoníková D, Hřibová E, Susek K, Naganowska B (2020) The Puzzling Fate of a Lupin Chromosome Revealed by Reciprocal Oligo-FISH and BAC-FISH Mapping. Genes 11:1489. https://doi.org/10.3390/genes11121489

Bonifácio EM, Fonsêca A, Almeida C, et al (2012) Comparative cytogenetic mapping between the lima bean (*Phaseolus lunatus L.*) and the common bean (*P. vulgaris* L.). Theor Appl Genet 124:1513–1520. https://doi.org/10.1007/s00122-012-1806-x

Boukar O, Fatokun CA, Huynh B-L, et al (2016) Genomic tools in cowpea breeding programs: status and perspectives. Front Plant Sci 7:1–13. https://doi.org/10.3389/fpls.2016.00757

Braz GT, He L, Zhao H, et al (2018) Comparative oligo-fish mapping: an efficient and powerful methodology to reveal karyotypic and chromosomal evolution. Genetics 208:513–523. https://doi.org/10.1534/genetics.117.300344

Braz GT, Vale Martins L, Zhang T, et al (2020a) A universal chromosome identification system for maize and wild *Zea* species. Chromosom Res 28:183–194. https://doi.org/10.1007/s10577-020-09630-5

Braz GT, Yu F, do Vale Martins L, Jiang J (2020b) Fluorescent *in situ* hybridization using oligonucleotide-based probes. In: In Situ Hybridization Protocols, Methods in Molecular Biology. pp 71–83. http://link.springer.com/10.1007/978-1-0716-0623-0_4.

Braz GT, Yu F, Zhao H, et al (2021) Preferential meiotic chromosome pairing among homologous chromosomes with cryptic sequence variation in tetraploid maize. New Phytol 229:3294–3302. https://doi.org/10.1111/nph.17098

Broughton WJ, Hern A, et al (2003) Beans (*Phaseolus* spp.) - model food legumes. Plant Soil 252:55–128

Chen L, Su D, Sun J, et al (2020) Development of a set of chromosome-specific oligonucleotide markers and karyotype analysis in the Japanese morning glory *Ipomoea nil*. Sci Hortic (Amsterdam) 273:109633. https://doi.org/10.1016/j.scienta.2020.109633

Darlington CD, Wylie AP (1955) Chromosome atlas of cultivated plants. Chromosome atlas of flowering plants., Second edn, London, UK.

De Carvalho CR, Saraiva LS (1993) An air drying technique for maize chromosomes without enzymatic maceration. Biotech Histochem 68:142–145. https://doi.org/10.3109/10520299309104684

Ferraz ME, Fonsêca A, Pedrosa-Harand A (2020) Multiple and independent rearrangements revealed by comparative cytogenetic mapping in the dysploid Leptostachyus group (*Phaseolus* L., Leguminosae). Chromosom Res 28:395–405. https://doi.org/10.1007/s10577-020-09644-z

Fonsêca A, Ferraz ME, Pedrosa-Harand A (2016) Speeding up chromosome evolution in *Phaseolus*: multiple rearrangements associated with a one-step descending dysploidy. Chromosoma 125:413–421. https://doi.org/10.1007/s00412-015-0548-3

Fonsêca A, Ferreira J, dos Santos TRB, et al (2010) Cytogenetic map of common bean (*Phaseolus vulgaris* L.). Chromosom Res 18:487–502. https://doi.org/10.1007/s10577-010-9129-8

Fonsêca A, Pedrosa-Harand A (2013) Karyotype stability in the genus *Phaseolus* evidenced by the comparative mapping of the wild species *Phaseolus microcarpus*. Genome 56:335–343. https://doi.org/10.1139/gen-2013-0025

Forni-Martins ER (1986) New chromosome number in the genus *Vigna* Savi (Leguminosae-

Papilionoideae). Bull du Jard Bot Natl Belgique / Bull van Natl Plantentuin van België 56:129. https://doi.org/10.2307/3667759

Freire Filho RF, Ribeiro VQ, Rocha M de M, et al (2011) Feijão-Caupi no Brasil, 1st edn. EMBRAPA Meio-Norte, Teresina-PI

Garcia T, Duitama J, Zullo S, et al (2020) Comprehensive genomic resources related to domestication and crop improvement traits in Lima bean. Nat Res. https://doi.org/10.21203/rs.3.rs-95762/v1 (preprint)

Geffroy V, Macadré C, David P, et al (2009) Molecular analysis of a large subtelomeric nucleotide-binding-site–leucine-rich-repeat family in two representative genotypes of the major gene pools of *Phaseolus vulgaris*. Genetics 181:405–419. https://doi.org/10.1534/genetics.108.093583

Gepts P, Aragão FJL, Barros E de, et al (2008) Genomics of *Phaseolus* beans, a major source of dietary protein and micronutrients in the tropics. In: Genomics of Tropical Crop Plants. Springer New York, New York, NY, pp 113–143

Han Y, Zhang T, Thammapichai P, et al (2015) Chromosome-specific painting in *Cucumis* species using bulked oligonucleotides. Genetics 200:771–779. https://doi.org/10.1534/genetics.115.177642

Han Y, Zhang Z, Liu C, et al (2009) Centromere repositioning in cucurbit species: Implication of the genomic impact from centromere activation and inactivation. Proc Natl Acad Sci 106:14937–14941. https://doi.org/10.1073/pnas.0904833106

Hasing T, Tang H, Brym M, et al (2020) A phased *Vanilla planifolia* genome enables genetic improvement of flavour and production. Nat Food 1:811–819. https://doi.org/10.1038/s43016-020-00197-2

He L, Braz GT, Torres GA, Jiang J (2018) Chromosome painting in meiosis reveals pairing of specific chromosomes in polyploid *Solanum* species. Chromosoma 127:505–513. https://doi.org/10.1007/s00412-018-0682-9

He L, Zhao H, He J, et al (2020) Extraordinarily conserved chromosomal synteny of *Citrus* species revealed by chromosome-specific painting. Plant J 103:2225–2235. https://doi.org/10.1111/tpj.14894

Hou L, Xu M, Zhang T, et al (2018) Chromosome painting and its applications in cultivated

and wild rice. BMC Plant Biol 18:110. https://doi.org/10.1186/s12870-018-1325-2

Hougaard BK, Madsen LH, Sandal N, et al (2008) Legume anchor markers link syntenic regions between *Phaseolus vulgaris* , *Lotus japonicus* , *Medicago truncatula* and *Arachis*. Genetics 179:2299–2312. https://doi.org/10.1534/genetics.108.090084

Ishii T, Juranić M, Maheshwari S, et al (2020) Unequal contribution of two paralogous CENH3 variants in cowpea centromere function. Commun Biol 3:775. https://doi.org/10.1038/s42003-020-01507-x

Iwata A, Tek AL, Richard MMS, et al (2013) Identification and characterization of functional centromeres of the common bean. Plant J 76:47–60. https://doi.org/10.1111/tpj.12269

Iwata-Otsubo A, Radke B, Findley S, et al (2016) Fluorescence *in situ* hybridization (FISH)-based karyotyping reveals rapid evolution of centromeric and subtelomeric repeats in common bean (*Phaseolus vulgaris*) and relatives. G3 Genes, Genomes, Genet 6:1013–1022. https://doi.org/10.1534/g3.115.024984

Jiang J (2019) Fluorescence *in situ* hybridization in plants: recent developments and future applications. Chromosom Res 27:153–165. https://doi.org/10.1007/s10577-019-09607-z

Jiang J, Gill BS (1994) Nonisotopic *in situ* hybridization and plant genome mapping: the first 10 years. Genome 37:717–725. https://doi.org/10.1139/g94-102

Jiang J, Gill BS (2006) Current status and the future of fluorescence *in situ* hybridization (FISH) in plant genome research. Genome 49:1057–1068. https://doi.org/10.1139/g06-076

Kirov I, Khrustaleva L, Van Laere K, et al (2017) DRAWID: user-friendly java software for chromosome measurements and idiogram drawing. Comp Cytogenet 11:747–757. https://doi.org/10.3897/compcytogen.v11i4.20830

Krzywinski M, Schein J, Birol I, et al (2009) Circos: an information aesthetic for comparative genomics. Genome Res 19:1639–1645. https://doi.org/10.1101/gr.092759.109

Landegent JE, Jansen in de Wal N, Dirks RW, van der Ploeg M (1987) Use of whole cosmid cloned genomic sequences for chromosomal localization by non-radioactive *in situ* hybridization. Hum Genet 77:366–370. https://doi.org/10.1007/BF00291428

Langer-Safer PR, Levine M, Ward DC (1982) Immunological method for mapping genes on

Drosophila polytene chromosomes. Proc Natl Acad Sci 79:4381–4385. https://doi.org/10.1073/pnas.79.14.4381

Li G, Zhang T, Yu Z, et al (2020) An efficient Oligo-FISH painting system for revealing chromosome rearrangements and polyploidization in Triticeae. Plant J 105: 978-993. https://doi.org/10.1111/tpj.15081

Li H, Wang W, Lin L, et al (2013) Diversification of the phaseoloid legumes: effects of climate change, range expansion and habit shift. Front Plant Sci 4:1–9. https://doi.org/10.3389/fpls.2013.00386

Liu X, Sun S, Wu Y, et al (2020) Dual-color oligo-FISH can reveal chromosomal variations and evolution in *Oryza* species. Plant J 101:112–121. https://doi.org/10.1111/tpj.14522

Lonardi S, Muñoz-Amatriaín M, Liang Q, et al (2019) The genome of cowpea (*Vigna unguiculata* [L.] Walp.). Plant J 98:767–782. https://doi.org/10.1111/tpj.14349

Mandáková T, Hloušková P, Koch MA, Lysak MA (2020) Genome evolution in Arabideae was marked by frequent centromere repositioning. Plant Cell 32:650–665. https://doi.org/10.1105/tpc.19.00557

Martins L do V, Bustamante FO, Oliveira ARS, et al (2021) BAC- and oligo-FISH mapping reveals chromosome evolution among *Vigna angularis*, *V. unguiculata* and *Phaseolus vulgaris.* Chromosoma (accepted).

Martins L do V, Yu F, Zhao H, et al (2019) Meiotic crossovers characterized by haplotype-specific chromosome painting in maize. Nat Commun 10:4604. https://doi.org/10.1038/s41467-019-12646-z

Meng Z, Han J, Lin Y, et al (2020) Characterization of a *Saccharum spontaneum* with a basic chromosome number of $x = 10$ provides new insights on genome evolution in genus *Saccharum*. Theor Appl Genet 133:187–199. https://doi.org/10.1007/s00122-019-03450-w

Meng Z, Zhang Z, Yan T, et al (2018) Comprehensively characterizing the cytological features of *Saccharum spontaneum* by the development of a complete set of chromosome-specific oligo probes. Front Plant Sci 9:1–11. https://doi.org/10.3389/fpls.2018.01624

Mercado-Ruaro P, Delgado-Salinas A (1996) Karyological studies in several Mexican species

of *Phaseolus* L. and *Vigna* Savi (Phaseolinae, Fabaceae). In: Advances in legume systematics 8, Legumes of economic importance. Royal Botanic Gardens, Kew., pp 83–87

Mercado-Ruaro P, Delgado-Salinas A (1998) Karyotypic studies on species of *Phaseolus* (Fabaceae: Phaseolinae). Am J Bot 85:1–9. https://doi.org/10.2307/2446547

Mercado-Ruaro P, Delgado-Salinas A (2000) Cytogenetic studies in *Phaseolus* L. (Fabaceae). Genet Mol Biol 23:985–987. https://doi.org/10.1590/S1415-47572000000400043

Murray J, Larsen J, Michaels TE, et al (2002) Identification of putative genes in bean (*Phaseolus vulgaris*) genomic (Bng) RFLP clones and their conversion to STSs. Genome 45:1013–1024. https://doi.org/10.1139/g02-069

Oliveira AR da S, Martins L do V, Bustamante FDO, et al (2020) Breaks of macrosynteny and collinearity among moth bean (*Vigna aconitifolia*), cowpea (*V. unguiculata*), and common bean (*Phaseolus vulgaris*). Chromosom Res. https://doi.org/10.1007/s10577-020-09635-0

Pecrix Y, Staton SE, Sallet E, et al (2018) Whole-genome landscape of *Medicago truncatula* symbiotic genes. Nat Plants 4:1017–1025. https://doi.org/10.1038/s41477-018-0286-7

Piperidis N, D'Hont A (2020) Sugarcane genome architecture decrypted with chromosome-specific oligo probes. Plant J 103:2039–2051. https://doi.org/10.1111/tpj.14881

Qin S, Wu L, Wei K, et al (2019) A draft genome for *Spatholobus suberectus*. Sci Data 6:1–9. https://doi.org/10.1038/s41597-019-0110-x

Qu M, Li K, Han Y, et al (2017) Integrated karyotyping of woodland strawberry (*Fragaria vesca*) with oligopaint FISH probes. Cytogenet Genome Res 153:158–164. https://doi.org/10.1159/000485283

Ribeiro T, dos Santos KGB, Richard MMS, et al (2017) Evolutionary dynamics of satellite DNA repeats from *Phaseolus* beans. Protoplasma 254:791–801. https://doi.org/10.1007/s00709-016-0993-8

Schneider KL, Xie Z, Wolfgruber TK, Presting GG (2016) Inbreeding drives maize centromere evolution. Proc Natl Acad Sci 113:E987–E996. https://doi.org/10.1073/pnas.1522008113

Schmutz J, McClean PE, Mamidi S, et al (2014) A reference genome for common bean and genome-wide analysis of dual domestications. Nat Genet 46:707–713. https://doi.org/10.1038/ng.3008

Schubert I (2018) What is behind “centromere repositioning”? Chromosoma 127:229–234. https://doi.org/10.1007/s00412-018-0672-y

Schubert I, Lysak MA (2011) Interpretation of karyotype evolution should consider chromosome structural constraints. Trends Genet. 27:207–216

Šimoníková D, Němečková A, Karafiátová M, et al (2019) Chromosome painting facilitates anchoring reference genome sequence to chromosomes *in situ* and integrated karyotyping in banana (*Musa* spp.). Front Plant Sci 10:1–12. https://doi.org/10.3389/fpls.2019.01503

Song X, Song R, Zhou J, et al (2020) Development and application of oligonucleotide-based chromosome painting for chromosome 4D of *Triticum aestivum* L. Chromosom Res 28:171–182. https://doi.org/10.1007/s10577-020-09627-0

Talbert PB, Henikoff S (2020) What makes a centromere? Exp Cell Res 389:111895. https://doi.org/10.1016/j.yexcr.2020.111895

Vallejos CE, Sakiyama NS, Chase CD (1992) A molecular marker-based linkage map of *Phaseolus vulgaris* L. Genetics 131:733–740

Varshney RK, Chen W, Li Y, et al (2012) Draft genome sequence of pigeonpea (*Cajanus cajan*), an orphan legume crop of resource-poor farmers. Nat Biotechnol 30:83–89. https://doi.org/10.1038/nbt.2022

Vasconcelos EV, de Andrade Fonsêca AF, Pedrosa-Harand A, et al (2015) Intra- and interchromosomal rearrangements between cowpea [*Vigna unguiculata* (L.) Walp.] and common bean (*Phaseolus vulgaris* L.) revealed by BAC-FISH. Chromosom Res 23:253–266. https://doi.org/10.1007/s10577-014-9464-2

Venora G, Blangifortil S, Cremonini R (1999) Karyotype analysis of twelve species belonging to genus *Vigna*. Cytologia (Tokyo) 64:117–127. https://doi.org/10.1508/cytologia.64.117

Wang J, Roe B, Macmil S, et al (2010) Microcollinearity between autopolyploid sugarcane and diploid sorghum genomes. BMC Genomics 11:261. https://doi.org/10.1186/1471-

2164-11-261

Wu F, Tanksley SD (2010) Chromosomal evolution in the plant family Solanaceae. BMC Genomics 11:182. https://doi.org/10.1186/1471-2164-11-182

Xin H, Zhang T, Han Y, et al (2018) Chromosome painting and comparative physical mapping of the sex chromosomes in *Populus tomentosa* and *Populus deltoides*. Chromosoma 127:313–321. https://doi.org/10.1007/s00412-018-0664-y

Yang L, Koo D-H, Li D, et al (2014) Next-generation sequencing, FISH mapping and synteny-based modeling reveal mechanisms of decreasing dysploidy in *Cucumis*. Plant J 77:16–30. https://doi.org/10.1111/tpj.12355

Zhao Q, Wang Y, Bi Y, et al (2019) Oligo-painting and GISH reveal meiotic chromosome biases and increased meiotic stability in synthetic allotetraploid *Cucumis* ×*hytivus* with dysploid parental karyotypes. BMC Plant Biol 19:471. https://doi.org/10.1186/s12870-019-2060-z

FIGURE LEGENDS

Fig. 1 Chromosome identification of *Vigna unguiculata* (*2n* = 22) and *Phaseolus vulgaris* (*2n* = 22) based on *V. unguiculata* oligo-FISH barcode. Two oligo-FISH probe sets (red and green) hybridized on mitotic metaphase chromosomes of *V. unguiculata* (a) and *P. vulgaris* (b). Homologous chromosomes in **a** and **b** were paired in karyograms to identify the 11 chromosome pairs of *V. unguiculata* (c) and *P. vulgaris* (d). Each chromosome shows a unique pattern of oligo-FISH red and/or green signals. Chromosomes were counterstained in DAPI (pseudocoloured in grey). Idiograms of the barcode for both species using the *V. unguiculata* reference genome and considering the conserved sequences of *P. vulgaris* genome (**e**, *V. unguiculata* and **f**, *P. vulgaris*). Chromosomes were named according to the species name abbreviations (*Vu* and *Pv*), followed by their chromosome numbering. Each region was selected and named according to its position in *V. unguiculata* pseudomolecules starting at 0 Mb in alphabetical order. Bars in **a**-**b** = 5 µm and in **c**-**d** = 10 µm

Fig. 2 Circular representation of pseudomolecules (internal) and chromosomes (external) of *Vigna unguiculata* (left side) and *Phaseolus vulgaris* (right side) showing the position of oligo

barcode, BAC, rDNA and markers. Each chromosome and pseudomolecule start at 0 Mb, indicating its orientation in the present representation. Barcode markers are represented by continuous lines, while the BAC markers by dashed lines. The colour of each chromosome marker was defined in accordance with *V. unguiculata* chromosomes/ pseudomolecules: *Vu*1 (dark blue), *Vu*2 (light green), *Vu*3 (red), *Vu*4 (gold), *Vu*5 (brown), *Vu*6 (purple), *Vu*7 (dark green), *Vu*8 (light pink), *Vu*9 (yellow), *Vu*10 (light blue), *Vu*11 (margeta). DNAr 5S and 35S marks colours were represented by red and green, respectively. Labels of markers that colocalize are separated by "/" and of markers that are adjacent, by "-". The first label represents the marker that is closer to 0 Mb (from right to left in *Vu* and from left to right in *Pv*). The orientation of some pseudomolecules (*Pv*2, *Pv*3, *Pv*4, *Pv*7, *Pv*9, *Pv*10, and *Pv*11) and chromosomes (*Pv*2, *Pv*3, *Pv*4, *Pv*7, *Pv*9, *Pv*11, and *Vu*5) was inverted for a better visualization of synteny and collinearity

Fig. 3 Circular representation of the chromosomes 1, 5, and 8 of *Vigna unguiculata* (*Vu*) and *Phaseolus vulgaris* (*Pv*), showing the translocation complex among them (a), and the reciprocal translocation between chromosomes 2 and 3 (b) both identified using the oligo barcode and BAC probes. The measurement scale is presented in Mb. Each chromosome starts at 0 Mb, indicating its orientation in the present representation. Barcode markers are represented by continuous lines, while the BAC markers by dashed lines

Fig. 4 Circular representation of chromosomes 7 (a) and 9 (b) of *Vigna unguiculata* (*Vu*) and *Phaseolus vulgaris* (*Pv*), both suggesting a centromere repositioning. The measurement scale is presented in Mb. Each chromosome starts at 0 Mb, indicating its orientation in the present representation. Barcode markers are represented by continuous lines, while the BAC markers by dashed lines

Fig. 5 Circular representation of chromosomes 4 (a) and 10 (b) of *Vigna unguiculata* (*Vu*) and *Phaseolus vulgaris* (*Pv*), evidencing a pericentric (a), and a paracentric (b) inversion, respectively. The measurement scale is presented in Mb. Each chromosome starts at 0 Mb, indicating its orientation in the present representation. Barcode markers are represented by continuous lines, while the BAC markers by dashed lines

SUPPLEMENTARY INFORMATION LEGENDS

Table S1 Genomic positions of oligo barcode and BAC markers in the reference genome of *Vigna unguiculata* (*Vu*) showing the scores of BLAST search, as well as the positions in bp. a

Total size and centromere regions by Lonardi et al. (2019). b BACs from V. unguiculata were previous used by Oliveira et al. (2020) and Martins et al. (2021) and are available at HarvEST:cowpea (harvest.ucr.edu). The colour of each chromosome marker was defined in accordance with Fig. 2 description.

Table S2 Genomic positions of oligo barcode and BAC markers in the reference genome of *Phaseolus vulgaris* (*Pv*) showing the scores of BLAST search, as well as the positions in bp. Genomic positions of oligo barcode and BAC markers in the reference genome of Phaseolus vulgaris (Pv) showing the scores of BLAST search, as well as the positions in bp. a Total size and centromere regions by Schmutz et al. (2014). c Gene markers ID and accessions for BAC sequences available at NCBI GenBank and EMBL-EBI. The colour of each chromosome marker was defined in accordance with Fig. 2 description.

Table S3 Chromosome positions of oligo barcode and BAC markers on *Vigna unguiculata* idiogram. Total chromosome size and position of centromere in bp are also indicated. The colour of each chromosome marker was defined in accordance with Fig. 2 description.

Table S4 Chromosome positions of oligo barcode and BAC markers on *Phaseolus vulgaris* idiogram. Total chromosome size and position of centromere in bp are also indicated. The colour of each chromosome marker was defined in accordance with Fig. 2 description.

Data S1 Sequences of the green oligo set used for oligo-FISH of *V. unguiculata* and *P. vulgaris* chromosomes. The sequences were selected using the reference genome of *V. unguiculata* 'IT97K-499-35' (Lonardi et al. 2019), based on regions conserved in *P. vulgaris* (Schmutz et al. 2014)

Data S2 Sequences of the red oligo set used for oligo-FISH of *V. unguiculata* and *P. vulgaris* chromosomes. The sequences were selected using the reference genome of *V. unguiculata* 'IT97K-499-35' (Lonardi et al. 2019), based on regions conserved in *P. vulgaris* (Schmutz et al. 2014)

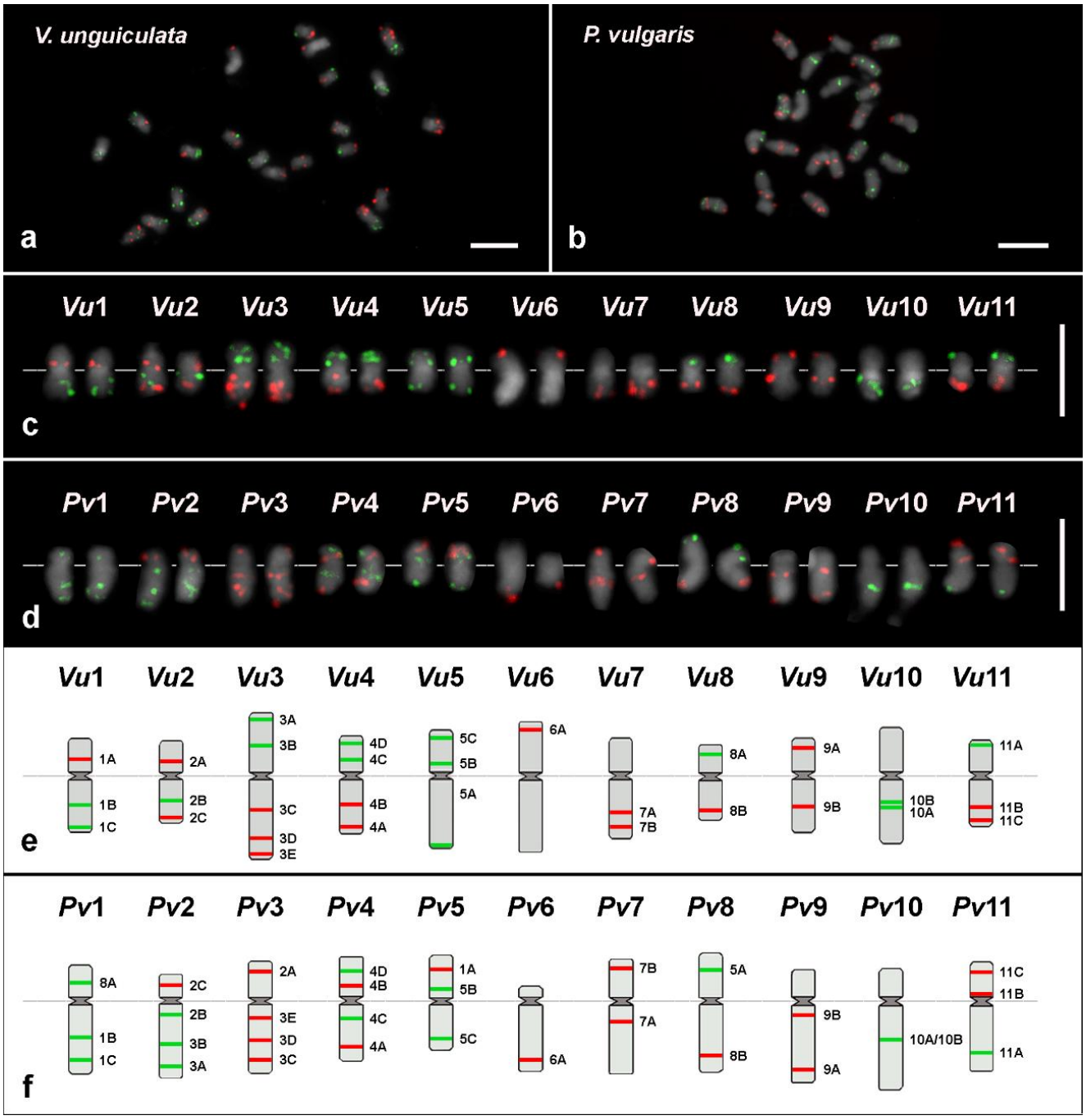

Fig. 1 Chromosome identification of *Vigna unguiculata* (*2n* = 22) and *Phaseolus vulgaris* (*2n* = 22) based on *V. unguiculata* oligo-FISH barcode. Two oligo-FISH probe sets (red and green) hybridized on mitotic metaphase chromosomes of *V. unguiculata* (a) and *P. vulgaris* (b). Homologous chromosomes in **a** and **b** were paired in karyograms to identify the 11 chromosome pairs of *V. unguiculata* (c) and *P. vulgaris* (d). Each chromosome shows a unique pattern of oligo-FISH red and/or green signals. Chromosomes were counterstained in DAPI (pseudocoloured in grey). Idiograms of the barcode for both species using the *V. unguiculata* reference genome and considering the conserved sequences of *P. vulgaris* genome (**e**, *V.*

unguiculata and **f**, *P. vulgaris*). Chromosomes were named according to the species name abbreviations (*Vu* and *Pv*), followed by their chromosome numbering. Each region was selected and named according to its position in *V. unguiculata* pseudomolecules starting at 0 Mb in alphabetical order. Bars in **a**-**b** = 5 µm and in **c**-**d** = 10 µm

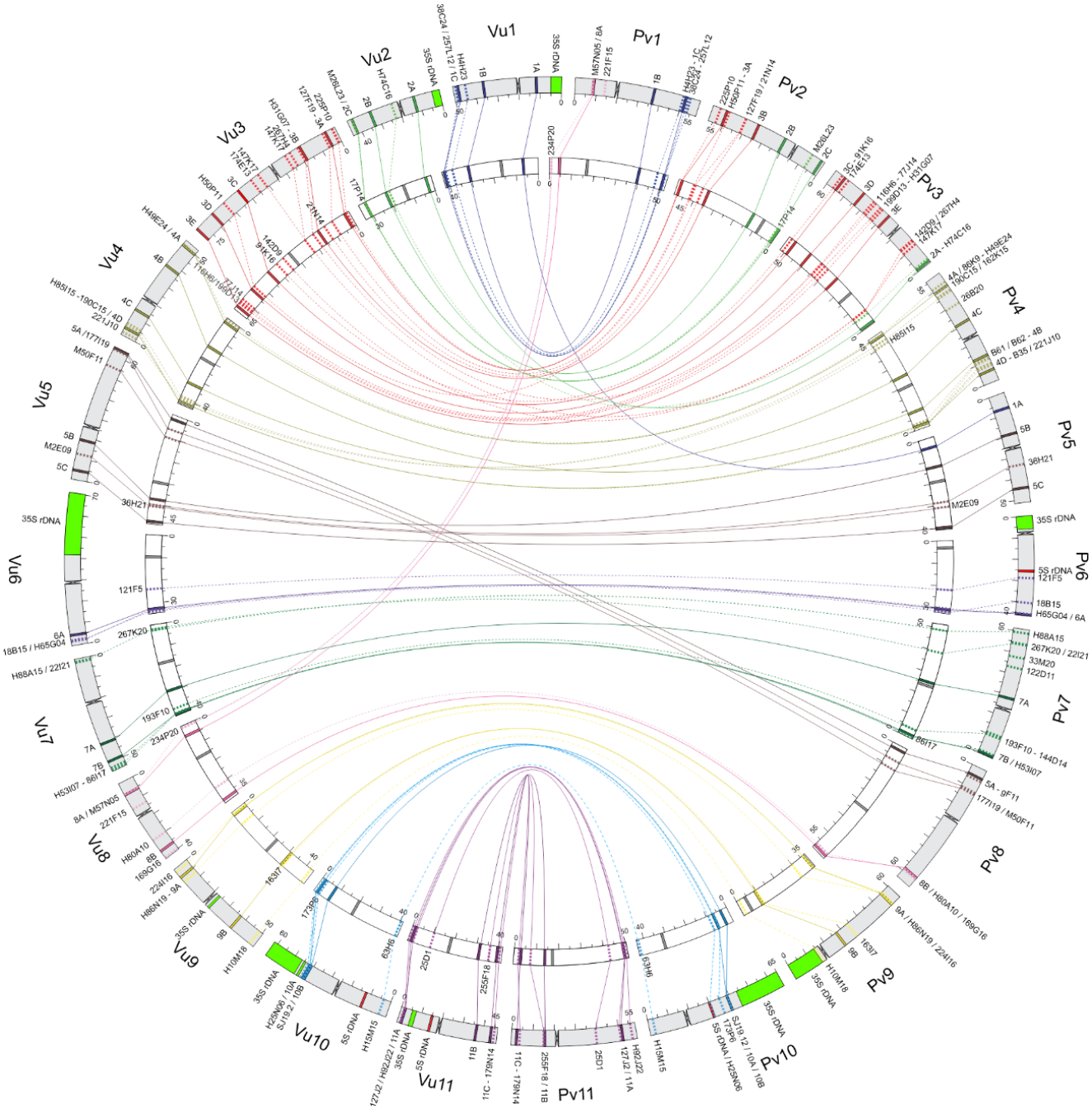

Fig. 2 Circular representation of pseudomolecules (internal) and chromosomes (external) of *Vigna unguiculata* (left side) and *Phaseolus vulgaris* (right side) showing the position of oligo barcode, BAC, rDNA and markers. Each chromosome and pseudomolecule start at 0 Mb,

indicating its orientation in the present representation. Barcode markers are represented by continuous lines, while the BAC markers by dashed lines. The colour of each chromosome marker was defined in accordance with *V. unguiculata* chromosomes/ pseudomolecules: *Vu*1 (dark blue), *Vu*2 (light green), *Vu*3 (red), *Vu*4 (gold), *Vu*5 (brown), *Vu*6 (purple), *Vu*7 (dark green), *Vu*8 (light pink), *Vu*9 (yellow), *Vu*10 (light blue), *Vu*11 (margeta). DNAr 5S and 35S marks colours were represented by red and green, respectively. Labels of markers that colocalize are separated by "/" and of markers that are adjacent, by "-". The first label represents the marker that is closer to 0 Mb (from right to left in *Vu* and from left to right in *Pv*). The orientation of some pseudomolecules (*Pv*2, *Pv*3, *Pv*4, *Pv*7, *Pv*9, *Pv*10, and *Pv*11) and chromosomes (*Pv*2, *Pv*3, *Pv*4, *Pv*7, *Pv*9, *Pv*11, and *Vu*5) was inverted for a better visualization of synteny and collinearity

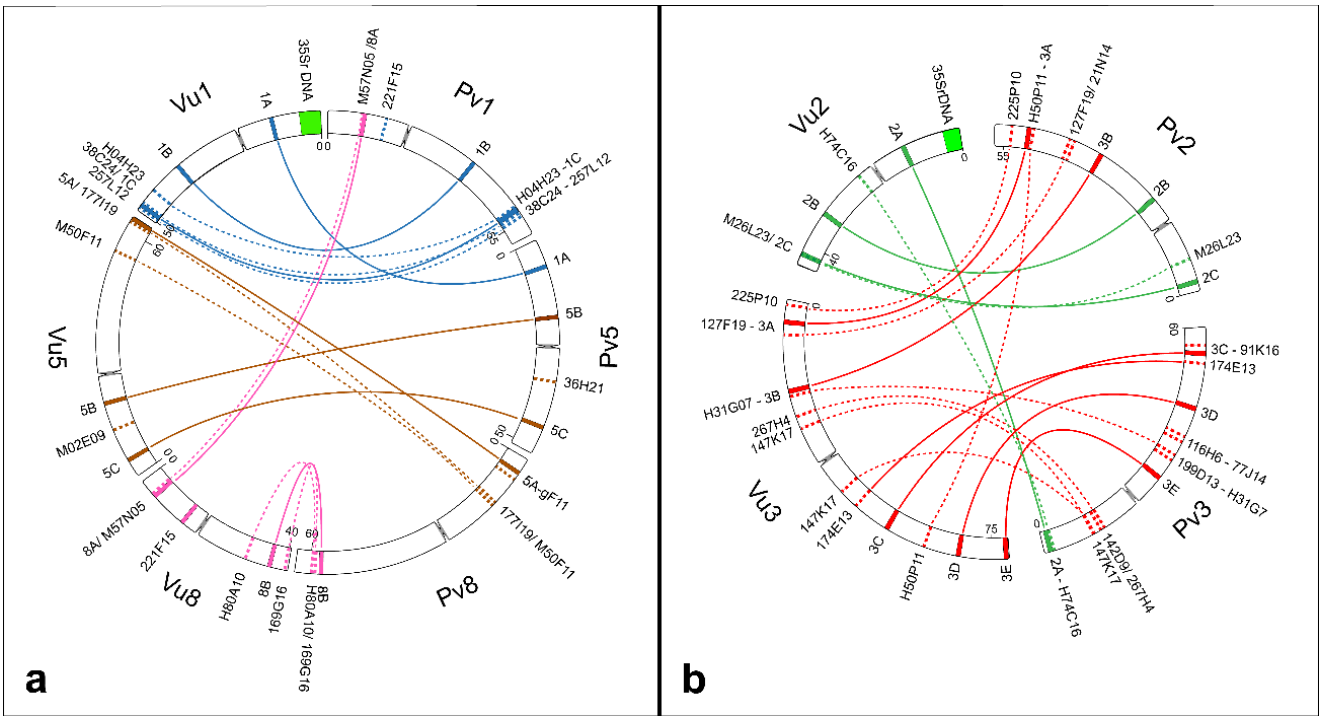

Fig. 3 Circular representation of the chromosomes 1, 5, and 8 of *Vigna unguiculata* (*Vu*) and *Phaseolus vulgaris* (*Pv*), showing the translocation complex among them (a), and the reciprocal translocation between chromosomes 2 and 3 (b) both identified using the oligo barcode and BAC probes. The measurement scale is presented in Mb. Each chromosome starts at 0 Mb, indicating its orientation in the present representation. Barcode markers are represented by continuous lines, while the BAC markers by dashed lines

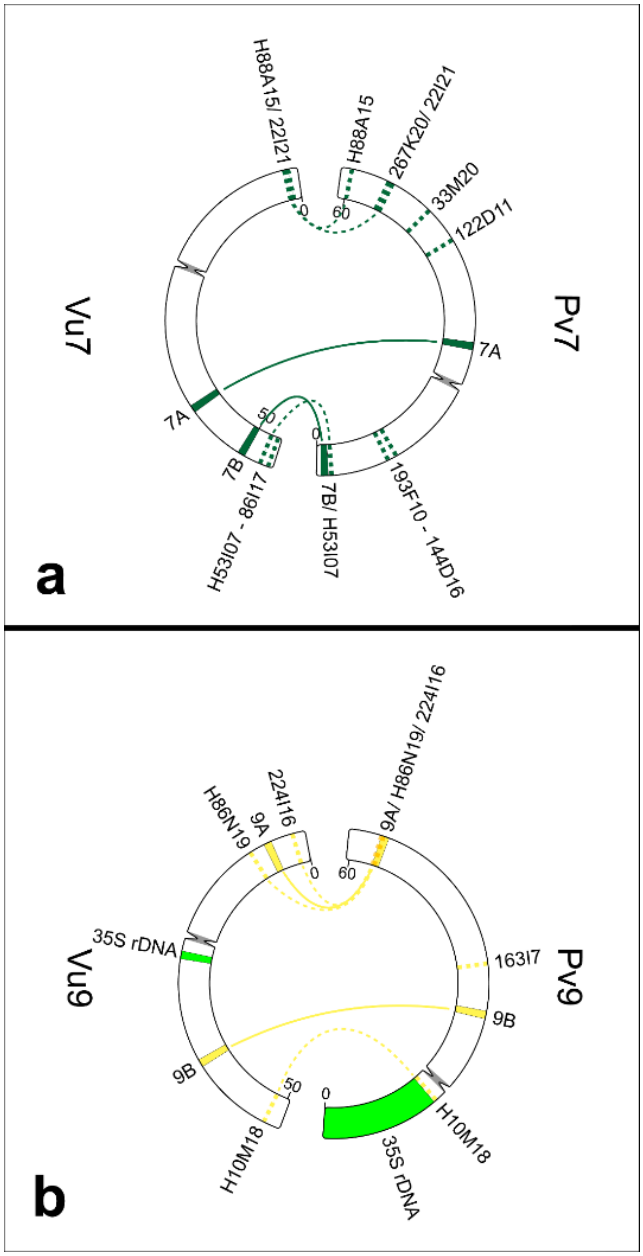

Fig. 4 Circular representation of chromosomes 7 (a) and 9 (b) of *Vigna unguiculata* (*Vu*) and *Phaseolus vulgaris* (*Pv*), both suggesting a centromere repositioning. The measurement scale is presented in Mb. Each chromosome starts at 0 Mb, indicating its orientation in the present representation. Barcode markers are represented by continuous lines, while the BAC markers by dashed lines

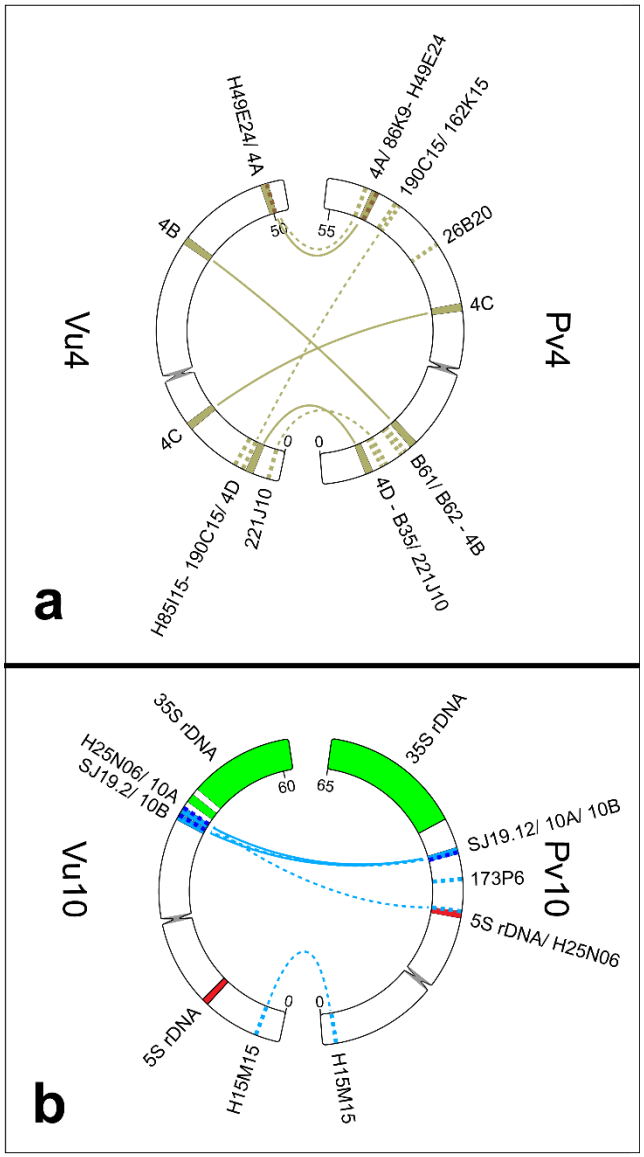

Fig. 5 Circular representation of chromosomes 4 (a) and 10 (b) of *Vigna unguiculata* (*Vu*) and *Phaseolus vulgaris* (*Pv*), evidencing a pericentric (a), and a paracentric (b) inversion, respectively. The measurement scale is presented in Mb. Each chromosome starts at 0 Mb, indicating its orientation in the present representation. Barcode markers are represented by continuous lines, while the BAC markers by dashed lines

Table S1 - https://static-content.springer.com/esm/art%3A10.1007%2Fs00122-021-03921-z/MediaObjects/122_2021_3921_MOESM1_ESM.xlsx

Table S2 – <https://static-content.springer.com/esm/art%3A10.1007%2Fs00122-021-03921-z/MediaObjects/122_2021_3921_MOESM2_ESM.xlsx>

Table S3 – <https://static-content.springer.com/esm/art%3A10.1007%2Fs00122-021-03921-z/MediaObjects/122_2021_3921_MOESM3_ESM.xlsx>

Table S4- <https://static-content.springer.com/esm/art%3A10.1007%2Fs00122-021-03921-z/MediaObjects/122_2021_3921_MOESM4_ESM.xlsx>

4. ARTIGO 2

Artigo a ser submetido ao periódico *The Plant Journal*

Oligo-FISH reveals the speed race in *Phaseolus* beans chromosome evolution

Thiago Nascimento and Andrea Pedrosa-Harand

Laboratory of Plants Cytogenetics and Evolution, Department of Botany, Federal University of Pernambuco, Recife, Brazil

✉ For correspondence (e-mail: andrea.harand@ufpe.br).

Thiago Nascimento - ORCID: 0000-0002-7742-0260

Andrea Pedrosa-Harand - ORCID: 0000-0001-5213-4770

Running head: Chromosome evolution in *Phaseolus* species

SUMMARY

Plant karyotypes evolve by structural chromosomal rearrangements associated or not to polyploidy or dysploidy. The *Phaseolus* genus comprises ~90 species, five of them domesticated due to their nutritional relevance. Most of the species have 2*n* = 22 and are highly syntenic, except for the three dysploid species from the Leptostachyus group (2*n* = 20), hypothesised to have accumulated several rearrangements. Here, we investigated the degree of structural rearrangements among Leptostachyus and other *Phaseolus* groups by estimating chromosomal evolution rates (CER). For this, we combined our oligo-FISH barcode system and chromosome-specific painting probes for chromosomes 2 and 3, with 5S and 35S rDNA loci and a centromeric repeat (CentPv1), for establishing chromosome orthologies and identifying structural rearrangements across nine *Phaseolus* species, including two *P. vulgaris* accessions. We integrated the detected rearrangements with a phylogenomic approach to estimate the CERs for each *Phaseolus* lineage. Our data allowed us to identify chromosome pairs in all species and to identify novel rearrangements, such as translocations, inversions, duplications, deletions and transpositions, mostly in species belonging to the Leptostachyus

group. *Phaseolus leptostachyus* showed the highest CER (11.68 rearrangements/My), followed by its sister species *P. macvaughii* (CER = 3.65). The remaining species had around one structural rearrangement per My or less. Our data support a ten-fold increase in the rate of chromosomal structural rearrangements in *P. leptostachyus*, and an absolute rate higher than any known plant or mammal, making this a model species to investigate the mechanisms behind a rapid genome reshuffling in species diversification.

Keywords: Barcode, chromosome painting, inversion, structural rearrangement, synteny, translocation

Significance statement:

Our comparative chromosome analysis using barcode and painting approaches enabled us to cytologically map the karyotype of ten *Phaseolus* bean accessions, revealing chromosome orthologies and identifying novel rearrangements within the genus. Mapping each chromosomal rearrangement along the branches of a dated phylogeny indicated more than ten-fold increase in the rate of chromosomal evolution of *P. leptostachyus*, suggesting a reshaping of its dysploid karyotype.

INTRODUCTION

Structural chromosomal rearrangements have a key role in species evolution. Inversions in heterozygosity preserve the linkage between alleles of different loci by reducing recombination despite gene flow and is associated with species adaptation and differentiation (Thompson and Jiggins, 2014; Wellenreuther and Bernatchez, 2018). Similarly, translocations, fusions and duplications are associated with adaptation and diversification (Mérot *et al.*, 2020). Duplications in the yellow monkeyflower, for example, are directly associated with its reproductive time and resistance to drought (Nelson *et al.*, 2019). The insertion of the 2.25-kb LTR retrotransposon in crows of *Corvus* genus changed gene expression related to plumage and, consequently, isolated subspecies (Weissensteiner *et al.*, 2020).

Chromosomal rearrangements also impact genome organization in different groups. It may, for instance, result in dysploidy events, with decrease (descending) or increase

(ascending) in chromosome number, such as in the genera *Phalaris* and *Senna* (Winterfeld *et al.*, 2018; Waminal *et al.*, 2021). Descending dysplody is particularly important during diploidization, frequent in plants that went through whole genome duplications (Mandáková and Lysak, 2018). A large number of chromosome rearrangements was described in Brassicaceae species (Mandáková *et al.*, 2020), marked by several cycles of polyploidy during its evolution, with different species experiencing different rates of evolution. When comparing *Arabidopsis thaliana* (2*n* = 5) and *Capsella rubella* (2*n* = 8) to the ancestral crucifer karyotype (ACK), for instance, *A. thaliana* experienced a higher incidence of rearrangements (Lysak *et al.*, 2016).

In groups with higher chromosomal evolution rates, these events can be assigned to specific clades and help unveil the phylogenetic relationships and evolution of its species. In bats of the Phyllostomidae family, high rates of structural rearrangements, such as fissions and fusions, have been reported and used as phylogenetic markers to investigate the evolution of this clade (Sotero-Caio *et al.*, 2015; Benathar *et al.*, 2019). In great apes, inversions are proportional to the phylogenetic distances and shed light into the genome evolution of apes and humans (Porubsky *et al.*, 2020). On the other hand, the evaluation of structural rearrangements in an evolutionary time context allows estimating a chromosomal evolution rate, as the calculated for mammals by Maruyama and Imai (1981), with ~0.4 rearrangements per million years (my), and the recently estimated for the Indian muntjac, the fastest evolving lineage known in mammals, with 3.5 changes/my (Mudd et al., 2020).

The identification of structural genomic variation depends on the methods applied. Different approaches can provide resolution at different scales, eventually detecting variations at base pair level (Mérot *et al.*, 2020). Advances in sequencing and bioinformatics enabled the detection of a wide range of variations through comparative genomics. However, whole genome assemblies of multiple species or individuals are still limited to few groups. In this context, the sequencing and assembly of a reference genome to produce oligonucleotide (oligo) probes for chromosome identification via FISH (Fluorescent *in situ* Hybridization) allows the identification of microscopic scale chromosomal rearrangements in a large number of closely related species that otherwise could not be analysed by using traditional cytogenetic strategies (Jiang, 2019).

The oligo-FISH technique has been applied to develop chromosome painting probes to investigate chromosome evolution, recombination, and homologous paring in different plant species such as cucumber, sugarcane, oranges and maize (Han *et al.*, 2015; do Vale Martins *et*

al., 2019; Piperidis and D'Hont, 2020; He *et al*., 2020). The oligo-based probes also allow to select specific regions of multiple chromosomes at different positions and combinations simultaneously, generating a barcode pattern able to identify all chromosome pairs in a single dual-colour FISH experiment (Braz *et al.*, 2018; Liu *et al.*, 2020; Braz, *et al.*, 2021). With the development of the oligo-FISH barcode for beans (De Oliveira Bustamante *et al*., 2021), a wide range of *Phaseolus* species can be karyotyped for identifying chromosome orthologies and structural rearrangements within the genus.

Phaseolus L. comprises ~90 species (POWO, 2021) with estimated origin around 6-8 million years ago (Mya) (Delgado-Salinas *et al.*, 2006). It belongs to Leguminosae (Fabaceae), the third largest family of angiosperms and the second in economic importance. *Phaselous* species are widely distributed, from Canada to Argentina, with two pools of diversification: the Mesoamerican and the Andean (Broughton *et al.*, 2003; Lewis *et al.*, 2005; Mercado-Ruaro *et al.*, 2009). *Phaseolus* is a monophyletic group, split into two main clades (A and B) which are subdivided into eight well-supported subclades defined as groups. Five species are domesticated and well-known for their economical and nutritional importance, such as the common bean (*Phaseolus vulgaris* L.), the scarlet runner bean (*P. coccineus* L.) and the lima bean (*P. lunatus* L.), all belonging to clade B and from the Vulgaris or Lunatus groups (Delgado-Salinas *et al.*, 2006). Due to its economic importance, four assembled genomes in chromosome scale are available for *Phaseolus: P. vulgaris* (both Mesoamerican, BAT93, and Andean, G19833) (Schmutz *et al.*, 2014; Vlasova *et al.*, 2016), *P. lunatus* (Garcia *et al.*, 2021) and *P. acutifolius* (Moghaddam *et al.*, 2021).

Most of *Phaseolus* species exhibit 2*n* = 22 chromosomes, while three dysploid species (*P. macvaughii*, *P. leptostachyus* and *P. micranthus*) form the Leptostachyus group and have 2*n* = 20 chromosomes (Mercado-Ruaro and Delgado-Salinas, 1996; Mercado-Ruaro and Delgado-Salinas, 1998). Few species have been compared by applying *Phaseolus vulgaris* bacterial artificial chromosomes (BACs) as FISH probes to construct cytogenetic maps, as for *P. vulgaris* (Vulgaris group) (Fonsêca *et al.*, 2010), *P. lunatus* (Lunatus group) (Bonifácio *et al.*, 2012), and *P. microcarpus* (Clade A) (Fonsêca and Pedrosa-Harand, 2013). These studies revealed a conserved synteny, with few inversions. Nonetheless, large variation in ribosomal DNA distribution was reported, mainly among *P. vulgaris* accessions (Moscone *et al.*, 1999; Pedrosa-Harand *et al.*, 2006). BAC-FISH mapping also showed that the descending dysploidy in the Leptostachyus group was a result of a nested chromosome fusion (NCF) between chromosomes 10 and 11 of the ancestral of *P. macvaughii* and *P. leptostachyus* when compared

to *P. vulgaris,* with several independent inversions and translocations observed between the former species (Fonsêca *et al.*, 2016; Ferraz *et al.*, 2020). Nevertheless, the evolution rate of the Leptostachyus group and other *Phaseolus* lineages has not been yet quantified. Furthermore, Leptostachyus group exclusive translocations remain to be confirmed, since the approaches used so far are laborious and did not allow the establishment of a cytogenetic map for *P. leptostachyus* nor the characterization of a wide range of species.

In this study, we aimed to compare the degree of structural rearrangements of two representatives of the Leptostachyus group (*P. leptostachyus* and *P. macvaughii*) to other *Phaseolus* species belonging to different groups and clades [Clade A (*P. microcarpus*) and B (Filiformis, Vulgaris and Lunatus groups]. For that we applied oligo-FISH barcode and painting to answer the following questions: 1) Which and how many were the main structural rearrangements that shaped *P. leptostachyus* and *P. macvaughii* karyotypes? 2) Are the rearrangements shared with other species? 3) How rearranged is the Leptostachyus dysploid group when compared to a larger sample of *Phaseolus* species? 4) What is the speed of chromosome evolution in the Leptostachyus group in comparison to other groups? Our hypothesis was that this group experienced a significantly increased rate of chromosome evolution, especially *P. leptostachyus*, even when considering a larger sample of the genus and additional chromosome markers that enable to identify previously undetected rearrangements. Indeed, we revealed an elevated rate of chromosome evolution in the Leptostachyus dysploid group, particularly in *P. leptostachyus*, an order of magnitude greater than other groups in the genus and higher than reported so far to other plants. In addition, we discuss the possible mechanisms that shaped *P. leptostachyus* karyotype evolution.

RESULTS

Chromosome identification of *Phaseolus* species by oligo-FISH

We combined the oligo-FISH barcode probes previously developed for *Vigna unguiculata* and *Phaseolus vulgaris* (De Oliveira Bustamante *et al*., 2021), the oligopaint probes for *P. vulgaris* chromosomes 2 (*Pv2*) and 3 (*Pv3*) (Do Vale Martins *et al*. 2020), with 5S and 35S rDNA, to efficiently identify all chromosomes in the analysed *Phaseolus* species (Fig.1). Considering the individual labelling pattern of each chromosome, as well as its size, morphology and eventual heterochromatic bands, all chromosome pairs could be individually distinguished (Figs. 1 and 2). For the Vulgaris group, the centromeric CentPv1 (*Nazca*) satellite

DNA (Iwata-Otsubo *et al.*, 2016) was also used to confirm the centromeric position of most pairs, except for chromosomes 5, 6 and 11, that lack this repeat.

We also attempted to establish chromosome orthologies among species (Fig. 2). For the Leptostachyus (*P. leptostachyus* and *P. macvaughii)* and Filiformis (*P. filiformis)* groups, three or more chromosome pairs did not present the *P. vulgaris* barcode patterns, hindering an undoubtful orthologous identification. Nevertheless, we established karyotypes for all species by attempting to maximize orthologies (indicated by the same chromosome numbers), by considering the most similar patterns. Among the Leptostachyus group species, *P. macvaughii* showed to be less rearranged than its sister *P. leptostachyus* when compared to *P. vulgaris*. Our results, combined to previous BAC-FISH mapping (Ferraz *et al.*, 2020), allowed the identification of all *P. macvaughii* orthologous pairs. Altogether, we possibly underestimated the number of rearrangements, especially for *P. leptostachyus*, but the reshuffling of *P. leptostachyus* genome was nevertheless clear.

Comparative chromosome painting in *Phaseolus*

Chromosome painting of the orthologous *Pv*2 and *Pv*3 revealed a conserved synteny in most *Phaseolus* species, except for *P. filiformis* and the species of the Leptostachyus group (Figs. 1 and 2). The painting of chromosome 3 revealed translocations in *Phaseolus filiformis*, with a segment of an unidentified chromosome corresponding to its short arm and a small segment of chromosome 3 in another pair (Figs. 3 and 4). In *P. macvaughii*, the painting pattern of *Pv*2 validated a translocation involving *Pma*2, previously described by Ferraz *et al.* (2020). Although *P. macvaughii* and *P. leptostachyus* belong to the same group, *P. leptostachyus* exhibited a larger number of translocations involving *Pv*2 and *Pv*3. Chromosome *Pv*2 was distributed in four different *P. leptostachyus* chromosome pairs. We assigned as the ortholog *Ple*2 the chromosome pair with *Pv*2 segments in both short and long arms. The *Pv*3 probe revealed signals in four chromosome pairs, but one chromosome pair was labelled in both short and long arms and was considered *Ple*3 (Fig. 2).

Comparative barcode pattern

The oligo-FISH barcode probes generated 16 red and 13 green signals for both Andean and Mesoamerican accessions of *P. vulgaris*, as previously described for ‘BAT93’ (De Oliveira Bustamante *et al.*, 2021). For *P. acutifolius, P. coccineus* and *P. dumosus*, as well as for *P.*

filiformis, we observed the same number of signals. However, for *P. microcarpus* and for Leptostachyus and Lunatus groups species, we observed changes in the number of signals. For *P. microcarpus,* 15 red and 13 green signals were detected, with absence of one red signal. *P. macvaughii* showed 16 red and 15 green signals, with two green signals duplicated, *P. leptostachyus* showed 15 red and 15 green signals, with deletions and duplications, while *P. lunatus* presented 14 green and 16 red signals due the duplication of one green signal, indicating additional small structural rearrangements in these four species (Figs. 2 and 3).

Breaks of collinearity indicated by different signal positions in respect to the chromosome arms were observed in a few orthologs of *P. microcarpus*, *P. acutifolius* and *P. lunatus* (indicated in Figs. 2 and 3). The barcode system revealed a pericentric inversion in chromosome 3 of *P. microcarpus*, followed by a deletion of one red signal on its long arm. We also identified in this species a change of the green signal in *Pmi10*, being located in the short arm and opposite to the 5S rDNA locus, what might indicate a transposition of the green signal. In, *P. acutifolius*, however, both 5S and green signals are present in the short arm, suggesting a pericentric inversion in *Pac*10. *Phaseolus lunatus* showed a duplication of one green signal in the short arm of *Plu4.* Furthermore, *P. filiformis* exhibited breaks of synteny due to a complex translocation involving orthologs *Pfi1*, *Pfi3* and *Pfi7*. According to the painting and the barcode patterns, we suggest that *Pfi1* received a segment containing a red barcode signal from *Pfi7*, which received a segment from *Pfi3*, while *Pfi3* received a segment with a green barcode signal, possibly from *Pfi1* (Figs. 2 and 4).

The Leptostachyus group exhibited a large number of synteny and collinearity breaks, additionally to the NCF that resulted in these dysploid karyotypes. For *P. macvaughii*, the barcode patterns of *Pma*1 and *Pma*2 are compatible with a single reciprocal translocation involving the short arm of *Pv*1 and the long arm of *Pv*2. Additionally, duplications of green signals were observed in the short arm of *Pma2* and in the long arm of *Pma*5 (Figs. 2 and 3). For *P. leptostachyus*, a larger number of rearrangements was inferred, including one deletion, two duplications, one inversion (excluding the inversion of the 5S rDNA) and eleven translocations. According to our results, only *Ple*8 conserved the same barcode pattern of *P. vulgaris* (Fig. 3).

Ribossomal DNA comparison in *Phaseolus* species and CentPv1 in the Vulgaris group

Our combined FISH probes helped us to identify the chromosome pairs (e.g. pairs 6 and 10) that carries rDNA sites, confirming their previously mapped positions at chromosomes of *P. leptostachyus, P. lunatus, P. macvaughii, P. microcarpus* and *P. vulgaris*, and their positions in *P. acutifolius, P. coccineus, P. dumosus* and *P. filiformis* (Figs. 1 and 2). *Phaseolus coccineus* presented 35S rDNA sites in *Pco*6, *Pco*9 and *Pco*10 and major 5S rDNA loci in *Pco*6 and *Pco*10, as observed for 'BAT93'. It also showed an additional 5S site in the short arm of *Pco*3, not shared with other species. *Phaseolus dumosus* showed eight 35S rDNA sites distributed in *Pdu*1,3,4,5,6,9,10 and 11, and two 5S rDNA loci in the long arms of *Pdu*6 and 10, suggesting a closely relation to *P. vulgaris* 'G19833'. The 35S loci in *Pdu*11 is exclusive of this species. *Phaseolus acutifolius* presented the ancestral 35S rDNA locus in *Pac*6 and 5S rDNA locus in *Pac*10, but at the short arm. This species also shows an exclusive additional 5S site in *Pac*8 (Figs. 2 and 3). *Phaseolus filiformis* presented a 35S rDNA locus in the short arm of *Pfi*6 and 5S rDNA loci close to the centromere at *Pfi*2, and in the long arm of *Pfi*4 and 10. The *Pfi*2 5S locus was exclusive of *P. filiformis*, while a 5S locus was also observed in *Pmi*4. Additionally, a second 5S rDNA signal was detected in the long arm of the 10/11 fused chromosome of *P. leptostachyus*, adjacent to the 5S signal, probably not detected before due to condensation of chromosomes (Fig 2 and Fig. S1).

We also mapped the centromeric repeat CentPv1 in *P. coccineus, P. dumosus* and both accessions of *P. vulgaris*. For *P. coccineus* the orthologs 1,2,3,4,5,6,7,9 and 10 exhibited centromeric signals, with special attention for Pco3 that presented the signal only in one of the homologues. *P. dumosus* and the two accessions of *P. vulgaris* exhibited the same number of centromeric signals in the orthologs 1,2,3,4,7,8,9 and 10 (Fig. 2).

Chromosomal evolution rates

In order to consider all detected karyotype changes in time, a dated phylogenetic analysis was performed using plastome assemblies. Despite the lower number of species, the resulting phylogenetic tree maintained the same topology as in Delgado-Salinas *et al.* (2006), with monophyletic groups and the expected relationships. Each rearrangement was placed along the branches considering the shared states as ancestral characters. Chromosomal evolution rates (CER) were estimated for each species or group by dividing the number of rearrangements in the lineage since the split from its sister group by the age of this clade in millions of years (my) (Table 1), providing the rate in number of rearrangements by my. For

this analysis, we calculated separately the number of structural rearrangements (referred here as CER), such as translocations and inversions detected by the painting and barcode procedures, and the number of rDNA sites changes (referred here as CErDNA), which may be a result of amplification of these tandem repeats without associated break of collinearity.

All Vulgaris group species presented less than a one chromosome rearrangement per my (CER = 0.91), except for *P. acutifolius* (CER = 0.45), with differences in CErDNA rates among species. For *P. vulgaris* 'BAT93', *P. coccineus*, and *P. vulgaris* 'G19833', the CErDNA was 1.36, 1.82 and 3.18 respectively, while *P. dumosus* and *P. acutifolius* presented CErDNA = 0.45 for both species. The Filiformis group presented CER = 0.36 and CErDNA = 0.71. The Lunatus group presented both CER and CErDNA of 0.40. *Phaseolus microcarpus* presented a CER of 0.65 and a CErDNA of 0.22. In comparison to *P. microcarpus*, the CER index was higher in Vulgaris group, since the rearrangements occurred in a shorter period of time, considering the species sampled in the present work. In the Leptostachyus group, *P. leptostachyus* exhibited the highest CER level (11.68) and a CErDNA of 1.46, followed by *P. macvaughii* with CER = 3.65 and a CErDNA = 0.73. Differences observed in the CER rates of the Leptostachyus species demonstrate the large number of rearrangements occurred in this group, particularly in *P. leptostachyus.*

DISCUSSION

We successfully applied our chromosome painting and barcode oligo probes to identify all chromosome pairs in the analysed *Phaseolus* species, representing both clades A and B, four formal groups and the unassigned *P. microcarpus* (Delgado-Salinas *et al*., 2006). Furthermore, we established chromosome orthologies for all species, confirming previous BAC-FISH mapping (Fonsêca *et al.*, 2010; Fonsêca and Pedrosa-Harand, 2013; Bonifácio *et al.*, 2012) and genomic sequencing (Garcia et al., 2021; Moghaddam et al., 2021), except for *P. leptostachyus*, which showed a higher number of synteny breaks than previously described (Fonsêca *et al.*, 2016; Ferraz *et al.*, 2020). *Phaseolus filiformis* exhibited novel translocations, changing the scenario of exclusivity of translocations in dysploid *Phaseolus* species. In this work, we compared a larger number of species, shedding light on the chromosome evolution of the genus.

In addition to the new rearrangements in species previously unmapped, the oligo-FISH approach enabled detecting previously undetected rearrangements, such as the multiple translocations of *Pv*2 and 3 in *P. leptostachyus* and the transposition in *Pmi*10. Nevertheless, a

few previously reported rearrangements were not detected by our oligo-FISH probe set, such as the paracentric inversion in the long arm of *Pmi*6 (Fonsêca and Pedrosa-Harand, 2013) or pericentric inversions in *Pma*3 and *Ple*7 (Ferraz *et al.*, 2020), demonstrated by BAC-FISH. Therefore, the number of rearrangements reported here is underestimated, especially considering small rearrangements and chromosomes with fewer barcode signals. Nevertheless, according to the comparisons between *P. vulgaris, P. lunatus* and *P. acutifolius* genomes, a high macrocollinearity was indeed maintained among these genomes. The inversions and intrachromosomal translocations involving orthologs *Pv*2/*Plu*2 and *Pv*9/*Plu*9 (Garcia *et al.*, 2021) can be associated to the differentiation in barcode pattern observed in *Plu2* and *Plu*9. The genomes of *P. acutifolius* and *P. vulgaris* are highly collinear, with a larger inversion observed only between *Pac*9 and *Pv*9 (Moghaddam *et al.*, 2021), what corroborates the results presented here.

Our chromosome identification system also confirmed the conservation of rDNA sites on chromosomes 10 (5S) and 6 (35S) (Fonsêca and Pedrosa-Harand, 2017), but identified new, exclusive 5S clusters for *Pfi2* and 4, *Pac*8 and *Pco*3. The presence of the 5S rDNA site at similar positions in *Pfi*4 and *Pmi*4 might be a homoplasy. Our results also indicate intraspecific variation in the position of 5S rDNA loci in *P. acutifolius*. Although the number of sites was the same as observed by Moscone *et al.* (1999), we did not detect synteny of 5S and 35S rDNA as previously reported. Intraspecific rDNA variation was detected for *P. vulgaris* and *P. lunatus* (Pedrosa-Harand *et al.*, 2006; Almeida and Pedrosa-Harand, 2011), but while the 35S is highly variable in number among *P. vulgaris* accessions (Pedrosa-Harand *et al.*, 2006), the 5S rDNA is much more variable in position, comparing orthologs, in the genus as a whole. Thus, the rDNA loci are not reliable for establishing chromosome orthologies among *Phaseolus* beans.

The barcode and painting pattern displayed by *P. dumosus* corroborate its similarity to *P. vulgaris*, especially with *P. vulgaris* 'G19833' accession, and *P. coccineus*. Indeed, *P. dumosus* is a hybrid between both species (Llaca *et al.*, 1994; Mina-Vargas *et al.*, 2016; Rendón-Anaya *et al.*, 2017). Our results corroborates its origin (Rendón-Anaya *et al.*, 2017), indicating that an Andean *P. vulgaris* accession was probably the maternal contributor. The difference observed between the hybrid and its parental species was the presence of a unique 35S rDNA locus in *Pdu*11. This new site might have originated after the hybridization event, in the last million year of its evolution. The restricted distribution of *P. dumosus* in South America is explained by its origin in Central America followed by a recent introduction (Llaca *et al.*, 1994). But this would imply that the hybridization event would have occurred after domestication of common

bean and the introduction of Andean domesticated beans to Central America more recently, or suggest more recent introgression with Andean beans. Further studies are required to confirm *P. dumosus* origin. Hybrids may undergo remarkable changes in regard to genomic organization, known as genomic shock (Barker *et al.*, 2012). But, apart from the new rDNA site, we do not have any evidence of a genomic shock in this particular case.

The species of Vulgaris group (*P. acutifolius*, *P. coccineus*, *P. dumosus* and *P. vulgaris*, clade B) presented conservation of synteny, as expected from previous BAC-FISH results between less related species, such as *P. vulgaris* and *P. lunatus* (clade B; Bonifácio *et al.*, 2012), and *P. vulgaris* and *P. microcarpus* (Clade A; Fonsêca and Pedrosa-Harand, 2013). The establishment of chromosome orthologies in a phylogenetic context enabled us to infer the ancestral states and place each detected rearrangement along the phylogenetic branches in a conservative approach, by calculating the rate of chromosome evolution in each lineage, considering only events not shared with its sister groups. Vulgaris and Leptostachyus groups have a similar age ~1.5 to 3 My (Delgado-Salinas *et al.*, 2006; and present work), but while the rate in the Vulgaris group is around one structural rearrangement per my, the Leptostachyus group showed several breaks of synteny and a rate at least three times higher. The rate observed for *P. leptostachyus*, however, was above 10 rearrangements/my, which is higher than the observed for mammals (~0.4 changes per million year; Maruyama and Imai, 1981), and even higher than the calculated rate for the Indian muntjac, *Muntiacus muntjak vaginalis*, (with a rate of ~5.3 changes/my; Mudd *et al.*, 2020), indicating it has the fastest rate of genome reshuffling so far known. Moreover, the sister group of Vulgaris group (Filiformis group, represented by *P. filiformis*; Delgado-Salinas *et al.*, 2006) showed three breaks of synteny, indicating that phylogenetic proximity cannot be used as an indicator of chromosome conservation in the genus, even when chromosome number is maintained.

We demonstrated the high number of changes exclusive of the Leptostachyus group, especially of *P. leptostachyus* genome, in comparison to other groups and revealed an increase in the speed of chromosome evolution within the *Phaseolus* genus. One of the main reasons that lead to the drastic changes in the genome organization is the effect of polyploidization followed by diploidization, affecting recombination and speciation (De Storme and Mason, 2014; Van De Peer *et al.*, 2017). No event of polyploidization was reported so far for *Phaseolus* species on the basis of cytogenetic or genome analyses (Mercado-Ruaro and Delgado-Salinas, 1996; Mercado-Ruaro and Delgado-Salinas, 1998; Schmutz *et al.*, 2014; Vlasova *et al.*, 2016; Garcia *et al.*, 2020). Otherwise, in *P. leptostachyus, P. macvaughii* and *P. micranthus* (2*n* = 20)

species, the descending dysploidy resulted from a Nested Chromosome Fusion (NCF) shared by the two less-related, mapped species, *P. leptostachyus* and *P. macvaughii* (Fonsêca *et al.*, 2016; Ferraz *et al.*, 2020). The instability promoted by polyploidy is well understood for Brassicaceae species (Lysak *et al.*, 2006), and descending dysploidy is pointed as the most crucial route to diploidization, turning polyploids into functional diploids (Mandáková and Lysak, 2018). Although we detected two and three small genomic duplications in *P. macvaughii* and *P. leptostachyus*, respectively, this could be related to segmental duplications or breaks within barcode segments, not previous whole genome duplication events. Furthermore, the age of the Leptostachyus group (~1.3 Mya) argue against a whole genome duplication followed by a reduction from $2n = 44$ to 20 in such short period of time. Another possible mechanism for genome reshuffling is the participation of repeats, since recent studies have demonstrated the role of repeats in chromosome rearrangements in *Senna tora* dysploid karyotype (Waminal *et al.*, 2021) and in *Arabidopsis* (Fransz *et al.*, 2016). A whole genome assembly will be necessary to elucidate the degree of rearrangements in *P. leptostachyus* genome and test for the presence of repeats in the rearrangement breakpoints.

EXPERIMENTAL PROCEDURES

Plant materials

Seeds of *P. acutifolius* (G40006B), *P. coccineus* (PHAS8577), *P. dumosus* (PHAS8544), *P. filiformis* (181315.00), *P. leptostachyus* (179671.00), *P. lunatus* (vermelhinha/GL0135), *P. macvaughii* (G40656), *P. microcarpus* (179698.00), *P. vulgaris* (BAT93/CNF04916), and *P. vulgaris* (G19833) were obtained from the germplasm banks of CIAT (International Center for Tropical Agriculture), EMBRAPA (Brazilian Agricultural Research Corporation) and IPK (Leibniz Institute of Plant Genetics and Crop Plant Research). The seeds were multiplied at the experimental garden of the Plant Cytogenetics and Evolution laboratory at the Department of Botany from the Federal University of Pernambuco, Recife, Brazil.

Chromosome preparation

Root tips from germinating seeds were pre-treated in 2 mM 8-hydroxyquinoline solution for 5 h at 18º C, fixed in methanol: acetic acid (3:1 v/v) for 2-24 h at room temperature, then stored at -20º C until use. For the chromosome preparation, tips were washed twice in distilled

water (5 minutes each), and treated with enzymatic solution containing 2% pectolyase (Sigma-Aldrich), 4% cellulase (Onozuka/ Sigma-Aldrich) and 20% pectinase (Sigma-Aldrich) in dark humid chamber at 37º C for 2 h. Chromosomes were spread using the air dry technique (De Carvalho and Saraiva, 1993) with minor modifications, as an additional bath in 60% acetic acid for at least 30 min to reduce the cytoplasm. Before FISH procedure, the slides were dried for ~15 min at 37º C.

FISH probes

The oligo-FISH barcode probes were designed based on the *Vigna unguiculata* 'IT97K-499-35' genome (Lonardi *et al.*, 2019), considering conserved regions with *P. vulgaris* genome (Schmutz *et al.*, 2014). One green and one red libraries are composed of ~27.000 oligos each (~ 45 nucleotides long), with 16 red and 13 green signals in *P. vulgaris*. One to four unique signals are present in each chromosome of *P. vulgaris*, in a specific combination of green and red signals in the short and long chromosome arms (De Oliveira Bustamante *et al*., 2021). The oligo painting probes for chromosomes 2 and 3 were selected and synthetized at the same conditions cited above but using the genome of *P. vulgaris* as reference (do Vale Martins *et al.*, 2021). The libraries were synthetized by Arbor Bioscience (Ann Arbor, MI, USA) and indirectly labelled with digoxigenin and biotin.

Additionally, a clone from *Triticum aestivum* L. (plasmid p*Ta*71) containing 25-28S, 5.8S and 18S (35S) rDNA and a 500-bp 5S rDNA clone (D2) of *Lotus japonicus* (Regel) K. Larsen. were used as rDNA probes, both directly labelled with Cy5-dUTP (GE Healthcare) by Nick translation. For *P. vulgaris*, *P. coccineus* and *P. dumosus* (Vulgaris group), the repeat probe CentPv1 (also known as *Nazca*; Iwata *et al.*, 2013) was directly labelled with Cy3-dUTP (GE Healthcare).

Oligo-FISH and image processing

The oligo-FISH procedure was conducted following the protocol proposed by Braz *et al.* (2020b) with small modifications. The hybridization mix consisted of 50% formamide, 2× SSC (Saline Sodium Citrate) solution (pH 7.0), 10% dextran sulphate, 350 ng of biotin labelled probe, 200 ng of digoxigenin labelled probe (15 µL of per slide). For the rDNA probes, we added 80 ng of one of the probes. The chromosomes were denatured at 75º C for 5-7 min and incubated for 18-72 h in dark humid chamber at 37º C. The coverslips were gently removed, and the material was submitted to stringency washes in 2× and 0.1× SSC solutions at 42º C (~76% of final stringency), followed by 1× TNB (Tris-NaCl-Blocking) buffer wash. For the

CentPv1 probe, the total stringency was lowered to ~40%, following the recommendations described by Iwata *et al.* (2013) and Ribeiro *et al.* (2017). A total of 20 µL solution containing 1:100 of Alexa Fluor 488 Streptavidin (Invitrogen) and 1:100 of Rhodamine Sheep anti-DIG (Roche) was applied, and the material was incubated in dark humid chamber at 37º C for 1h, with posterior washes in 4× SSC with 0.1% Tween-20 solution. The chromosomes were counterstained with 2 µg/mL DAPI in Vectashield H-100 antifade solution (Vector Laboratories). We used the same slides for the sequential FISH procedure, the first hybridization was made with the painting probes plus the 35S rDNA probe and the second FISH with the barcode plus 5S rDNA probes. We denatured the slides at 75º C for 3-5 min with no addition of the probes in the mix between the hybridizations for removing previous signals, followed by re-hybridization, as described above.

The metaphase images of each species or accession were captured with a Leica DM5500B fluorescence microscope and uniformly adjusted for brightness and contrast in Adobe Photoshop CC (2019) software. The chromosomes were ordered in karyograms following their orthology and the schematic representation of them was constructed based in the observation of at least five metaphases. Barcode and painting probes are visualized with the same colour as the fluorophore used during detection, while rDNA and CentPv1 were artificially coloured using Adobe Photoshop.

Molecular dated tree and estimative of chromosomal evolution rates

To estimate the rate of chromosome evolution at different lineages, we constructed and dated a phylogenetic tree, which included *Vigna nakashimae* and *Macroptilium atropurpureum* as outgroups and the nine *Phaseolus* species analysed in this work. Available low coverage sequencing data deposited in GenBank (Accession numbers are described in Table S1) for all the species were used to assemble circularized plastid contigs with NovoPlasty v. 4.3 (Dierckxsens *et al*., 2016). The contigs were analysed, aligned using MUSCLE as a plugin in Geneious platform v. 7.1.9 (Kearse *et al.*, 2012) and then concatenated. The phylogenetic relationships were inferred with Bayesian Inference model (BI) using BEAUti and BEAST (v. 1.10.4) for inference and dating (Drummond *et al.*, 2012). We selected the GTR substitution model and the uncorrelated relaxed clock with lognormal distribution. The Markov Chain Monte Carlo (MCMC) runs were conducted for 10,000,000 generations, sampling each 1,000 generations. Since *Phaseolus* is a recent group, we used the Birth-Death speciation model (Gernhard, 2008). The estimated divergence date between *Vigna* and *Phaseolus* (9.7 Mya) (Li *et al.*, 2013) was used as calibration point. The runs were analysed with the TRACER software

(v. 1.7) for parameters of distribution (Rambaut *et al.*, 2018). 95% of the generated trees were burned and the final tree was constructed with TreeAnnotator (v. 1.10.4) (Rambaut and Drummond, 2013), visualized and edited in FigTree (v. 1.4.4) (Rambaut, 2018) (Fig. S2). The chromosome rearrangements identified were indicated in the corresponding branches of the tree and the number of rearrangements were divided by the age of the most recent ancestral node for estimating chromosomal evolution rates for each lineage.

ACKNOWLEDGMENTS

We thank CIAT, Embrapa Cenargen and IPK for providing the seeds. We thank CNPq (Conselho Nacional de Desenvolvimento Científico e Tecnológico, Grant no. 310804/2017-5) and CAPES (Coordenação de Aperfeiçoamento de Pessoal de Nível Superior, Financial Code 001) for the financial support. We also thank Bruna Zirpoli for reading the first version of the manuscript and Fernanda de Oliveira Bustamante, Lívia do Vale Martins, Guilherme Tomaz Braz, Jiming Jiang and Ana Christina Brasileiro-Vidal for development of oligo-FISH probes.

AUTHORS CONTRIBUTIONS

THN: conducted the experiments, analysed the data, constructed the figures and wrote the paper. APH: conceived this research, provided the resources, discussed the results and helped to write the paper.

CONFLICT OF INTEREST

The authors declare no conflicts of interest.

ETHICS APPROVAL

Not applicable.

DATA AVABIALITY

All data generated or analysed during this study are included as supplementary materials.

SUPPORTING INFORMATION

Figure S1. *P. leptostachyus* zygotene exhibiting more than one 5S rDNA loci

Figure S2. Phylogenetic tree based on the circular plastidial contigs.

Table S1. Accessions of sequencing data deposited in GenBank.

REFERENCES

Almeida, C. and Pedrosa-Harand, A. (2011) Contrasting rDNA evolution in lima bean (*Phaseolus lunatus* L.) and common bean (*P. vulgaris L.*, Fabaceae). *Cytogenet. Genome Res.*, **132**, 212–217.

Barker, M.S., Baute, G.J. and Liu, S.-L. (2012) Duplications and Turnover in Plant Genomes. In J. F. Wendel, J. Greilhuber, J. Dolezel, and I. J. Leitch, eds. *Plant Genome Diversity Volume 1: Plant Genomes, their Residents, and their Evolutionary Dynamics*. Vienna: Springer Vienna, pp. 155–169. Available at: http://link.springer.com/10.1007/978-3-7091-1130-7.

Benathar, T.C.M., Nagamachi, C.Y., Rodrigues, L.R.R., O'Brien, P.C.M., Ferguson-Smith, M.A., Yang, F. and Pieczarka, J.C. (2019) Karyotype, evolution and phylogenetic reconstruction in Micronycterinae bats with implications for the ancestral karyotype of Phyllostomidae. *BMC Evolutionary Biology*, **19**.

Bonifácio, E.M., Fonsêca, A., Almeida, C., Santos, K.G.B. dos and Pedrosa-Harand, A. (2012) Comparative cytogenetic mapping between the lima bean (*Phaseolus lunatus* L.) and the common bean (*P. vulgaris* L.). *Theoretical and Applied Genetics*, **124**, 1513–1520.

Braz, G.T., He, L., Zhao, H., Zhang, T., Semrau, K., Rouillard, J.-M., Torres, G.A. and Jiang, J. (2018) Comparative Oligo-FISH Mapping: An Efficient and Powerful Methodology To Reveal Karyotypic and Chromosomal Evolution. *Genetics*, **208**, 513–523.

Braz, G.T., Yu, F., Vale Martins, L. do and Jiang, J. (2020) Fluorescent *In Situ* Hybridization Using Oligonucleotide-Based Probes. In *In Situ Hybridization Protocols, Methods in Molecular Biology*. pp. 71–83.

Braz, G.T., Yu, F., Zhao, H., Deng, Z., Birchler, J.A. and Jiang, J. (2021) Preferential meiotic chromosome pairing among homologous chromosomes with cryptic sequence variation in tetraploid maize. *New Phytologist*, **229**, 3294–3302. Available at: https://onlinelibrary.wiley.com/doi/10.1111/nph.17098.

Broughton, W.J., Hern, aacute, Ndez, G., Blair, M., Beebe, S., Gepts, P. and Vanderleyden, J. (2003) Beans (*Phaseolus* spp.) - model food legumes. *Plant and Soil*, **252**, 55–128.

Carvalho, C.R. De and Saraiva, L.S. (1993) An Air Drying Technique for Maize Chromosomes without Enzymatic Maceration. *Biotechnic & Histochemistry*, **68**, 142–145.

Chen, L., Su, D., Sun, J., Li, Z. and Han, Y. (2020) Development of a set of chromosome-specific oligonucleotide markers and karyotype analysis in the Japanese morning glory *Ipomoea* nil. *Scientia Horticulturae*, **273**, 109633.

De Oliveira Bustamante, F., Do Nascimento, T.H., Júnior, C.M., et al. (2021) Oligo-FISH barcode in beans: a new chromosome identification system. *Theor. Appl. Genet.* Available at: https://link.springer.com/10.1007/s00122-021-03921-z.

Delgado-Salinas, A., Bibler, R. and Lavin, M. (2006) Phylogeny of the Genus *Phaseolus* (Leguminosae): A Recent Diversification in an Ancient Landscape. *Systematic Botany*, **31**, 779–791.

Dierckxsens, N., Mardulyn, P. and Smits, G. (2016) NOVOPlasty: de novo assembly of organelle genomes from whole genome data. *Nucleic Acids Res*. Available at: https://academic.oup.com/nar/article-lookup/doi/10.1093/nar/gkw955.

Do Vale Martins, L., Oliveira Bustamante, F. de, Silva Oliveira, A.R. da, et al. (2021) BAC- and oligo-FISH mapping reveals chromosome evolution among *Vigna angularis*, *V. unguiculata*, and *Phaseolus vulgaris*. *Chromosoma*.

Do Vale Martins, L., Yu, F., Zhao, H., et al. (2019) Meiotic crossovers characterized by haplotype-specific chromosome painting in maize. *Nature Communications*, **10**, 4604. Available at: http://dx.doi.org/10.1038/s41467-019-12646-z.

Drummond, A.J., Suchard, M.A., Xie, D. and Rambaut, A. (2012) Bayesian Phylogenetics with BEAUti and the BEAST 1.7. *Molecular Biology and Evolution*, **29**, 1969–1973.

Ferraz, M.E., Fonsêca, A. and Pedrosa-Harand, A. (2020) Multiple and independent rearrangements revealed by comparative cytogenetic mapping in the dysploid Leptostachyus group (*Phaseolus* L., Leguminosae). *Chromosome Research*, **28**, 395–405.

Fonsêca, A., Ferraz, M.E. and Pedrosa-Harand, A. (2016) Speeding up chromosome evolution in *Phaseolus*: multiple rearrangements associated with a one-step descending dysploidy. *Chromosoma*, **125**, 413–421. Available at: http://dx.doi.org/10.1007/s00412-015-0548-3.

Fonsêca, A., Ferreira, J., Santos, T.R.B. dos, et al. (2010) Cytogenetic map of common bean (*Phaseolus vulgaris* L.). *Chromosome Research*, **18**, 487–502.

Fonsêca, A. and Pedrosa-Harand, A. (2013) Karyotype stability in the genus *Phaseolus* evidenced by the comparative mapping of the wild species *Phaseolus microcarpus* G. J. Scoles, ed. *Genome*, **56**, 335–343.

Fonsêca, A. and Pedrosa-Harand, A. (2017) Cytogenetics and Comparative Analysis of *Phaseolus* Species. In *The comoon bean Genome*. pp. 57–68. Available at: http://link.springer.com/10.1007/978-3-319-63526-2_3.

Fransz, P., Linc, G., Lee, C., et al. (2016) Molecular, genetic and evolutionary analysis of a paracentric inversion in Arabidopsis thaliana. *Plant J.*, **88**, 159–178. Available at: https://onlinelibrary.wiley.com/doi/10.1111/tpj.13262.

Garcia, T., Duitama, J., Zullo, S., et al. (2020) Comprehensive genomic resources related to domestication and crop improvement traits in Lima bean. *Nat. Res.* Available at: https://doi.org/10.21203/rs.3.rs-95762/v1.

Gernhard, T. (2008) The conditioned reconstructed process. *Journal of Theoretical Biology*, **253**, 769–778.

Han, Y., Zhang, T., Thammapichai, P., Weng, Y. and Jiang, J. (2015) Chromosome-Specific Painting in *Cucumis* Species Using Bulked Oligonucleotides. *Genetics*, **200**, 771–779. Available at: http://www.genetics.org/lookup/doi/10.1534/genetics.115.177642.

He, L., Zhao, H., He, J., et al. (2020) Extraordinarily conserved chromosomal synteny of Citrus species revealed by chromosome-specific painting. *Plant J.*, **103**, 2225–2235. Available at: https://onlinelibrary.wiley.com/doi/10.1111/tpj.14894.

Iwata, A., Tek, A.L., Richard, M.M.S., et al. (2013) Identification and characterization of functional centromeres of the common bean. *Plant Journal*, **76**, 47–60.

Jiang, J. (2019) Fluorescence *in situ* hybridization in plants: recent developments and future applications. *Chromosome Research*, **27**, 153–165. Available at: http://link.springer.com/10.1007/s10577-019-09607-z.

Kearse, M., Moir, R., Wilson, A., et al. (2012) Geneious Basic: An integrated and extendable desktop software platform for the organization and analysis of sequence data. *Bioinformatics*, **28**, 1647–1649.

Lewis, G., Schrire, B., Mackinder, B. and Lock, M. (2005) *Legumes of the world* 1 ed., London, UK: Royal Botanic Garden, Kew.

Li, H., Wang, W., Lin, L., Zhu, Xiangyun, Li, J., Zhu, Xinyu and Chen, Z. (2013) Diversification of the phaseoloid legumes: effects of climate change, range expansion and habit shift. *Frontiers in Plant Science*, **4**, 1–9.

Liu, X., Sun, S., Wu, Y., et al. (2020) Dual-color oligo-FISH can reveal chromosomal variations and evolution in *Oryza* species. *The Plant Journal*, **101**, 112–121.

Llaca, V., Delgado Salinas, A. and Gepts, P. (1994) Chloroplast DNA as an evolutionary marker in the *Phaseolus vulgaris* complex. *Theor. Appl. Genet.*, **88**, 646–652.

Lonardi, S., Muñoz-Amatriaín, M., Liang, Q., et al. (2019) The genome of cowpea (*Vigna unguiculata* [L.] Walp.). *The Plant Journal*, **98**, 767–782.

Lysak, M.A., Berr, A., Pecinka, A., Schmidt, R., McBreen, K. and Schubert, I. (2006) Mechanisms of chromosome number reduction in *Arabidopsis* thaliana and related Brassicaceae species. *Proc. Natl. Acad. Sci.*, **103**, 5224–5229. Available at: http://www.pnas.org/cgi/doi/10.1073/pnas.0510791103.

Lysak, M.A., Mandáková, T. and Schranz, M.E. (2016) Comparative paleogenomics of crucifers: Ancestral genomic blocks revisited. *Curr. Opin. Plant Biol.*, **30**, 108–115.

Mandáková, T., Hloušková, P., Koch, M.A. and Lysak, M.A. (2020) Genome Evolution in Arabideae Was Marked by Frequent Centromere Repositioning. *The Plant Cell*, **32**, 650–665. Available at: http://www.plantcell.org/lookup/doi/10.1105/tpc.19.00557.

Mandáková, T. and Lysak, M.A. (2018) Post-polyploid diploidization and diversification through dysploid changes. Curr. Opin. Plant Biol., 42, 55–65. Available at: https://linkinghub.elsevier.com/retrieve/pii/S1369526617301899.

Maruyama, T. and Imai, H.T. (1981) Evolutionary rate of the mammalian karyotype. *J. Theor. Biol.*, **90**, 111–121. Available at: https://linkinghub.elsevier.com/retrieve/pii/0022519381901259.

Meng, Z., Han, J., Lin, Y., et al. (2020) Characterization of a *Saccharum spontaneum* with a basic chromosome number of $x = 10$ provides new insights on genome evolution in genus *Saccharum*. *Theoretical and Applied Genetics*, **133**, 187–199.

Mercado-Ruaro, P. and Delgado-Salinas, A. (1996) Karyological studies in several Mexican species of *Phaseolus* L. and *Vigna* Savi (Phaseolinae, Fabaceae). In *Advances in legume systematics 8, Legumes of economic importance*. Royal Botanic Gardens, Kew., pp. 83–87.

Mercado-Ruaro, P. and Delgado-Salinas, A. (1998) Karyotypic studies on species of *Phaseolus* (Fabaceae: Phaseolinae). *American Journal of Botany*, **85**, 1–9. Available at: http://doi.wiley.com/10.2307/2446547.

Mercado-Ruaro, P., Delgado-Salinas, A. and Chiang, F. (2009) Taxonomic re-assessment of *Phaseolus dasycarpus* (Leguminosae): Systematic position, chromosome studies and re-description. *Brittonia*, **61**, 8–13.

Mérot, C., Oomen, R.A., Tigano, A. and Wellenreuther, M. (2020) A Roadmap for Understanding the Evolutionary Significance of Structural Genomic Variation. *Trends in Ecology and Evolution*, **35**, 561–572. Available at: https://doi.org/10.1016/j.tree.2020.03.002.

Mina-Vargas, A.M., McKeown, P.C., Flanagan, N.S., Debouck, D.G., Kilian, A., Hodkinson, T.R. and Spillane, C. (2016) Origin of year-long bean (*Phaseolus dumosus* Macfady, Fabaceae) from reticulated hybridization events between multiple Phaseolus species. *Ann. Bot.*, **118**, 957–969

Moghaddam, S.M., Oladzad, A., Koh, C., et al. (2021) The tepary bean genome provides insight into evolution and domestication under heat stress. *Nat. Commun.*, **12**, 1–14.

Moscone, E.A., Klein, F., Lambrou, M., Fuchs, J. and Schweizer, D. (1999) Quantitative karyotyping and dual-color FISH mapping of 5S and 18S-25S rDNA probes in the cultivated *Phaseolus* species (Leguminosae). *Genome*, **42**, 1224–1233.

Mudd, A.B., Bredeson, J. V., Baum, R., Hockemeyer, D. and Rokhsar, D.S. (2020) Analysis of muntjac deer genome and chromatin architecture reveals rapid karyotype evolution. *Commun. Biol.*, **3**, 480. Available at: http://dx.doi.org/10.1038/s42003-020-1096-9

Nelson, T.C., Monnahan, P.J., McIntosh, M.K., Anderson, K., MacArthur-Waltz, E., Finseth, F.R., Kelly, J.K. and Fishman, L. (2019) Extreme copy number variation at a tRNA ligase gene affecting phenology and fitness in yellow monkeyflowers. *Molecular Ecology*, **28**, 1460–1475. Available at: https://onlinelibrary.wiley.com/doi/10.1111/mec.14904.

Pedrosa-Harand, A., Almeida, C.C.S. De, Mosiolek, M., Blair, M.W., Schweizer, D. and Guerra, M. (2006) Extensive ribosomal DNA amplification during Andean common bean (*Phaseolus vulgaris* L.) evolution. *Theor. Appl. Genet.*, **112**, 924–933.

Peer, Y. Van De, Mizrachi, E. and Marchal, K. (2017) The evolutionary significance of polyploidy. *Nat. Rev. Genet.*, **18**, 411–424. Available at: http://dx.doi.org/10.1038/nrg.2017.26.

Piperidis, N. and D'Hont, A. (2020) Sugarcane genome architecture decrypted with chromosome-specific oligo probes. *Plant J.*, **103**, 2039–2051. Available at: https://onlinelibrary.wiley.com/doi/10.1111/tpj.14881.

Porubsky, D., Sanders, A.D., Höps, W., et al. (2020) Recurrent inversion toggling and great ape genome evolution. *Nature Genetics*, **52**, 849–858.

POWO (2021) Plants of the World Online. Facilitated by the Royal Botanic Gardens, Kew. Published on the Internet; http://www.plantsoftheworldonline.org/. Retrieved 14 December 2021.

Rambaut, A. (2018) FigTree v 1.4.4.

Rambaut, A. and Drummond, A.J. (2013) TreeAnnotator v1.10.4. Available as Part of the BEAST package. *http://beast.bio.ed.ac.uk.*

Rambaut, A., Drummond, A.J., Xie, D., Baele, G. and Suchard, M.A. (2018) Posterior Summarization in Bayesian Phylogenetics Using Tracer 1.7 E. Susko, ed. *Systematic Biology*, **67**, 901–904.

Rendón-Anaya, M., Montero-Vargas, J.M., Saburido-Álvarez, S., et al. (2017) Genomic history of the origin and domestication of common bean unveils its closest sister species. *Genome Biol.*, **18**, 1–17.

Ribeiro, T., Santos, K.G.B. dos, Richard, M.M.S., Sévignac, M., Thareau, V., Geffroy, V. and Pedrosa-Harand, A. (2017) Evolutionary dynamics of satellite DNA repeats from *Phaseolus* beans. *Protoplasma*, **254**, 791–801.

Schmutz, J., McClean, P.E., Mamidi, S., et al. (2014) A reference genome for common bean and genome-wide analysis of dual domestications. *Nature Genetics*, **46**, 707–713.

Sotero-Caio, C.G., Volleth, M., Hoffmann, F.G., Scott, L.A., Wichman, H.A., Yang, F. and Baker, R.J. (2015) Integration of molecular cytogenetics, dated molecular phylogeny, and

model-based predictions to understand the extreme chromosome reorganization in the Neotropical genus *Tonatia* (Chiroptera: Phyllostomidae). *BMC Evol. Biol.*, **15**, 1–15. Available at: http://dx.doi.org/10.1186/s12862-015-0494-y.

Storme, N. De and Mason, A. (2014) Plant speciation through chromosome instability and ploidy change: Cellular mechanisms, molecular factors and evolutionary relevance. *Curr. Plant Biol.*, **1**, 10–33. Available at: http://dx.doi.org/10.1016/j.cpb.2014.09.002.

Thompson, M.J. and Jiggins, C.D. (2014) Supergenes and their role in evolution. *Heredity*, **113**, 1–8. Available at: http://www.nature.com/articles/hdy201420.

Vlasova, A., Capella-Gutiérrez, S., Rendón-Anaya, M., et al. (2016) Genome and transcriptome analysis of the Mesoamerican common bean and the role of gene duplications in establishing tissue and temporal specialization of genes. *Genome Biol.*, **17**, 1–18. Available at: http://dx.doi.org/10.1186/s13059-016-0883-6.

Waminal, N.E., Pellerin, R.J., Kang, S.-H. and Kim, H.H. (2021) Chromosomal Mapping of Tandem Repeats Revealed Massive Chromosomal Rearrangements and Insights Into *Senna tora* Dysploidy. *Frontiers in Plant Science*, **12**, 1–13. Available at: https://www.frontiersin.org/articles/10.3389/fpls.2021.629898/full.

Weissensteiner, M.H., Bunikis, I., Catalán, A., et al. (2020) Discovery and population genomics of structural variation in a songbird genus. *Nature Communications*, **11**, 3403. Available at: http://www.nature.com/articles/s41467-020-17195-4.

Wellenreuther, M. and Bernatchez, L. (2018) Eco-Evolutionary Genomics of Chromosomal Inversions. *Trends in Ecology and Evolution*, **33**, 427–440. Available at: https://doi.org/10.1016/j.tree.2018.04.002.

Winterfeld, G., Becher, H., Voshell, S., Hilu, K. and Röser, M. (2018) Karyotype evolution in *Phalaris* (Poaceae): The role of reductional dysploidy, polyploidy and chromosome alteration in a wide-spread and diverse genus L. Peruzzi, ed. *PLOS ONE*, **13**, e0192869. Available at: https://dx.plos.org/10.1371/journal.pone.0192869.

TABLES

Table 1. Summary of the chromosomal rearrangement number and type, ages (in My) of each clade and their respective chromosomal evolution rates calculated separately for structural rearrangements (CE) and changes in rDNA (CErDNA).

Groups/ clades	Species	Number of Structural changes	Description	Number of rDNA changes	Description	Age	CER	CErDNA
Clade A	*P. microcarpus*	3	Inv3/Del3/TP10	1	5S4	4.6	0.65	0.22
Filiformis	*P. filiformis*	3	Tr1-3/Tr3-7/Tr7-1	2	5S2/5S4	2.8	1.07	0.71
Vulgaris	*P. acutifolius*	1	Inv10	1	5S8	2.2	0.45	0.45
	P. coccineus	2	Inv2/Inv9	4	5S3/5S6/35S9/35S10	2.2	0.91	1.82
	P. dumosus	2	Inv2/Inv9	1	35S11	2.2	0.91	0.45
	P. vulgaris 'G19833'	2	Inv2/Inv9	7	5S6/35S1/35S3/35S4/35S5/35S9/35S10	2.2	0.91	3.18
	P. vugaris 'BAT93'	2	Inv2/Inv9	3	5S6/35S9/35S10	2.2	0.91	1.36
Leptostachyus	*P. leptostachyus*	16	2Tr1/Tr2/Dup2/Dup3/Del 3/3Tr4/3Tr5/Tr6/Tr7/Inv9 /NCF10-11	2	Dup5S10-11/Inv5S10	1.37	11.68	1.46
	P. macvaughii	5	Tr1-2/Dup2/Dup5/NCF10-11/Inv4	1	Inv5S10	1.37	3.65	0.73
Lunatus	*P. lunatus*	1	Dup4	1	Inv5S10	2.5	0.40	0.40

Del- Deletion; Inv- Inversion; F- Fusion, Tr- Translocation; TP- Transposition; NCF- Nestled Chromosome Fusion; CER- Chromosomal Evolution Rate; CErDNA- CER for rDNA loci

LEGENDS

Figure 1. Chromosome identification by oligo-FISH barcode, *Pv2* and *Pv3* painting, 5S and 35S rDNA and CentPv1 centromeric repeat in *Phaseolus* species. **(a** and **a')** *P. microcarpus* (*Pmi*), insets in **a** highlight the pericentric inversion in *Pmi2*, the deletion of one red signal in *Pmi3* and small signals in *Pmi4* and *Pmi5*. **(b** and **b')** *P. filiformis*, insets in **b** and **b'** display the small green barcode signal in *Pfi3* and small signals in *Pfi5*, besides of segment of *Pfi3* translocated to *Pfi7*, respectively. **(c** and **c')** *P. acutifolius* (*Pac*), insets in **c** show details of *Pac2* and *Pac3***. (d** and **d')** *P. coccineus* (*Pco*), inserts in **d'** evidence the CentPv1 centromeric signal in *Pco6* co-localized with 5S rDNA locus. **(e** and **e')** *P. vulgaris* 'G19833' (*Pv* 'G19833'), insets in **e'** evidence a small 35S rDNA *locus* in *Pv4*. **(f** and **f')** *P. vulgaris* 'BAT93' (*Pv* 'BAT93'), insets in **f** evidence weak signals in *Pv2*, *4* and *11*, while insert in **f'** amplify the 5S rDNA locus in *Pv10*. **(g** and **g')** *P. dumosus* (*Pdu*), inserts in **g'** highlight smaller 35S rDNA loci. **(h** and **h')** *P. leptostachyus* (*Ple*) with inset in **h** evidencing small signals in *Ple2*. **(i** and **i')** *P. macvaughii* (*Pma*), insers in **i** display signals of *Pma1*, *2* and *3*. **(j** and **j')** *P. lunatus* (*Plu*), insert in **j** evidences a small green signal in *Plu8*. Bar corresponds to 5 µm.

Figure 2. Karyograms of the nine analysed *Phaseolus* species and two *P. vulgaris* accessions plotted in a phylogenetic tree. For each species, the upper lane shows the barcode signals in green and red, and the bottom lane shows the *Pv*2 (green) and *Pv*3 (red) painting probes, as well as the 5S (yellow) and 35S (purple) rDNA probes. For *P. coccineus*, *P. dumosus* and *P. vulgaris*, CentPv1 probe (blue) is present in the centromeric region of some chromosome pairs. The chromosomes are ordered according to putative orthology to *P. vulgaris*, with centromere aligned by a dotted white line. The arrowheads point to differences in the barcode or painting pattern in comparison to *P. vulgaris*.

Figure 3. Schematic representation of *Phaseolus* karyotypes based on the distribution of oligo-FISH barcode signals (green and red dots), painting (green and red segments for *Pv2* and *Pv3*, respectively), 5S (yellow dots) and 35S (purple segments) rDNA loci and CentPv1 (blue segments at centromeric regions of *P. coccineus, P. dumosus and P. vulgaris*). Vertical arrows in different directions represent inversions (except for the indication of the hybrid origin of *P. dumosus*), Tr translocations, while NCF represents Nested Chromosome Fusion; minus signs represent deletions, while plus signs represent duplications of signals. Exclusive rDNA sites are indicated with black dots. Independent

and shared rearrangements are indicated in the nodes and clades of the dated phylogenetic tree. Rearrangements in rDNA loci are represented in blue and rearrangements detected by oligo-FISH probes in red. All codes are preceded by the occurrence number and followed by the respective rearranged ortholog. In the right side, numbers after G and R letters represent the total number of barcode green and red signals, respectively.

Figure 4. Schematic representation of the complex translocation involving chromosomes 1, 3 and 7 of *P. filiformis*. *Pfi*1 probably received a segment from *Pfi*7 containing one barcode red signal and donated a segment to *Pfi*3 containing one barcode green signal. *Pfi*3 donated a segment to *Pfi*7 detected by the red painting probe.

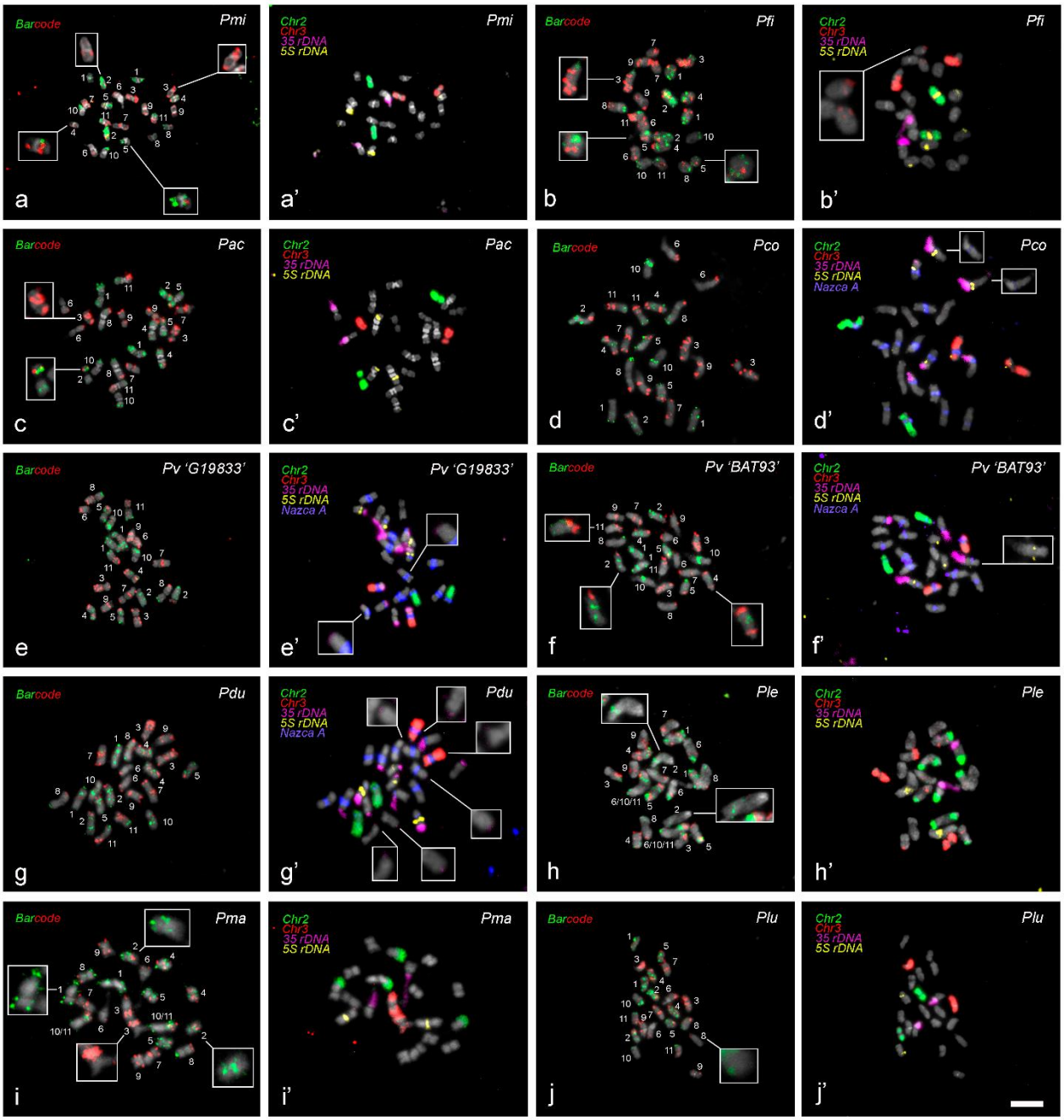

Figure 1. Chromosome identification by oligo-FISH barcode, *Pv2* and *Pv3* painting, 5S and 35S rDNA and CentPv1 centromeric repeat in *Phaseolus* species. **(a** and **a') ***P. microcarpus* (*Pmi*), insets in **a** highlight the pericentric inversion in *Pmi2*, the deletion of one red signal in *Pmi3* and small signals in *Pmi4* and *Pmi5*. **(b** and **b') ***P. filiformis*, insets in **b** and **b'** display the small green barcode signal in *Pfi3* and small signals in *Pfi5*, besides of segment of *Pfi3* translocated to *Pfi7*, respectively. **(c** and **c') ***P. acutifolius* (*Pac*), insets in **c** show details of *Pac2* and *Pac3*. **(d** and **d') ***P. coccineus* (*Pco*), inserts in **d'** evidence the CentPv1 centromeric signal in *Pco6* co-localized with 5S rDNA locus. **(e** and **e') ***P.*

vulgaris 'G19833' (*Pv* 'G19833'), insets in **e'** evidence a small 35S rDNA *locus* in *Pv4*. **(f** and **f')** *P. vulgaris* 'BAT93' (*Pv* 'BAT93'), insets in **f** evidence weak signals in *Pv2*, *4* and *11*, while insert in **f'** amplify the 5S rDNA locus in *Pv10*. **(g** and **g')** *P. dumosus* (*Pdu*), inserts in **g'** highlight smaller 35S rDNA loci. **(h** and **h')** *P. leptostachyus* (*Ple*) with inset in **h** evidencing small signals in *Ple2*. **(i** and **i')** *P. macvaughii* (*Pma*), insers in **i** display signals of *Pma1*, *2* and *3*. **(j** and **j')** *P. lunatus* (*Plu*), insert in **j** evidences a small green signal in *Plu8*. Bar corresponds to 5 µm.

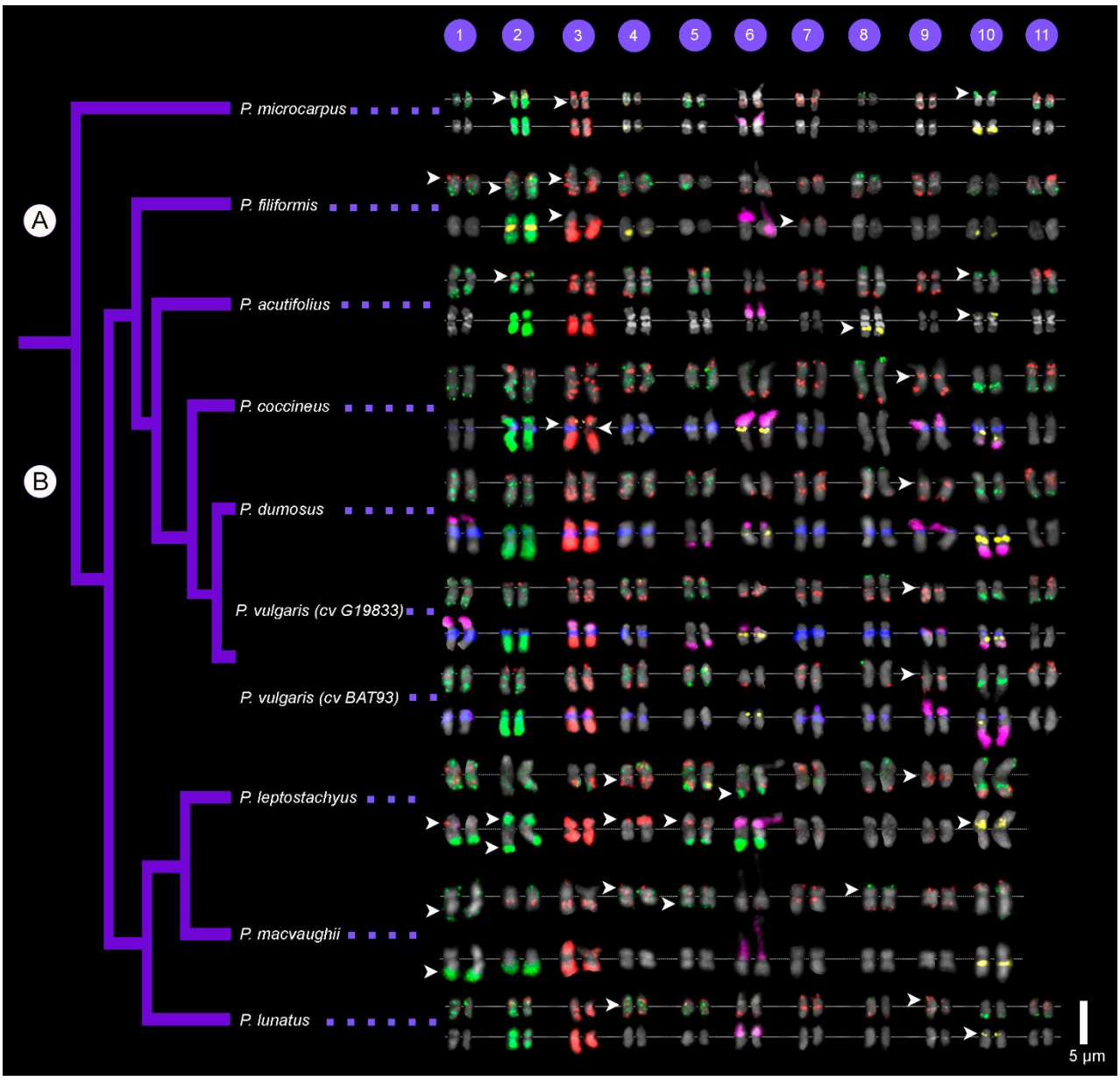

Figure 2. Karyograms of the nine analysed *Phaseolus* species and two *P. vulgaris* accessions plotted in a phylogenetic tree. For each species, the upper lane shows the barcode signals in green and red, and the bottom lane shows the *Pv*2 (green) and *Pv*3 (red)

painting probes, as well as the 5S (yellow) and 35S (purple) rDNA probes. For *P. coccineus*, *P. dumosus* and *P. vulgaris*, CentPv1 probe (blue) is present in the centromeric region of some chromosome pairs. The chromosomes are ordered according to putative orthology to *P. vulgaris*, with centromere aligned by a dotted white line. The arrowheads point to differences in the barcode or painting pattern in comparison to *P. vulgaris*.

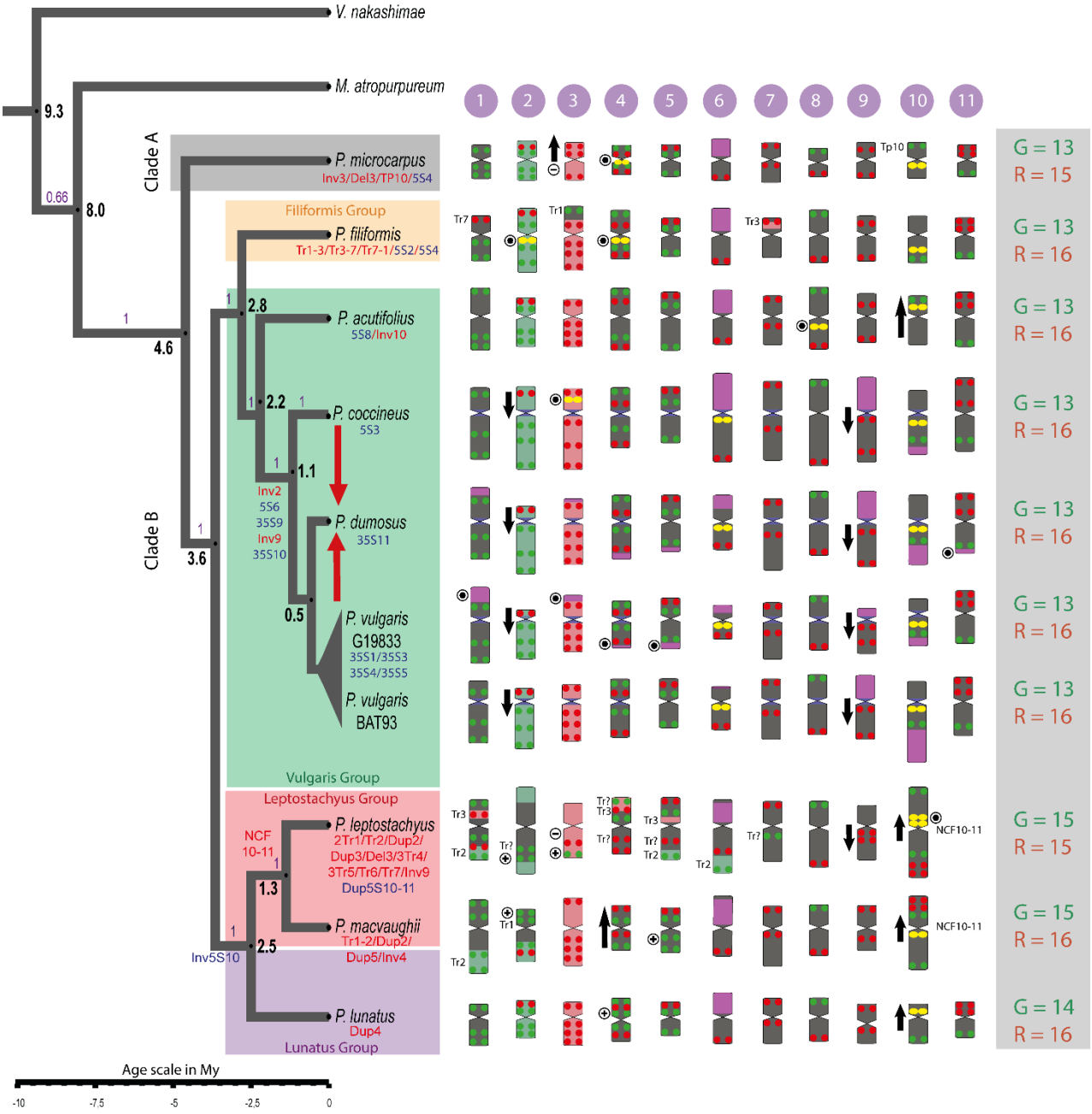

Figure 3. Schematic representation of *Phaseolus* karyotypes based on the distribution of oligo-FISH barcode signals (green and red dots), painting (green and red segments for

Pv2 and *Pv3*, respectively), 5S (yellow dots) and 35S (purple segments) rDNA loci and CentPv1 (blue segments at centromeric regions of *P. coccineus*, *P. dumosus and P. vulgaris*). Vertical arrows in different directions represent inversions (except for the indication of the hybrid origin of *P. dumosus*), Tr translocations, while NCF represents Nested Chromosome Fusion; minus signs represent deletions, while plus signs represent duplications of signals. Exclusive rDNA sites are indicated with black dots. Independent and shared rearrangements are indicated in the nodes and clades of the dated phylogenetic tree. Rearrangements in rDNA loci are represented in blue and rearrangements detected by oligo-FISH probes in red. All codes are preceded by the occurrence number and followed by the respective rearranged ortholog. In the right side, numbers after G and R letters represent the total number of barcode green and red signals, respectively.

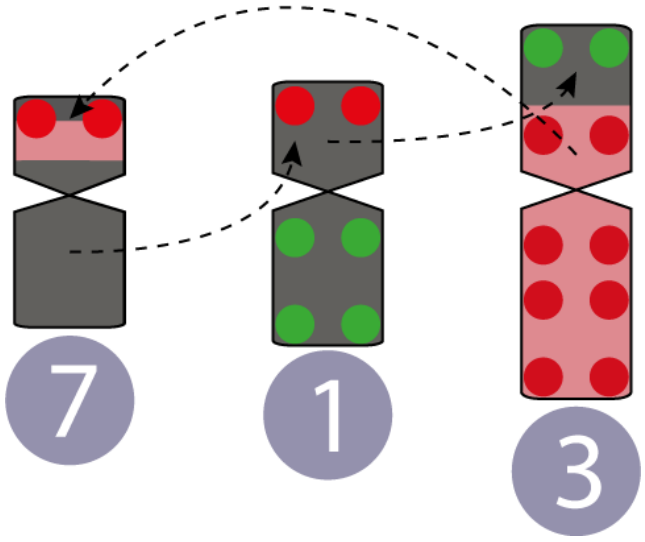

Figure 4. Schematic representation of the complex translocation involving chromosomes 1, 3 and 7 of *P. filiformis*. *Pfi*1 probably received a segment from *Pfi*7 containing one barcode red signal and donated a segment to *Pfi*3 containing one barcode green signal. *Pfi*3 donated a segment to *Pfi*7 detected by the red painting probe.

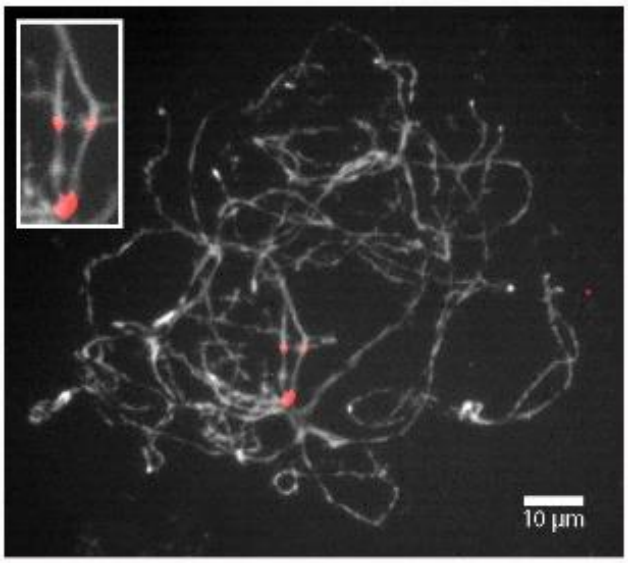

Figure S1. *P. leptostachyus* zygotene exhibiting more than one 5S rDNA loci

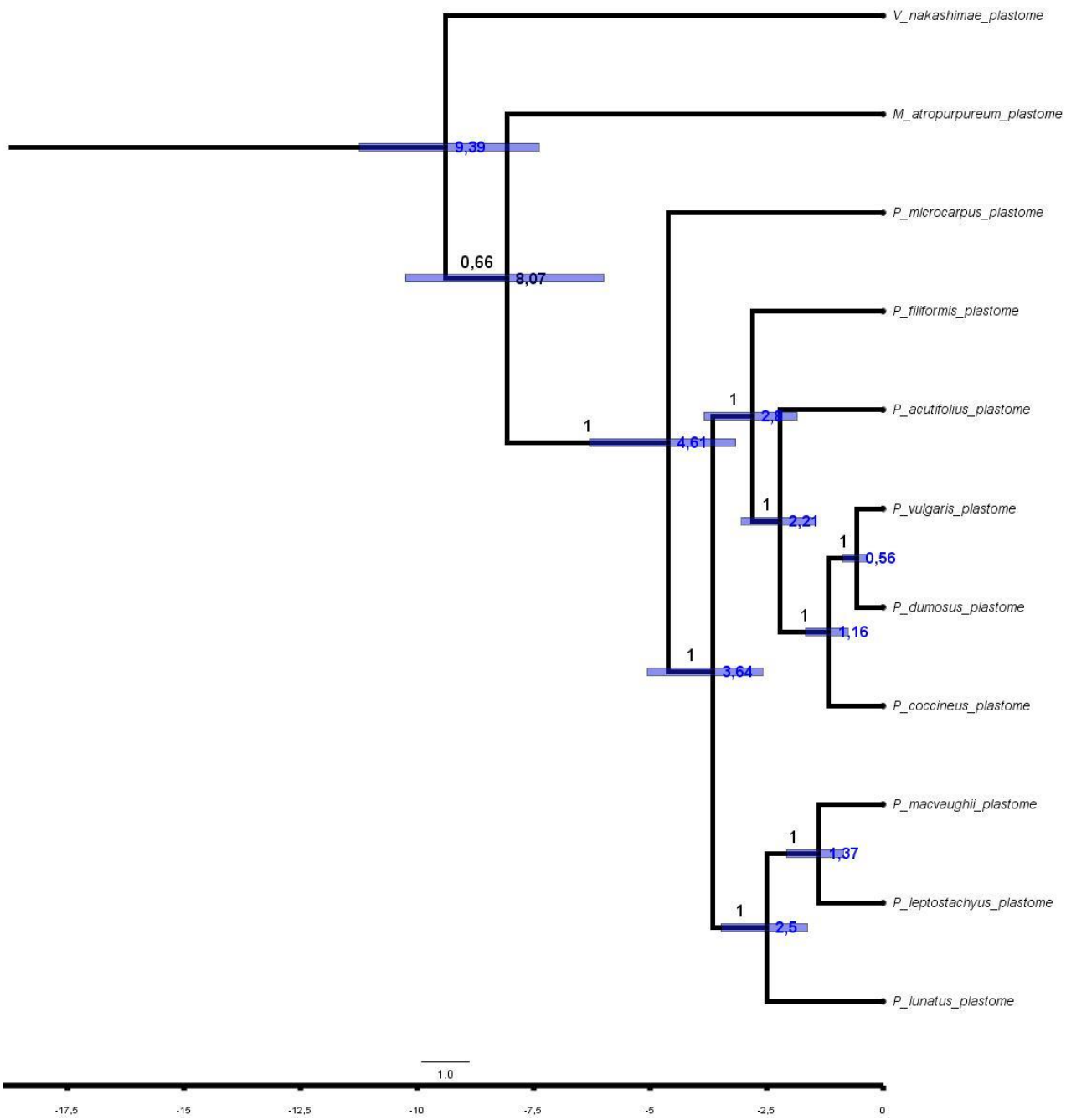

Figure S2. Phylogenetic tree based on the circular plastidial contigs.

Table S1. Sequence data of the species used for the Phylogenetic analyses.

Species	Accession numbers
Vigna nakashimae	SRX758247
Macroptilium atropurpureum	xxxxxx
Phaseolus microcarpus	SRS1938373
Phaseolus filiformis	SRS1938376
Phaseolus acutifolius	SRS1938375
Phaseolus coccineus	SRS1938377
Phaseolus vulgaris	SRR1005889
Phaseolus dumosus	SRS1938378
Phaseolus leptostachyus	SRS1938371
Phaseolus macvaughii	xxxxxx
Phaseolus lunatus	SRS1938374

5. CONCLUSÕES

- Foi estabelecido o primeiro sistema oligo-FISH *barcode* para leguminosas com base no genoma de *Vigna unguiculata* em comparação com o genoma de *Phaseolus vulgaris*;
- O sistema oligo-FISH *barcode* se mostrou eficiente e permitiu estabelecer as ortologias cromossômicas entre *V. unguiculata* e *P. vulgaris*, corroborando rearranjos previamente identificados por meio de BAC-FISH e revelando rearranjos inéditos entre as duas espécies;
- O uso de oligo-FISH *barcode*, pintura cromossômica, DNAr e um *repeat* centromérico (CentPv1) como sondas, aliadas a uma abordagem filogenômica, tornou possível o estabelecimento de ortologias em uma ampla amostragem de espécies do gênero *Phaseolus*, permitindo inferir taxas de evolução cromossômica (rearranjos estruturais/milhão de ano);
- Translocações em *Phaseolus*, antes hipostenizadas como exclusivas do grupo disploide Leptostachyus, foram reveladas no grupo Filiformis;
- O grupo Leptostachyus sofreu uma reestruturação genômica significativa em um curto espaço de tempo evolutivo, em especial *P. leptostachyus* que apresentou uma taxa de evolução cromossômica 10 vezes maior que a do grupo Vulgaris. *Phaseolus leptostachyus* é a planta que sofreu reestruturação genômica mais rápida registrada até o momento, superando inclusive taxas de evolução cromossômica descritas para vertebrados.

6. ANEXOS

6.1. Regras para submissão no periódico Theoretical and Appplied Genetics

Versão completa disponível em: <https://www.springer.com/journal/122/submission-guidelines>

Submission guidelines

Instructions for Authors

Manuscript Submission

Manuscript Submission

Submission of a manuscript implies: that the work described has not been published before; that it is not under consideration for publication anywhere else; that its publication has been approved by all co-authors, if any, as well as by the responsible authorities – tacitly or explicitly – at the institute where the work has been carried out. The publisher will not be held legally responsible should there be any claims for compensation.

Permissions

Authors wishing to include figures, tables, or text passages that have already been published elsewhere are required to obtain permission from the copyright owner(s) for both the print and online format and to include evidence that such permission has been granted when submitting their papers. Any material received without such evidence will be assumed to originate from the authors.

Online Submission

Please follow the hyperlink “Submit manuscript” on the right and upload all of your manuscript files following the instructions given on the screen.

Please ensure you provide all relevant editable source files. Failing to submit these source files might cause unnecessary delays in the review and production process.

6.2. Regras para submissão no periódico The Plant Journal

the plant journal

Edited By: Lee Sweetlove
Impact factor: 6.417
CiteScore: 11
2020 Journal Citation Reports (Clarivate Analytics): 15/235 (Plant Sciences)
CiteScore Ranking: 2020: 10/603 (Plant Science)
Online ISSN: 1365-313X

Versão complete disponível em:
<https://onlinelibrary.wiley.com/page/journal/1365313x/homepage/forauthors.html>

Author Guidelines

1. SUBMISSION

Thank you for your interest in *The Plant Journa*l (*TPJ*). Note that submission implies that the content has not been published or submitted for publication elsewhere except as a brief abstract in the proceedings of a scientific meeting/symposium or on a preprint server such as BioRxiv.

***TPJ* has removed all formatting requirements for the initial submission of articles to the journal. Under this scheme new manuscripts, or manuscripts previously considered by other journals, can be submitted to *TPJ* without excessive formatting/reformatting requirements. As long as manuscripts contain a title, author list, abstract, introduction, results/discussion, methods, and bibliography, we will be happy to process the submission through our normal procedures, irrespective of exactly how it is formatted. The aim is to allow swift consideration of the work, with only those manuscripts that have to be resubmitted following review, or which directly go on to be provisionally accepted for publication, needing to be reformatted to *TPJ* style. The review process itself will proceed in exactly the same way as in previous years.**

Once you have prepared your submission, or resubmission in accordance with the Guidelines, manuscripts should be submitted online at **https://mc.manuscriptcentral.com/tpj**